THE CHARACTERIZATION OF COLLAPSIN RESPONSE MEDIATOR PROTEIN-1 (CRMP-1) FOR ARP2/3 DEPENDENT ACTIN STRUCTURES

BY

HUI-CHIA YU-KEMP

DISSERTATION

Submitted in partial fulfillment of the requirements
For the degree of Doctor of Philosophy in Cell and Developmental Biology
in the Graduate College of the
University of Illinois at Urbana-Champaign, 2016

Urbana, Illinois

Doctoral Committee:

Associate Professor William M Brieher, Chair and Director of Research
Professor Martha U Gillette
Professor Claudio Grosman
Professor Phillip A Newmark

ABSTRACT

The actin cytoskeleton, composed of actin and its binding proteins, drives cell motility, determines cell shape, and is necessary for strong cell-matrix and cell-cell adhesion. Consistent with its critical function in cell physiology, actin assembly is highly regulated. One of the key factors controlling actin assembly is the actin nucleator, the Arp2/3 complex. Upon the hierarchical regulation of the activity of the Arp2/3 complex, the cell can build the control actin framework spatially and temporally in response to different cellular signals. Understanding the molecular mechanism of how Arp2/3 is regulated would provide crucial insights into how actin polymerization is normally controlled to direct cell movements. It will also provide insights into how misregulation of actin assembly can cause disease such as metastasis. Even though many factors have been shown to contribute to Arp2/3 dependent actin assembly, these known factors are not sufficient to account for Arp2/3 mediated actin assembly detected in cells, implying there are still missing factors that contribute to this reaction. The bacterial pathogen *Listeria monocytogenes*, for example, uses host Arp2/3 to assemble an actin comet tail. We used *Listeria* as a tool to screen brain cytosol for new factors that promote comet tail assembly. We identified Collapsin Response Mediator Protein-1 (CRMP-1) as a new factor for Arp2/3 dependent actin polymerization. CRMP-1 is essential for *Listeria monocytogenes* actin tail formation, as well as for actin filament accumulation inside MDCK epithelial cells. CRMP-1 acts as an enhancer for Arp2/3 complex in the *Listeria* system; yet CRMP-1 works with EVL as a novel Arp2/3 activator in the mammalian system. Perturbing CRMP-1 function results in the loss of actin assembly in both systems. CRMP-1 belongs to CRMP family which has been long studied as a microtubule binding protein. Our results reveal that this family protein might help the crosstalk between actin and microtubule cytoskeleton.

To my husband Jim, our son Jimmy, and our families.

獻給我最親愛的家人

Acknowledgement

- Thanks to my thesis adviser, Dr. William Brieher, for giving me the chance to work on the CRMP-1 project and for his support along the way.
- Many thanks to my thesis committee, Dr. Martha Gillette, Dr. Claudio Grosman, and Dr. Phillip Newmark, as well as past committee members, Dr. Michel Bellini and Dr. Fei Wang, for providing suggestions for both my project and my career. Special thanks to Dr. Newmark and Dr. Gillette, who were willing to spare some time from their busy schedules to meet with me whenever I felt lost; thank you for lightening hope on pursuing a research career. Special thanks to Dr. Grosman and Dr. Bellini, with whom I had many delightful conversations about different further possibilities.

My Ph.D. is like running a marathon, without being able to reach the finish line. Whenever I thought I got close, the line got pushed farther away. I would not have been able to maintain my strength to endure this process without the love and support from my family, and my friends.

I am grateful to have my husband, James Kemp, to be on my side with my every mood. I cannot thank him enough for his endless patience toward me and his strong belief in humanity. With so many obstacles in my Ph.D., having his love and support are the reason why I can smile even when the times were hard.

I am blessed to have my family's support. To my family in Taiwan, sorry for my absence for all the years. The messages and phone calls from you always cheer me up. To my family in U.S.A., thank you for always being there whenever I need help. To my son, Jimmy, I am so glad to have you. You bring joys to my life and color my Ph.D.

I am very lucky to meet and make friends with many loving people. Among them, I would like to emphasize my gratitude to my best friends, Koh Eun Narm and Christina Rosenberger. Thank you for listening to me and empathizing with my feelings. The sarcastic response from Koh Eun always made me laugh about my own situation; the optimistic attitude from Christina drove me through many down times. The time we shared together are one of the best memories I cherish in my Ph.D.

I am also thankful for some of the not ideal situations I encountered during these years, which strengthened me and pushed me to think over many things I would have never thought of. The unpleasant experience with the people I met in science taught me the importance of treating people kindly and politely, and the importance of being a helpful labmate or a respectful senior scientist. Many thanks to the labmates, Kieran Normoyle, James Kemp and Krista Angileri, who always generously provide their know-how and offer help to those in need, and Ambika Nadkarni, whose bright spirit brings laughs to the lab. If I had a chance to restart my Ph.D in 2009, I might have chosen a different path. But if that were the case, I would not have experienced the same, and would not met these people who helped me grow and helped me realize that I am so loved and supported.

Table of Contents

CHAPTER 1: INTRODUCTION 1

I. Actin and Actin Cytoskeleton 1

II. Arp2/3 Complex and Nucleation Promoting Factors 2

III. Cadherin Mediated Adherens Junction 5

IV. *Listeria monocytogenes* 6

V. Collapsin Response Mediator Protein (CRMP) Family Proteins 8

i. Overview 8

ii. The CRMP variants 9

iii. The varied functions of CRMP variants 10

iv. CRMPs and cytoskeleton 11

v. Post-translational modification of CRMPs 13

vi. Sequence and the related function of the CRMPs 15

CHAPTER 2: MATERIAL AND METHODS 19

I. Plasmids and Sequence 19

i. Plasmids 19

ii. Sequence 19

II. Protein Purification 20

i. Purification of CRMP-1 from brain cytosol 20

ii. Recombinant protein purification 21

iii. Endogenous protein purification 21

III. Biochemical Assays 22
i. *Listeria* preincubation assays 22
ii. Immunodepletion of CRMP-1 and rescue experiments 22
iii. In vitro actin assembly assays 23
iv. Filament branching assay 24
v. F-actin co-sedimentation 24
vi. Protein interaction assays 24
IV. Tissue Cultured Cells and Imaging 26
i. Cell line 26
ii. Calcium switch assay 26
iii. Fixation and staining 26
iv. Hanging drop adhesion assays 27
v. Cell spreading experiment 28
vi. Wound healing experiment and live cell imaging 28
V. Data analysis 28

CHAPTER 3: RESULTS 30
I. CRMP-1 contributes to *Listeria* Actin Tail Formation 30
i. Identification of CRMP-1 as a new factor for *Listeria* actin tail formation 30
ii. CRMP-1 is essential for *Listeria* Actin Tail Formation 30
iii. CRMP-1 and CRMP family proteins facilitate Arp2/3-dependent assembly 32
iv. CRMP-1 increases Arp2/3-dependent branching 34

II. Localization and Functional Study of CRMP-1 at Cadherin-Mediated Adherens Junction in MDCK Cells....34

i. CRMP-1 locates at cadherin-mediated cell-cell contacts 34

ii. CRMP-1 is recruited to cell-cell contact at the early stage of the contact re-formation.... 35

iii. Depletion of CRMP-1 reduces cadherin and F-actin amount at the apical junction 36

iv. Reduced stress fiber was detected in the CRMP-1 knockdown cells 36

v. CRMP-1 knockdown cells share similar many attributes with the Arp2/3 knockdown MDCK cells.... 37

vi. Arp2/3 might be less active under the CRMP-1-knockdown background 38

vii. CRMP-1 highly associates with cadherin-enriched membrane fraction and contributes to de novo Arp2/3 polymerization in the purified liver membrane system 39

viii. CRMP-1, rather than using VCA fragment of WAVE, works with EVL to activate Arp2/3 complex 41

ix. EVL and CRMP localize to cadherin mediated junction and mediate junctional actin assembly.... 43

x. Depletion of CRMP-1 or EVL decrease cell-cell attachment and reduces the rate of junction formation 45

III. Localization and Functional Study of CRMP-1 in Lamellipodia 46
i. CRMP-1 locates to the leading edge of protrusive structures in MDCK cell.... 46
ii. CRMP-1 is essential for cell spreading in an Arp2/3-dependent manner..... 46
iii. CRMP-1 contributes to F-actin accumulation at the leading edge of lamellipodia of a wounded cell 47
iv. No obvious change in microtubule organization was detected in CRMP-1-depleted or –overexpressing cells 48
v. Semaphorin 3A does not attenuate the formation of the protrusive structures in MDCK cells 49
vi. CRMP-1 contributes to the stability of the protrusive edge 50
vii. CRMP-1 contributes to the directionality in wounded monolayers..... 50
CHAPTER 4: DISCUSSION..... 52
CHAPTER 5: REFERENCES 56
CHAPTER 6: FIGURES..... 68
APPENDIX A 106
APPENDIX B 118

CHAPTER 1: INTRODUCTION

I. Actin and Actin Cytoskeleton

Actin is a protein containing 375 residues. It is one of the most abundant proteins inside the cell. It polymerizes into long filaments that organize into networks to form the actin cytoskeleton. The actin cytoskeleton is a dynamic structure, that is constantly be assembled, disassembled, and reassembled in response to internal and external signals. A collection of dozens perhaps hundreds of actin binding proteins control actin organization to perform diverse cellular processes, such as cell migration, cytokinesis, and endocytosis as well as an important structural role in reinforcing cell-matrix and cell-cell adhesive contacts.

Actin can exist in a globular monomeric form (G-actin) and as filamentous form (F-actin) inside the cell. In vitro, under low salt condition, actin remains in its monomeric state. Upon the addition of ions, G-actin can self-assemble into F-actin. This process is called polymerization. Polymerization can be further divided into a nucleation phase and an elongation phase. The nucleation phase is slow because the actin subunits must first form an actin trimer in order for actin to then polymerize; yet this trimer state is unstable. Therefore, a kinetic barrier of actin polymerization is usually seen as a long lag phase before fast actin assembly begins.

Cells express actin nucleation factors, such as the Arp2/3 complex, which can help bypass the barrier by structurally mimicking the trimeric state of actin, therefore actin filaments can be generated rapidly provided an active actin nucleation factor is present (see the next chapter). After nucleation, the filament can be elongated by just adding actin monomers to the end of the existing filament. This process is very fast relative to nucleation. During elongation, new actin monomers are added only to one end of the filament. We call this end the growing end, or the plus end. The other end is called the shrinking end, or the minus end. This polarity of actin filament results from the consistent orientation of all the monomers within the polymer such that they all face the same direction (Fujii et al., 2010).

Opposite to polymerization, F-actin can be disassembled (depolymerized) into G-actin. Disassembly usually takes place at the minus end of the filament. Polymerization is

essential for the actin cytoskeleton to perform its function in many situations, (see examples in Chapter 1, III and IV). Depolymerization, therefore, ensures the turnover of actin filaments and maintains a substantial pool monomeric actin that allows continual growth of the actin filaments.

The actin cytoskeleton has two major structural arrangements inside the cell: the filaments are either organized into branched actin networks or they are crosslinked into parallel bundles. In the branched networks, the minus end of one actin filament is anchored to the side of another filament through the Arp2/3 complex (see the next chapter). In the bundled situation, actin filaments are aligned in a parallel array through the side binding activity of various actin bundling proteins, such as vasodilator-stimulated phosphoprotein (Ena/VASP), alpha-actinin and fascin (Honda et al., 1998; Kane, 1975; Reinhard et al., 1992). During cell migration, the leading edge can contain two kinds of protruding structures, lamellipodia and filopodia, which consist of branched arrays and parallel bundles of filaments, respectively (Yang and Svitkina, 2011a; Yang and Svitkina, 2011b). Despite the distinct F-actin organizations of lamellipodia and filopodia, the two structures might be dynamically interrelated. Their filaments may be generated by common nucleator(s), since electron microscopy study indicates that the reorganization of dendritic network in the lamellipodia can be bundled together to form filopodial structure (Svitkina et al., 2003). Branched and bundled actin networks were also detected in the actin cytoskeleton formed by the pathogen *Listeria monocytogenes*. Understanding how the different organizations are formed is one important topic in order to understand how cell regulates the actin cytoskeleton.

II. Arp2/3 Complex and Nucleation Promoting Factors

Cells use the branched actin network at different cellular locations to perform different functions: at the leading edge of motile eukaryotic cells to push the membrane forwards (Svitkina and Borisy, 1999; Svitkina et al., 1997), at adherens junction to establish and maintain cell-cell adhesive contacts (Kovacs et al., 2011; Verma et al., 2012), and at the surface of certain pathogens like *Listeria* for its invasion and intracellular movement (Cossart, 2000; Welch and Way, 2013).

The formation of the branched network requires a protein complex called the Arp2/3 complex (Pollard and Beltzner, 2002; Pollard and Borisy, 2003). Arp2/3 is often referred to as an actin nucleator, since it can rapidly generate new filaments. The key mechanism to forming a dendritic meshwork relies on the binding of Arp2/3 complex to the side of a preexisting filament (mother filament), followed by initiating a new filament (daughter filament) with angle of 70 on the side of the old filament (Mullins et al., 1998). The Arp2/3 complex consists of seven subunits, Arp2, Arp3, p16, p20 (ARPC4), p21 (ARPC3), p34 (ARPC2), and p40 (ARPC1). Among all the subunits, p20, p34 and p40 of Arp2/3 contact the mother filament. Subunits Arp2 and Arp3 contact the daughter filament. Subunits Arp2 and Arp3 form a pocket to accommodate new actin monomers, therefore initiating the growth of the new filament. This pocket also provides the anchoring site for the pointed end of the daughter filament after the filament is formed. In the inactive state, the Arp2 and Arp3 subunits are too apart from each other and therefore structurally unfavorable to incorporate an actin monomer. It has been shown that various molecules need to contribute to the activation of Arp2/3 complex, including ATP, binding to the mother filament, and binding to nucleation promoting factors (NPFs) (Goley et al., 2004; Rouiller et al., 2008; Zencheck et al., 2009).

To grow a new filament out of the mother filament, several conformational changes have been detected during this process. Interestingly, those conformational changes are not limited to the Arp2/3 complex. Actin molecules in the mother filament also undergo several conformational changes. It is thought that those conformational changes result in the reinforcement of the interface between Arp2/3 and the mother filament, leading a strong(er) anchoring for the daughter filament (Rouiller et al., 2008). Therefore, the filament can exert force to push a membrane outward or to push a pathogen forward. A conformational change on Arp2/3 was observed upon ATP binding. As a result, the spatial distance between Arp2 and Arp3 gets narrower (Goley et al., 2004; Rouiller et al., 2008). Arp2/3 also adjusts its conformation while contacting the mother filament. After Arp2/3 binds to the mother filament, NFP helps recruit the first monomeric actin to Arp2-Arp3 pocket, establishing a template for the elongation of the branched daughter filament. Upon this branching formation, Arp2/3 complex and the mother filament adapt their

conformation at the contacting interface to reinforce and stabilize the branching structure (Rouiller et al., 2008).

The cell regulates the formation of new Arp2/3 dependent filaments through NPFs. The most well-known NPFs inside the cells are the Wiskott-Aldrich syndrome protein (WASP) family of proteins and the WASP family verprolin-homologous protein (Scar/WAVE or WAVE). NPFs themselves require activation through upstream signaling, which therefore provide cells with a mechanism for the spatial and temporal regulation of Arp2/3 activity and actin nucleation. The major signaling pathways involve the small G proteins Cdc42 and Rac. Cdc42 activates neural (N)-WASP (Rohatgi et al., 1999); Rac activates WAVE (Eden et al., 2002).

WASP and WAVE contain a VCA domain that binds and activates Arp2/3. To be more specific, WASP contains two V regions. So it is often referred to as the VVCA region for the WASP protein, whereas VCA is for WAVE. The V (verprolin homology) sequence, (also called the WASP homology 2 (WH2) domain), binds actin monomers; the C (central, connecting, or cofilin homology) sequence and A (acidic) sequence interacts with and activates Arp2/3 (Pollard and Borisy, 2003).

Even though NPFs are viewed as Arp2/3 activators in general, they could have other functions. Sometimes different NPFs colocalize in cell yet each NPF plays a distinct role. For example, N-WASP and WAVE are both localized to adherens junction (Ivanov et al., 2005) and in lamellipodia (Nakagawa et al., 2001). At the adherens junction, WAVE-2 activates Arp2/3 (Verma et al., 2012), whereas N-WASP regulates and maintains junctional filament stability rather than actin nucleation (Kovacs et al., 2011). Inside lamellipodia, N-WASP seems to control the formation of actin bundles, in addition to its activation activity on the Arp2/3 complex (Nakagawa et al., 2001).

Besides WASP and WAVE, which are the canonical VCA/VVCA-domain-containing NFPs, other proteins were also identified that activate or co-activate the Arp2/3 complex in a non-canonical fashion. Those molecules include, but are not limited to, cortactin and Dip1 (Wagner et al., 2013; Weaver et al., 2001). Revealing the mechanism of how different NPFs function independently and cooperatively is the key to understand how a cell effectively activates and controls Arp2/3 in response to various cellular environments and signals.

III. Cadherin Mediated Adherens Junction

Cadherin-mediated adherens junctions are a type of cell-cell contact mediated by cadherin molecules along the apical-lateral surface of the neighboring plasma membranes. This junction is important during embryonic development, cell growth, cell migration, differentiation, and even cancer cell invasion (Christofori and Semb, 1999; Takeichi, 1993). Cadherin mediated cell-cell junctions are also required for maintaining strong cell-cell adhesion throughout life. In certain epithelia, such as in Caco 2 cells, the adherens junction is highly developed with the vast majority of the cadherin concentrated in an "adhesion belt" that forms around the border of the contacting cells. The cadherins in the belt colocalize with a prominent ring of F-actin lining just beneath the cadherins. This highly specialized form of cadherin dependent contacts is called the "zonula adherens" (Verma et al., 2012). In other cell types, adherens junction display different morphologies: spotty and discontinuous more mesenchymal cells and in epithelial MDCK cells (Yonemura et al., 1995), or as tiny puncta as a constituent of the synaptic junctions in neurons (Uchida et al., 1996).

To form cadherin-mediated cell contacts, cadherins use their N-terminal extracellular domain to form hemophilic interactions with an identical cadherin isoform extending from an adjacent cell to connect the neighboring cells in a calcium-dependent manner. The cytoplasmic tail of cadherin provides anchoring sites for cytoskeletal elements, such as different catenins (Kemler, 1993). Cadherin recruits beta-catenin, which in turn binds alpha-catenin; and thus, it has been thought that cadherin can be passively linked to the actin filament through alpha-catenin (Jou et al., 1995). Yet later researches debate whether or not those interactions are mutually exclusive. Some said that cadherin-catenin complexes cannot bind actin (Drees et al., 2005; Yamada et al., 2005); whereas others presented data showing this interaction would exist only under tension (Buckley et al., 2014). Other than catenins, there are multiple different mechanisms that could provide the linkage between cadherin and F-actin. For example, cadherin (E-cadherin) can associate with the Arp2/3 complex, the actin nucleator (Kovacs et al., 2002; Kovacs and Yap, 2002). Cadherins therefore also have an active influence in the formation of actin filaments at cell-cell contacts. Different pharmacological agents

that interfere the actin cytoskeleton, such as cytochalasin D and latrunculin, can rapidly and efficiently disrupt adherens junctions, indicating the crucial role of actin cytoskeleton to cell-cell contact integrity. It is believed that the actin cytoskeleton provides mechanical force to maintain and reinforce cell-cell contacts (Vasioukhin et al., 2000). Many factors have been shown contribute to the formation of actin network at the junction. Understanding the mechanism and the relationship of those factors would not only help us understand the regulatory pathway of adherens formation, but also provide pharmaceutical input on diseases such as cancer.

IV. *Listeria monocytogenes*

Listeria monocytogenes (*Listeria*) is a gram-positive food-borne pathogen. *Listeria* can tolerate a wide range of pH and temperatures; therefore it can survive in refrigerated and even pasteurized food. Ingestion of contaminated food can lead to gastrointestinal symptoms or even lysteriosis.

The virulence of *Listeria* relates to its ability to transmit from cell to cell. After entering the cell, *Listeria* multiplies and is encapsulated by actin filaments. Those actin filaments later organized and extended to form an actin comet tail. Comet tail assembly creates the propulsive force for *Listeria*'s intracellular movement. Using this actin tail, *Listeria* can then translocate and spread into the adjacent cells (Sanger et al., 1992; Tilney and Portnoy, 1989).

This actin-based motility of *Listeria* requires one *Listeria* membrane protein, ActA. This surface protein mimics the function of cellular NPFs. ActA contains an acidic domain and a cofilin homology domain at its N-terminus; ActA hence binds and activates the Arp2/3 complex (Cossart, 2000; Welch et al., 1997). ActA can also recruit other cellular protein, such as Ena/VASP family proteins. Ena/VASP uses its EVH1 domain to bind to the proline-rich domain of ActA, and its EVH2 domain to bind to F-actin. It has been believed that Ena/VASP proteins contribute to *Listeria* actin tail growth by enhancing the contact and the elastic linkage of the bacteria to the actin filaments (Laurent et al., 1999; Skoble et al., 2001; Suei et al., 2011). Despite the unknown details of *Listeria* propulsion, ActA clearly recruits factors from the host to trigger actin assembly at the bacterial surface.

Many other actin-binding proteins also have roles in this actin comet tail. For instance, cofilin is necessary for depolymerizing the tail therefore controlling the tail length (Rosenblatt et al., 1997). Interestingly, a protein usually shares a similar function for the *Listeria* actin tail and for actin networks found inside the cell, which indicates that *Listeria* actin comet can be used as a model system for understanding other actin arrays used by the cell. The *Listeria* actin comet tail has other characteristics that are similar to the cellular actin systems: the rate of this tail assembly equals the rate of actin polymerization (Theriot et al., 1992), and the structure of the actin filaments: the comet tail contains a branched meshwork and/or paralleled bundles, which is similar to the actin organization detected in protruding lamellipodia and filopodia (Brieher et al., 2004). This structural similarity supports the notion that *Listeria* is driven by the same machinery responsible for the protrusion structures of a mirgrating cell (Borisy and Svitkina, 2000). Because of all those key resemblances, people have used *Listeria* as a model system for the in vitro study of the actin cytoskeleton. *Listeria* has been used to characterize proteins with actin-related function (David et al., 1998; Welch et al., 1997), examine the organization of the actin network (Brieher et al., 2004) and investigate the turnover of actin arrays (David et al., 1998; Rosenblatt et al., 1997).

A more recent publication from Van Troys and colleagues revealed the complexity of the proteins in the *Listeria* actin tail using proteomic techniques (Van Troys et al., 2008). Many of the proteins identified in their screen have no known actin-related functions, implying that this actin tail system might be far more sophisticated than we thought, in terms of participating components and regulatory pathways. In addition, independent researches mentioned that the reconstituted actin comet tail built out of purified components could be less efficient than the one formed in complex cytosol (Brieher et al., 2004; Laurent et al., 1999; Welch et al., 1997). Our knowledge on this actin tail might limited to the minimal components yet not the whole machinery. My Ph.D. project aims to characterize proteins that are novel for the *Listeria* tail formation, and follow with a mechanistic study of the protein in vitro and the functional study of the protein inside the cell. This project was initiated by my Ph.D. advisor William M. Brieher. He established an approach that combines unbiased chromatography and *Listeria* to screen through the potential factors from bovine brain cytosol that contribute to comet

tail assembly (Brieher et al., 2004). Using his method, he discovered Collapsin Response Mediator Protein-1 (CRMP-1) as one factor enhancing *Listeria* actin tail formation. CRMP-1 was a surprise as it had never been considered as an actin assembly factor in the past. My PhD project was to critically evaluate whether or not CRMP-1 actually contributes to Arp2/3 dependent actin assembly.

V. Collapsin Response Mediator Protein (CRMP) Family Proteins

i. Overview

The CRMP family consists of five family members in vertebrates: CRMPs 1-5 (Byk et al., 1996; Gaetano et al., 1997; Goshima et al., 1995; Inatome et al., 2000; Minturn et al., 1995b). The CRMP family is highly homologous to the enzyme dihydropyrimidinase (DHPase). However, CRMP proteins lack a key amino acid in the active site necessary for enzymatic activity. *C. elegans* and *Drosophila* express only one CRMP gene, which will produce one CRMP and one DHPase through alternative splicing (Morris et al., 2012). The function of CRMP family protein was first mentioned in 1985 by Hedgecock and colleagues (Hedgecock et al., 1985). They found that unc-33, the homolog of human CRMP-2 and chick CRMP-62, contributes to axon growth in *Caenorhabditis elegan*. Goshima and colleagues later identified vertebrate chick CRMP-62 as a component for transduction pathway of the extracellular semaphorin 3A (Sema3A) signal (Goshima et al., 1995). Sempahorin 3A is an important axon guidance cue in the developing nervous system. When applied to neuronal growth cones, it causes the growth cone to collapse. CRMP-62 got its name because it was required for collapse, hence "Collapsing Response Mediator Protein". The work done Goshima that identified chicken CRMP-62 is the same as CRMP-2. Since then, the vast majority of CRMP researcher has been focused on studying CRMP-2 and how it regulates various aspects of axon pathfinding and neurite outgrowth (Goshima et al., 1995; Hedgecock et al., 1985; Inagaki et al., 2001; Minturn et al., 1995b; Quinn et al., 2003; Quinn et al., 1999; Siddiqui and Culotti, 1991; Yoshimura et al., 2005).

Researchers are interested to know how CRMP family proteins achieve their physiological function. The very early study by Hedgecock et al. described that mutation

of unc-33 causes disruption of microtubule organization and abnormal microtubule structure in the neuronal cells, but not in muscle or hypodermal cells (Hedgecock et al., 1985). They proposed thought unc-33 can bind to microtubules and control the assembly or stability of neuronal microtubules. Subsequent biochemical and cell biological work successfully detected that CRMP-2 binds tubulin and promotes microtubule growth. Not until the early 2000s did the studies on CRMPs start to reveal their possible involvement in actin. With more and more studies published, we now know that CRMPs can bind both actin and microtubules, CRMPs function in various cell types (not just neuronal cells), and CRMPs are post-translationally modified in response to various cellular demands.

ii. The CRMP variants

After the discovery of chick CRMP-62 (CRMP-2) as a factor for Sema3A-mediated signaling (Goshima et al., 1995), a whole family of cytoplasmic proteins was described to be involved in the same signal transduction cascade. This family is now called collapsin response mediator protein (CRMP), which has replaced older names as turned on after division (TOAD) (Minturn et al., 1995a; Minturn et al., 1995b), or Unc-33-like-phosphoprotein (Ulip) (Byk et al., 1996; Byk et al., 1998; Gaetano et al., 1997). CRMP is also often referred to as DHPase-related protein due to its high sequence homology and structural similarity to DHPase (Goshima et al., 1995; Hamajima et al., 1996). The key distinction between DHPase and CRMP is that CRMP does not carry the enzymatic activity as DHPase (Goshima et al., 1995). DHPase is zinc-coupled dihydropyrimidine hydrolases; CRMPs lack this hydrolase activity as well as one or more zinc-binding site residues found in DHPase (Hamajima et al., 1998; Takemoto et al., 2000; Wang and Strittmatter, 1996).

The CRMP family was once consisted of four members: CRMP-1, -2, -3 and -4 (Quinn et al., 1999). Relatively recently, a new member CRMP-5, also called CRAM (CRMP3-associated molecule) or unc33-link phosphoprotein 6, was identified by different groups (Fukada et al., 2000; Horiuchi et al., 2000; Inatome et al., 2000). Unlike CRMPs 1-4 which share ~70-85 identity in sequence, CRMP-5 shares ~50% sequence identity with CRMPs 1-4 and DHPase.

The complexity of the CRMP family was further extended in 2003 by Yuasa-Kawada and colleagues (Yuasa-Kawada et al., 2003). They described the alternatively

spliced isoforms for several CRMPs (1, 2, and 4). The original isoform is now referred to as short isoform CRMP (S-CRMP) or CRMPa; the variant with a longer N-terminus is now called long isoform CRMP (L-CRMP) or CRMPb (Alabed et al., 2007; Pan et al., 2011; Quinn et al., 2003; Yuasa-Kawada et al., 2003). Researches on the functional difference between the two isoforms showed that different isoforms might perform different functions; sometimes one isoform can be an antagonist against the function of another isoform (see later chapters). In my thesis, the CRMP-1 I studied is the short isoform.

iii. The varied functions of CRMP variants

1. Different CRMP homologous

Emerging evidence shows that different CRMPs and different CRMP isoforms can have different or even antagonist functions. For example, even though CRMP-1 and CRMP-2 both contribute to neuronal outgrowth, they function differently in growth cone steering. Irradiation of CRMP-1 in the half region of the growth cone causes the growth cone turning away from the irritated site. In contrast, the growth cone turned toward the irritated site while inactivating CRMP-2 (Higurashi et al., 2012). This result shows that despite their high sequence homology, the members in the CRMP family might work through distinct mechanisms or different pathways.

Another example for the antagonistic effects among CRMPs can be found in the literature describing the conflicting function of CRMP-5 to other CRMPs. CRMP-5 showed the opposite function to other CRMP homologs. The binding of CRMP-2 to tubulin promotes neurite outgrowth; yet CRMP-5 can act as dominant signal and abrogate the outgrowth effect from CRMP-2 by antagonizing the tubulin-CRMP-2 interaction (Brot et al., 2010). Note that this counter-effect seems to involve a pathways that excludes the direct molecular interaction between CRMP-2 and CRMP-5. CRMP-1 and CRMP-5 are also shown to have antagonistic effects. CRMP1 stimulates the proliferation of neuronal progenitors, while CRMP-5 has negative effects (Veyrac et al., 2011). In other conditions, CRMP-5 helps filopodia extension in growth cone even in the presence of Sema3A (Hotta et al., 2005), yet other CRMPs, at least CRMP-1 and CRMP-2, function downstream of Sema3A (Uchida et al., 2005).

2. Different isoforms

Different splice variants of a CRMP can also have opposite cellular functions. L-CRMP-1 enhances filopodia formation, cancer cell migration and invasion via stabilization of actin; yet S-CRMP-1 has the opposite effect (Pan et al., 2011). L- and S-CRMP-2 can both bind to the kinase ROCKII. L-CRMP-2, however, has an extra ROCKII binding site at it N-terminus, which allows L-CRMP-2 to preferably bind to ROCKII and inhibit ROCK-dependent carcinoma cell migration and fibronectin matrix assembly (Yoneda et al., 2012). Similarly, L-CRMP-4 uses its unique N-terminal region to provide a better binding to its binding partner RhoA. Both of the isoforms of CRMP-4 bind RhoA; yet L-CRMP-4 shows a more robust binding to RhoA than S-CRMP-4 (Alabed et al., 2007; Alabed et al., 2010). In addition, only the L-CRMP4 isoform shows GSK3β- or Nogo-regulated RhoA binding, even though the regulation of GSK3β affects phosphorylation of both S- and L-CRMP-4 (Alabed et al., 2007).

iv. CRMPs and cytoskeleton

1. CRMPs and microtubule dynamics

CRMP-2 is the first described and most studied member of this family (Goshima et al., 1995). Its studies started on investigating its role in neuronal outgrowth and collapse. CRMP-2 can regulate neuronal polarity and axon elongation (Yoshimura et al., 2005). Overexpression of CRMP-2 in hippocampal neurons induces the formation of multiple axons for promotes elongation of the primary axon (Inagaki et al., 2001). On the other hand, CRMP-2 also contributes to growth cone collapse. This opposite effects of CRMP-2 can be explained by its tubulin binding ability and its post-translational modifications. Unphosphorylated CRMP-2 binds directly to tubulin dimer (Fukata et al., 2002). CRMP-2 also also binds to the kinesin-1 light chain, therefore regulates the transport of soluble tubulin to the distal parts of growing axon (Kimura et al., 2005). The binding of CRMP-2 to tubulin would be disrupted when CRMP-2 is phosphorylated in response to repulsive guidance cue, Sema3A (Goshima et al., 1995). Other CRMP family protein, such as CRMP-5, was also shown to bind to tubulin. However, instead of functioning as a downstream regulator for Sema3A to affect axon morphology, CRMP-5 inhibits axon

outgrowth by binding to tubulin itself and preventing the tubulin-CRMP-2 interaction (Brot et al., 2010).

Other than their roles in the neuronal cells, CRMPs contribute to other cellular functions through binding to microtubules. For example, CRMP-2 has been detected in the mitotic spindle of transformed mouse and human cells (Tahimic et al., 2006). It binds to tubulin during mitosis and can regulate mitosis and mitosis duration (Lin et al., 2011; Oliemuller et al., 2013; Tahimic et al., 2006). Perturbing CRMP functions results in multinucleated cells and causes apoptosis in A549 non-small-cell lung cancer (NSCLC) (Oliemuller et al., 2013).

2. CRMPs and actin cytoskeleton

The first direct evidence showing the direct interaction between CRMP and actin was published in 2005: CRMP-4 can bundle F-actin in vitro (Rosslenbroich et al., 2005). A later study using truncational analysis revealed that CRMP-4 uses its C-terminus to bind F-actin (Khazaei et al., 2014). Even though not many in vitro biochemical studies have been done to further dissect the molecular mechanism of CRMPs on actin dynamics, independent groups have observed the localization of CRMPs to actin-related structures.

Evidence showing CRMPs locate to the actin cytoskeleton could be traced back to the early growth cone researches. Early work emphasized the role of CRMPs in regulating growth cone collapse through modulating microtubule dynamics. Yet the growth cone staining indicates endogenous CRMP localizes to the very tip of the growth cone, which is organized by the actin cytoskeleton, not microtubules (Arimura et al., 2005; Minturn et al., 1995a; Nishimura et al., 2003). Not until recently, have researchers started to discuss the localization of CRMPs to actin structures in growth cones. CRMP-1, for example, overlaps with actin in the growth cones of dorsal root ganglion (DRG) neurons (Higurashi et al., 2012).

Growth cone collapse can be an downstream effect of actin bundle loss, actin redistribution or through actin depolymerization (Zhou and Cohan, 2001). CRMPs could possibly cause the loss of actin bundles through different ways. CRMP-1 was recently reported to bind to filamin-A, which is a known actin bundling protein. Sema3A signaling may augment the CRMP-filamin interaction and thus attenuate the ability of filamin to crosslink F-actin into bundles (Nakamura et al., 2014). Furthermore, CRMP

binds to another known regulator of actin dynamics in neurons known as MICAL. MICAL directly binds F-actin and disassembles both individual and bundled actin filaments. MICAL alone, however, is autoinhibited. CRMP is thought to release the auto-inhibition of MICAL (Schmidt et al., 2008). CRMP can therefore link Sema3A signaling from Plexin, the receptor for Sema3A, to F-actin disassembly through MICAL (Hung et al., 2010; Terman et al., 2002). It is unclear if the actin bundling activity of CRMP would be altered after post-translational modification. Even though the Kaibuchi group mentioned that phosphorylation or un-phosphorylated CRMP-2 can pull-down the same amount of actin from cell extract (Arimura et al., 2005), a more careful quantitative assay needs to be done to support this statement.

Other actin-related functions for CRMPs have been mentioned in the literatures. CRMPs were detected in filopodia, suggesting their role in regulating filopodial dynamics and/or growth cone development: CRMP-4 for filopodial extension in hippocampal neurons (Khazaei et al., 2014); CRMP-5 for filopodia growth in mouse DRG neurons (Hotta et al., 2005); L-CRMP-1 for filopodia formation in NSCLC (Pan et al., 2011). Inactivation of CRMP-1 was even described to cause lamellipodia retraction in chick DRG (Higurashi et al., 2012). This localization and effect of CRMPs, at least in filopodia, seems best explained by its actin binding or actin bundling activity. Yet the detailed molecular mechanisms remain obscure.

v. Post-translational modification of CRMPs

1. Phosphorylation

CRMPs are cytosolic phospho-proteins with extensive studies on its kinases and the corresponding phosphorylated residues. The physiological functions of the CRMP family protein in growth cones have been shown to be highly related to its phosphorylation.

For being a downstream effector of the repulsive cues, CRMP is phosphorylated by different kinases. CRMP-2 is phosphorylated at Theronine 555 by Rho kinase in response to lysophosphatic acid (Arimura et al., 2000). Downstream of Sema3A signaling, Fes/Fps phosphorylates CRMP-1, -2, and -4 (Fukata et al., 2002); CdK5 and GSK3-beta phosphorylate CRMP-2 at Serine 522 (priming phosphorylated site), Theronine 509, Threonine 514 and Serine 518 (Brown et al., 2004; Gu and Ihara, 2000; Uchida et al.,

2005; Yoshimura et al., 2005). Dephosphorylation of CRMP-2 at Threonine 514 can be processed by protein phosphatase 1A and protein phosphoatase 2A (Cole et al., 2008; Zhu et al., 2010). Phosphorylation of CRMP-2 at Serine 522 has an essential role for regulating dendritic branch trajectories in the cerebral cortical neurons in vivo in mice (Yamashita et al., 2012). Tyrosine 32 of CRMP-2 is phosphorylated in response to Sema3A mediated activation of the tyrosine kinase Fyn (Yamashita et al., 2007). Fyn can also phosphorylate CRMP-1 at Y504, providing an isoform specific phosphorylation. The upstream signal for this phosphorylation on CRMP-1 remains unclear (Buel et al., 2010). Overall, it is generally believed that these phosphorylations would decrease CRMPs' ability to bind tubulin dimers with consequences for microtubule disassembly resulting in growth cone collapse.

Phosphorylation of CRMP family protein can regulate neuronal morphology with molecules other than tubulin. As mentioned, CRMP-1 can bind to filamin. Phosphorylated CRMP-1 at Serine 522 increases its affinity with filamin. Therefore, in response to Sema3A, phosphorylated CRMP-1 might deprive filamin from crosslinking actin filaments in order to facilitate cytoskeletal remodeling (Nakamura et al., 2014). The effect of different phosphorylation of CRMP on its ability to directly bind to actin filaments is not clear. Kaibuchi and colleagues proposed that phosphorylation of CRMP-2 at Threonine 555 (by Rho Kinase) or at Theronine 514/Serine 518/Serine 522 (by Cdk5 and GSK3-beta) does not affect the protein binding to actin (Arimura et al., 2005).

Phosphorylation of CRMPs also has a role in non-neuronal cells. Perturbing phosphorylation of CRMPs causes abnormal phenotypes in a lung cancer cell line: alanine mutation on CRMP-2 substituting for Serine 522 increases the number of multinucleated cells in A549 NSCLC (Oliemuller et al., 2013). In immune cells, CRMP-2 functions as a transducer for chemokine signaling. The chemokine CXCL12 induces Yes-dependent Tyrosine 479 phosphorylation of CRMP2 and decreases GSK3-beta induced phosphorylation at Threonine 509/514, resulting in chemokine-mediated T-cell polarization and motility (Varrin-Doyer et al., 2009; Vincent et al., 2005).

With all the different phosphorylation sites on CRMPs, the cell might have established a hierarchical regulatory system to control CRMP function. For example, phosphorylation generated by GSK3-beta requires CDK5 to "prime" a phosphorylation at

Serine 522 (Cole et al., 2008). Another example can be found in the phosphorylation of CRMP-2 Tyrosine 479. Tyrosine 479 is not exposed on the protein surface. Dephosphorylation of CRMP-2 at Threonine509/514 might be essential to alter the overall charges in the vicinity of Tyrosine 479, and hence enhance the stability of phosphorylation at this residue in response to chemokine signal (Varrin-Doyer et al., 2009).

2. O-glycosylation

There is only one paper mentioned the glycosylation on CRMP-2. CRMP-2, in the synaptosomal cytosol, is O-glycosylated by a single beta-N-acetylglucosamine at serine/threonine (Cole and Hart, 2001). The authors also proposed the interrelationship of *O*-glycosylation and *O*-phosphorylation for regulating the function of CRMP-2 in synaptosomes: when CRMP-2 is *O*-glycosylated, the phosphorylation of CRMP-2 is blocked. As a consequence, CRMP-2, in its non-phosphorylated state, functions to promote growth cone formation.

Many actin binding proteins, such as vinculin, talin and synapsin (Cole and Hart, 1999; Hagmann et al., 1992; Hart, 1997), are *O*-glycosylated, yet with little understanding about the related function. The glycosylation of other CRMPs in synamptosome, or the glycosylation of CRMPs in other tissue, has not yet been addressed. We do not know if different CRMPs or different isoforms represent distinct *O*-glycosylation either. Deciphering the post-translational modifications and the upstream regulatory pathway of CRMPs would help understand how proteins were regulated spatially and temporarily. It will also help extend our understanding on the CRMP function. A major challenge in the future will be to examine how all the various CRMP isoforms and their posttranslational modifications alter microtubule and actin organization in cells to promote or inhibit cell motility.

vi. Sequence and the related function of the CRMPs

CRMPs have a core DHPase-like domain and a positively charged C-terminal region, which is highly susceptible to proteolysis (Deo et al. 2004). Domains and motifs in CRMP-1 were predicted through structure modeling and motif prediction (Shih et al.,

2003). This chapter summarizes the truncation studies of CRMPs and the prediction from Shih et al. to provide an overall view of the sequence and the related function.

1. Sequence for tubulin related function

The Kaibuchi group in 2002 provided the first evidence that CRMP family proteins physically interact with tubulin (Fukata et al., 2002). So far, two tubulin binding sites in human CRMP-2 were proposed: amino acids 323-381 (Fukata et al., 2002), and amino acids 480-509 (or, the 82 amino acids at the C-terminal) (Chae et al., 2009; Lin et al., 2011). Even CRMP-5, the least conserved member in the CRMP family, uses similar residues (residues 475-522) for tubulin binding (Brot et al., 2010). Deletion and point mutation studies of human CRMP-2 further indicated that the region 480-509 contains a GAP activity for tubulin dimers. This 480-509 region is the essential region for tubulin polymerization by stimulating tubulin GTPase activity, while 323-381 region stimulates microtubule assembly in a tubulin GTPase activity-independent manner (Chae et al., 2009).

CRMP itself might regulate its tubulin-binding ability in an auto-inhibitory manner. The first 300 amino acid of rat CRMP-4 was shown to have a counter-effect for tubulin polymerization. Deletion of this domain enhanced tubulin polymerization (Khazaei et al., 2014). C-terminal truncated CRMP-1 (reside 1-490) alone failed to bind to tubulin, suggesting that the central region of CRMP is unlikely to serve as a binding site without conformational alteration (Lin et al., 2011). Similarly, an earlier study of the corresponding region in human CRMP-2 (amino acid 150-299) demonstrated that this is a self-inhibitory region that binds the tubulin-binding site (Chae et al., 2009). Structurally, residues 323-381 in both CRMP-1 (Deo et al., 2004) and CRMP-2 (Stenmark et al., 2007) are largely buried in the tetramer, indicating that tubulin binding to this region might require conformational change to release the protein from auto-inhibition. A more critical view of this result would be that CRMP-1 and CRMP-2 binding to tubulin is a complete artifact because the residues necessary for “tubulin binding” are buried deep within the molecule.

2. Sequence for actin related function

CRMP-4 can bundle F-actin with the last 50 amino acids (amino acid 520-570) (Khazaei et al., 2014; Rosslenbroich et al., 2005). Consistently, this region was also

shown to contribute to filopodial length of the growth cones (Khazaei et al., 2014). Other than F-actin bundling activity, research also showed that CRMP-1 can interact with filamin A with residue 225-256, which might in turn indirectly regulate the amount of the bundled actin inside the cell (Nakamura et al., 2014).

Domain predictions done by Shih and colleagues reveals some interesting putative motifs that might contribute to actin-related functions (Shih et al., 2003). In their prediction, CRMP-1 contains two proline-rich extension signatures at residue 306-322 and 503-528. Many cytoskeletal proteins contain proline-rich region, such as zyxin, Ena/VASP, vinculin, and *Listeria monocytogenes* ActA. The proline-rich domain serves as a binding site to interact with other cytoskeleton proteins. *Listeria* ActA and vinculin, for example, use the proline-rich domain to bind to the EVH1 domain of Ena/VASP protein. Ena/VASP can help link *Listeria* to the actin filaments through F-actin binding ability of Ena/VASP (Laurent et al., 1999; Niebuhr et al., 1997). It would be intriguing to know if CRMP-1, or CRMPs, can use its proline-rich extension signatures to connect to other cytoskeletal factors.

3. Sequence for oligomerization and related function

CRMP family proteins form homotetramers and heterotetramers (Deo et al., 2004; Wang and Strittmatter, 1997). The N-terminal residues 8-134 and the core region residues 281-435 (in CRMP-1) are sufficient for homo-oligomerization (Majava et al., 2008; Stenmark et al., 2007; Wang and Strittmatter, 1997). Studies have shown that CRMP-2 and CRMP-3 can form heterotetramers (Wang and Strittmatter, 1997); CRMP-5 can interact with all the other CRMPs, yet with various affinity. For instance, CRMP-5 binds CRMP-2 better than CRMP-1 (Fukada et al., 2000; Ponnusamy and Lohkamp, 2013).

Through oligomerization, one CRMP variant might influence the function of a whole oligomer. For example, C-terminal deletion constructs of CRMP-2 (with C-terminal 191 or 222 residues deleted) can have dominant-negative effects in cultured cells. In those truncations, the tubulin-binding site is deleted yet the oligomerization site is not. The truncated protein can bind and sequester the function of the endogenous full-length CRMP-2. Hence, the neuron transfected with those constructs display short or no axon (Inagaki et al., 2001). Note that this phenotype might also be a result from hetero-interaction. How CRMPs regulate the formation of different hetero-oligomer and what

the physiological role of different hetero-oligomers are interesting questions that need to be explored.

4. Calpain-cleavage site

Calpain is a calcium-dependent protease, which cleaves a large number of proteins including cytoskeletal elements such as spectrins (Siman et al., 1996) and regulatory protein CDK-5 (Smith et al., 2006). CRMPs, the S- CRMPs, are all substrates for calpain cleavage, resulting in products of 55 and 58 kDA (Bretin et al., 2006; Hou et al., 2006). However, the cleavage site is not clear. Even though clapain can digest all the CRMPs, the cleavage sites do not seem to be conserved among different CRMPs. The cleavage site for calpain for CRMP-2 has been mapped to the C-terminal between Serine 465 and Isolueucine 558 (Bretin et al., 2006). CRMP-4 is cut near the C-terminus (Bretin et al., 2006; Chung et al., 2005; Deo et al., 2004; Kowara et al., 2005); whereas CRMP-3 is cleaved at the N-terminus (Hou et al., 2006). CRMP-1 was also detected as two protein products around 55 and 58 kDa in the mouse brain in a calpain-dependent manner (Jiang et al., 2007).

The physiological role of calpain cleavage is not fully understood. One result showed that cleaved CRMP-3 subsequently translocates to the nucleus and evokes neuronal death in response to excitotoxicity and cerebral ischemia (Hou et al., 2006). It is still unknown if it is also the case for other CRMPs. The function of calpain cleavage on CRMPs remains to be discovered.

CHAPTER 2: MATERIAL AND METHODS

I. Plasmids and Sequence

i. Plasmids

For recombinant protein expression in *Escherichia coli* (*E. coli*), we used different vectors that provide different affinity tags: pET30a (His-tag). pMAL (MBP-tag) and pGEX5-1 (GST-tag). Human CRMP-1, -2, -3, -5, DHPase and human EVL were and cloned into pET30a; human EVL was also cloned into pMAL; VVCA was cloned into pGEX5-1. His-tagged human CRMP-4 was purchased from Origene (Rockville, MD). His-tagged ActA was kindly provided by Mullins' lab (University of California, San Francisco) (Akin and Mullins, 2008). GST-VCA was provided by Kovar lab (University of Chicago). For protein expression in MDCK II cells, human CRMP-1 was cloned into pLenti-III-HA with GFP-tag. For dominant negative EVL (EVL-DN), the tetramerization domain of the EVL is cloned into pLenti-III-HA. For shRNA-expressing plasmids, hybridized oligonucleotides were cloned into pLKO.1.

ii. Sequence

For knockdown approaches, the following target sequences were used: Scramble: plasmid 1864 (Addgene); CRMP-1 sh1: 5'- ACCTGGAAGATGGACTTATAA -3'; CRMP-1 sh2: 5'- CCAAGTCTACATGGCATATAA -3'; CRMP-1 sh3: 5'- GATGGATGAGCTAGGAATAAA -3'; p34 sh1: 5'- TACGGGAGTTTCTTGGTAAAT -3'; p34 sh2: 5'- TACAATGTCTCTTTGCTATAT -3'; p34 sh3: 5'- GCCTCTGTCTTTGAGAAATAT -3'; APR3 sh1: 5'- GTAGATGCCAGACTGAAATTA -3'; ARP3 sh2: 5'- AGAAATTGGACCTAGCATTTG -3'; ARP3 sh3: 5'- GTCGTCACAATCCAGTGTTTG -3'; EVL sh1: 5'- CAGCAGGTTGTGATCAATTAT -3'; EVL sh2: 5'- GCAGGGATTCAGCCGGATAAA -3'; EVL sh3: 5'- AGGAGGCCTCATGGAAGAAAT -3'; WAVE-2 sh1: 5'- TGGGCAGCCTGAGTAAATATG -3'; WAVE-2 sh2: 5'-

GGTCGACCGCCTACAAGTTAA -3'; WAVE-2 sh3: 5'-TCCAAATCGAGGGAATGTAAA -3'.

II. Protein Purification

i. Purification of CRMP-1 from brain cytosol

1. Initial unbiased fractionation

All chromatographic media were purchased from GE Health Care. 150 grams of frozen bovine calf brain (Animal Technologies, Tyler, TX) was homogenized in two volumes of buffer B (20 mM Sodium Phosphate, pH7.5, 25 mM NaCl, 2 mM EGTA, 10 mM beta-mercaptoethanol and 0.1 mM PMSF). The homogenate was first centrifuged at 15,000X g for 30 minutes. The pellet was discarded and the supernatant centrifuged at 100,000 X g for 2 hours. The supernatant was applied to a 60 ml DE-52 column equilibrated in buffer A. The flow through, which contained the activity, was applied to a 70 ml S HP column equilibrated in buffer A. The column was eluted with a 500 ml gradient to 400 mM NaCl in buffer A. Active fractions were pooled and solid ammonium sulfate was added slowly to a final concentration of 1.25 M. Insoluble material was removed by centrifugation at 20,000X g for 30 minutes at 4^{o}C. The supernatant was applied to a 70 ml Phenyl HP column equilibrated in 1.25 M ammonium sulfate in buffer A. The column was eluted with a one liter gradient to buffer A. Active fractions were concentrated in a centricon with a 100 kD nominal cutoff and the retentate applied to a Superdex 200 gel filtration column equilibrated in 20 mM MES, pH 6.5, 100 mM NaCl. Active fractions were pooled, diluted with an equal volume of water and applied to Mono S column equilibrated in 20 mM MES, pH 6.5, 20 mM NaCl. The column was eluted with a 25 column volume gradient to 300 mM NaCl in the same buffer.

2. Mass spectrometry

Gel slices were destained in 50% acetonitrile+25 mM AMBIC, crushed using a plastic pestle and dried. The dried gel was suspended in 25 mM AMBIC and digested with MSG-Trypsin (G-Biosciences, St. Louis, MO) at a ratio of 1:10 – 1:50 using a CEM Discover Microwave Digestor (Mathews, SC) at 55˚ C and maximum power of 60 watts

for 15minutes. Digested peptides were extracted using 50% Acetonitrile + 5% formic acid twice and lyophilized. The digested peptides were dissolved in 5% acetonitrile + 0.1% formic acid for LC/MS. LC/MS was performed using a Thermo Dionex Ultimate RSLC3000 operating in nano mode at 300 microliters/min with a gradient from 0.1% formic acid to 100% acetonitrile + 0.1% formic acid in 120 minutes. The trap column used was a Thermo Acclaim PepMap 100 (100 µm x 2 cm) and the analytical column was a Thermo Acclaim PepMap RSLC (75 µm x 15 cm). Xcalibur raw file was converted by Mascot Distiller into peaklists that were submitted to an in-house Mascot Server and searched against specific NCBI-NR protein databases.
(Experimental procedure of section II. i: Courtesy of William M. Brieher).

ii. Recombinant protein purification

Rosetta *E. coli* cells (EMD Millipore) were used for expressing recombinant proteins. Recombinant proteins were induced at room temperature and then purified according to manufacture's instructions (Qiagen, USA). Purification was undergoing native condition, except for ActA. In brief, the bacteria expressed His-tagged CRMP-1 was pelleted and lysed with lysozyme in lysis buffer (150 mM NaCl and 50 mM Tris, pH 8.0) in the presence of 2-mercaptoethanol and 0.2 mM PMSF. For His-tagged ActA, we used denaturing condition, in which 3 M guanidine hydrochloride was added to the lysis buffer. We applied the supernatant to Ni-NTA column. The column was then washed with lysis buffer and eluted with increasing concentrations of imidazole. The final eluted fraction was dialyzed against a different buffer according to the experimental need. Final elution of His-tagged ActA was dialyzed into 1 mM EGTA, 50 mM KCl, 1 mM $MgCl_2$, 10 mM Tris or Hepes, pH8.0).

iii. Endogenous protein purification

Arp2/3 complex was purified from calf thymus as described (Welch et al., 1997). Filamin was purified from chicken as described previously (Shizuta et al., 1976). Actin was purified from rabbit muscle; pyrene actin was prepared as described (Bryan and Coluccio, 1985).

III. Biochemical Assays

i. *Listeria* preincubation assays

1. Listeria 2-step preincubation assay

Listeria actin assembly reactions were performed in perfusion chambers as described previously (Brieher et al., 2004). Briefly, *Listeria* absorbed to glass coverslips in perfusion chambers were incubated for 5 minutes with brain cytosol, column fractions, or recombinant protein at concentrations listed in the main text (step 1, preincubation step). Chambers were washed three times with buffer A (1 mM EGTA, 50 mM KCl, 1 mM $MgCl_2$, 10 mM Tris, pH7.8). Chambers were then filled with a solution containing 100 nM Arp2/3 complex and 2 μM G-actin labeled with Oregon Green (10% labeled) (step 2, nucleation step). After 10 minutes, this solution was washed out of the chamber and actin cloud and comet tail assembly were imaged with a 20X (NA 0.7) objective attached to a 1,000 × 1,000 charge-coupled device camera (ORCA-ER; Hamamatsu Photonics) on a Zeiss AxioImager with the Colibri illumination system using Zeiss acquisition software (Carl Zeiss).

2. Listeria 3-step preincubation assay

The 3-step preincubation assay is similar to the 2-step assay described in the previous paragraphs with an additional step (step 3. Elongation/nucleation step). After step 2 (initial nucleation step), the chambers were washed three times with buffer A and then provided with solution with 2 μM G-actin. Different G-actin solutions was used in different steps in order to distinguish the actin built during each step.

ii. Immunodepletion of CRMP-1 and rescue experiments

Polyclonal rabbit anti-CRMP antibodies were raised against purified recombinant human CRMP-1. The CRMP-1 antiserum itself was specific and sufficient for all western blotting procedures. For immunodepletion experiments, however, the antibodies were affinity purified using recombinant CRMP-1 coupled to affi-10 according to the manufacturer's instructions (Bio-Rad, USA). The affinity purified antibodies were coupled to affi-10 beads at a ratio of 1 mg of protein to 1 ml of beads. For immunodepletion of CRMP-1 from brain cytosol, 100 μl of affinity purified anti-CRMP-1-antibody coated beads or beads coupled with non-immune rabbit IgG were added to

200 μl of brain cytosol and incubated at 4°C for one hour with constant tumbling. Beads were then pelleted by centrifugation. The supernatant was diluted 1:3 into buffer A supplemented with 0.2 mM ATP and with additional 62.5 nM Arp2/3 complex and 2 μM 25% fluorophore-labeled actin. This mixture was applied to a perfusion chamber, containing *L. monocytogenes,* for 5 minutes at room temperature. In rescue experiments, recombinant CRMP was added to the same amount as endogenous CRMP-1 (0.01 mg/mL), which was determined by western blot, into the perfusion chamber to preincubate with *Listeria*. Comet tail assembly was analyzed by fluorescence imaging using a 63× objective lens (NA 1.4) under a Hamamatsu camera described above. The number of *Listeria* with actin tail and actin tail length were quantified using Fiji software (Schindelin et al., 2012). Depletion of CRMP-1 was confirmed by western blotting.

iii. In vitro actin assembly assays

1. Pyrene actin polymerization assay

Actin polymerization was monitored by the increase in fluorescence of pyrenyl-actin with excitation at 365 nm and emission at 410 nm. The reaction contains 2.5 uM actin (25% pyrene-labeled) and different protein mixture in buffer B (1 mM EGTA, 50 mM KCl, 1 mM $MgCl_2$, 10 mM imidazole, pH7.0) with 2 mM ATP. We used 25 nM or 50 nM Arp2/3. The concentration of other proteins used was indicated in the figures.

2. Actin assembly on the purified membrane

Actin assembly and immunofluorescence of purified rat liver membrane were proceeded as following: described before . In brief, the lyophilized rat liver membrane was resuspended in buffer A at 4 °C for 30 minutes. Potassium chloride was added into the buffer to a final concentration of 500 mM. The membranes were incubated in this high salt condition for 30 minutes on ice, then were centrifuged at 10,000 g for 30 minutes. The pellet was reserved and resuspened in buffer with 2 mM ATP. To test actin polymerization on the salt-stripped membrane, 0.5 μM fluorescently labeled actin, 1 μM recombinant alpha-actininin-4 and 5 μL preimmune serum were incubated with membrane and incubate for 10 minutes at room temp. In parallel, preimmune serum was replaced with 5 μL purified anti-CRMP-1 antibodies. For immunofluorescence of membranes, homemade polyclonal alpha-actinin-4 antibodies and E-cadherin antibodies

(DECMA-1; sc-59778) (Santa Cruz Biotech) were used as primary antibodies followed with a secondary antibody conjugated with fluorophore (Life Technologies).

iv. Filament branching assay

Pre-polymerized filaments were first prepared by incubating 2.5 μM Alexa-Fluor 647-labeled actin (10% labeled) in buffer B for 30 minutes at room temperature. These filaments were then diluted 10 fold into solutions containing 2.5 μM Alexa-Fluor 647-labeled G-actin with or without 0.6 μM Arp2/3, 0.4 μM ActA, and/or 0.125 μM CRMP-1, for 10 minutes. The filaments from this reaction were then diluted 1:50 into Buffer B with 15 mM glucose, 20 μg/ml catalase, 100 μg/ml glucose oxidase, and 1 mM TROLOX, then immediately applied into the chambers which had been pre-coated with 40 μg/mL filamin. Filaments were allowed to attach to the chamber for 10 minutes then detected by fluorescence imaging using a 63× objective lens as described above.

v. F-actin co-sedimentation

Four sets of co-sedimentation experiments were conducted. Two sets used CRMP-1 concentrations of 0.125 μM, 0.25 μM, 0.5 μM, 0.75 μM, and 2.5 μM. Two other sets used CRMP-1 concentrations of 0.75 μM, 1.25 μM, 2.5 μM, and 4 μM. Actin was provided at constant 2 μM with various concentration of CRMP-1 in different tubes. Actin was polymerized at 4^{o}C overnight in buffer B and 2mM ATP in the absence or presence of various concentrations of CRMP-1. The tubes were then centrifuged in a Beckman TLA 100 rotor at 350,000 × *g* (*k* factor, 8.1) for 20 min at 4 °C to separate supernatant and pellet fractions. The fractions were separated using SDS-PAGE. The gel was stained with coomassie blue and analyzed using Fiji software. Curve fitting was done using OriginLab software.

vi. Protein interaction assays

1. ActA and CRMP-1 interaction

The affinity of ActA for CRMP-1 was determined using the approach described by Pollard (Pollard, 2010). Recombinant ActA was immobilized onto affi-10 gel (Bio-Rad, USA) according to manufacturer's manual. Briefly, after the affi-10 gel was activated, recombinant ActA protein was added to the gel solution containing 50 mM KCl, 1 mM

$MgCl_2$, and 10 mM Hepes, pH7.8. ActA was allowed to couple onto the gel overnight at 4 °C. The final coupling density was 1.5 mg of ActA per ml of gel. The gel was blocked in casein solution for 30 minutes then washed with buffer A before use. The control gel was only coated in casein.

Twelve point five μL of the ActA-coated gel was used to incubate with various concentration of CRMP-1 to final volume of 112.5 μL. For control reactions, the blank gel was used. After an hour of incubation at 4 °C, the gel was pelleted using centrifugation. The supernatant was carefully separated from the gel, separated on SDS-PAGE followed by western blotting using our custom polyclonal antisera (not affinity purified) against CRMP-1. HRP-conjugated secondary antibodies (Bio-Rad, catalog number: 1706515) and chemiluminscence were used to visualize the amount of CRMP-1 in the supernatants by exposing the blots to autoradiography film. Multiple exposures were obtained to ensure the signals were in the linear range. The amount of CRMP-1 bound to ActA was determined by subtracting the total amount of CRMP-1 in the control condition from the amount of CRMP-1 left in the supernatant. This approach permitted the estimation of binding affinity from the concentration of CRMP-1 required for half-maximal binding to ActA beads. The results from 3 independent western blotting were analyzed using Fiji software and the curve was fitted using OriginLab software.

2. CRMP-1 and EVL interaction

His-tagged CRMP-1 and MBP-tagged EVL were used for the interaction assay. Recombinant MBP-EVL was immobilized onto 0.5 micron carboxylated polystyrene beads (Bangs Laboratoris Inc., Fishers, Indiana) using two-step coupling of protein through EDC and Sulfo-NHS according to manufacturer's manual (Thermo Fisher Scientific, Waltham, MA). Briefly, after the beads were activated, recombinant MBP-EVL was added to the solution containing 500 mM NaCl, 100 mM MES, pH6.0. MBP-EVL was allowed to couple onto the beads 30 minutes at room temperature. For the control condition, control gel was coated with MBP-tag peptide. The reaction was terminated with 2-mercaptoethanol. The final coupling density was 1 mg of protein per ml of beads.

Fifty μL of the beads was used to incubate with 200 μL of 1 mg/mL CRMP-1. After an hour of incubation at 4 °C, the gel was pelleted using centrifugation. The beads were

then fixed with formaldehyde for 20 minutes. After washing twice with PBS buffer, the gels were probed with anti-CRMP-1 antibodies follow with secondary antibody conjugated with fluorophore (Life Technologies). Centrifugation was used in between each step in order to remove unbound materials from the previous step.

IV. Tissue Cultured Cells and Imaging

i. Cell line

Madin-Darby Canine Kidney II cells (MDCK) and HEK 293 were used for the experiments. The cells were cultured at 37ºC under 5% CO2 in Dulbecco's Modified Eagle's Medium with 5% FBS. MDCK cells were used to carry all the experiments; except for expressing Sema3A, HEK 293 cells were used. Transfection was carried using calcium phosphate precipitation. Western blotting was used to validate the knockdown efficiency. For western blotting, we used Bradford assay (Bio-Rad) to verify that the same amount of sample from different condition was provided for each lane. All the cells were plated on coverslips coated with collagen and analyzed within 96 hours after transfection.

ii. Calcium switch assay

The cells were plated on collagen coated coverslip with a concentration that would allow the cells to reach confluency in 2 days. The calcium switch experiment were done on the 3rd day of the confluency. Confluent monolayers were first washed PBS with 2 mM $MgCl_2$, then were incubated in PBS with 2 mM $MgCl_2$ and 4 mM EGTA for 30 minutes in the tissue culture incubator. For cells to recover and reform cell-cell junction, the PBS buffer was removed and regular media with 5% FBS were added. Cells were fixed at different time point followed with immunostaining procedures in order to detect actin and E-cadherin signals.

iii. Fixation and staining

To probe the desired proteins and actin structures, various fixation procedure were used. For single spreading cells, formaldehyde fixation and TCA fixation were used. In formaldehyde fixation, the cells were fixed with 1% formaldehyde, permeabilized with

0.2% Triton X-100, and followed with immunostaining and phalloidin statining. For immunostaining, cells were probed with primary antibodies for one hour. After the primary antibodies, the cells were washed three times with PBS and then provided secondary antibodies conjugated with fluorophore. After proper wash to remove residual antibodies, phalloidin actin were added to staining F-actin. All the antibodies and phalloidin were diluted into PBS according to manufacturers' manual. For TCA fixation, 10% TCA were used. For detecting proteins in a monolayer, extraction and fixation procedures were adopted from Takenawa group (Yamazaki et al., 2007). The cells were first extracted in the presence of 2 μM phalloidin. Next, primary antiboides were added prior to formaldehyde fixation. The fixation reaction was quenched with 50 mM Tris in the absence of detergent. Secondary antibodies conjugated with fluorophore were provided in the last step. For staining microtubule, methanol fixation was used. In brief, the cells were treated with -20ºC methanol for 5 minutes. After 3 times of PBS washes, the cells were permeabilized with 0.1% Triton X-100 at room temperature for 30 minutes. Primary (anti-tubulin antibodies, Sigma) and secondary antibodies conjugated with fluorophore were provided afterwards. Fluorescence images were collected by 63x objective attached to a 1,000 × 1,000 charge-coupled device camera (ORCA-ER; Hamamatsu Photonics) on a Zeiss AsioImager with the Colibri illumination system under Zeiss acquisition software (Carl Zeiss).

iv. Hanging drop adhesion assays

This assay was performed as described by Nelson group with some modifications (Ehrlich et al., 2002). In brief, cells were allowed to grow in a 10 cm dish for 2 days. Cells were trypsinized, centrifuged and resuspended in the media at 1.2 * 106 cells/ml. Twenty microliter drops of cell suspension were pipetted on the inside surface of 6 cm culture dish lids. At the bottom of the dish, 5 mL of media was provided to prevent evaporation. At each time point, two individual drops will be used and quantified. Each drop has five microliter of suspension spread directly on the glass slide, as the sample before trituration. Another five microliter of suspenstion was taken out from each drop, triturated ten times with a 20 microliter pipet before putting down on a glass slide. At least 3 random fields from each drop were photographed under Zeiss 20x objective. The

number of the cells and the size of clusters were determined. Note that same amount of cells were quantified in different conditions.

v. Cell spreading experiment

For cell spreading experiment, freshly trypsinized MDCK II cells were plated on glass coverslips which were coated 0.5 μg/mL Type I collagen (BD Bioscience). Cells were allowed to spread for 1 hour, then were fixed with 1% formaldehyde, permeabilized with 0.2% Triton X-100, and followed with immunostaining. For Arp2/3 inhibitor experiments, 100 nM CK-636 and 100 nM CK-548 (Nolen et al., 2009) were added into the medium during the 1 hour spreading time.

vi. Wound healing experiment and live cell imaging

For detecting lamellipodia formation in response to wounding, a sharpened needle was used to wound a confluent MDCK II monolayer grew on collagen-coated coverslip. The monolayers were then allowed to recover in MEM with 5% FBS for one hour before immunostaining, or 5 minutes before collecting live cell images. Immunostaining of endogenous CRMP-1 was performed using the primary antibodies we generated, followed by secondary antibody conjugated with fluorophore (Life Technologies) at 1:200 dilution in PBS for 1 hr. Alexa Fluor 647 Phalloidin (Life Technologies) was applied at the last step to stain for F-actin. Immunostaining of p34 subunit of Arp2/3 complex was using the protocol described before (Yamazaki et al., 2007), with commercial polyclonal anti-rabbit antibody purchased from Millipore. Fluorescence images were collected under 63x objective as described before. Cell protrusive activity under wound healing condition were imaged at 24.5 ^{o}C. DIC images were acquired every 5 seconds for a total of 5 minutes using 40× objective lens (NA 0.7) under a Hamamatsu camera described above.

V. Data analysis

Data analysis of the results was carried out with Fiji software. Quantification results for the purified membrane and the tissue cultured cells, except live cell imagining, are mean ± s.d., from 3 repeats of the experiment. Quantifications for live cell imaging were analyzed with n=13. * $p<0.05$. ** $p<0.01$. For measuring actin intensity on purified

membrane, we manually outline the edge and divided the value with the size of the outline area. For quantifying high-intensity puncta on the purified membrane, the puncta were circled with radius of 0.5 μm and the intensity were calculated. For measuring protein intensity at cell-cell contact or at the leading edge, we manually outlined the leading edge of protrusive structure. Average intensity value was the value of total intensity of the line drawn divided by the length of the line. To compare the amount of different proteins, the raw value was ratio to scramble or wildtype sample. For live cell image, tacking plug-in under Fiji was used to track the trajectory of the leading edge, in which the middle of the leading edge was followed.

CHAPTER 3: RESULTS

I. CRMP-1 contributes to *Listeria* Actin Tail Formation

i. Identification of CRMP-1 as a new factor for *Listeria* actin tail formation

Previous research implied that there are uncharacterized factors in the cytosol that could help *Listeria* actin tail formation. We were interested in finding those factors; more specifically, we wanted to identify the factors that can enhance the initiation of the *Listeria* actin tail. To pursue this goal, we set up a two-step preincubation assay which allowed us to visualize and compare actin polymerization under different conditions (Fig. 1 A). In this assay, we pre-coated *Listeria* in a perfusion chamber. Brain cytosol was later applied into the chamber followed by a buffer wash to remove any unbound materials. A new solution containing Arp2/3 and fluorescently labeled actin was later introduced into the chamber; actin cloud formation was scored by fluorescence imaging. Under this experimental design, we focused on screening the factors that are able to associate tightly with the *Listeria* surface, and have contribution to actin assembly. We observed a greater fraction of *Listeria* preincubated with brain cytosol formed actin clouds than *Listeria* preincubated with buffer alone, confirming there are such desired factors in the brain cytosol.

In order to further purify those factors, we used conventional chromatography to fraction the cytosol. The activity of the individual fraction for enhancing actin cloud formation was then tested with the two-step preincubation assay described above. Only the active fractions were then being applied to the next column. After serial fractionation and activity test, the final active fraction contained two bands of approximately 65 kilodaltons (Fig. 1 B). Mass spectrometry result indicates both of the bands are Collapsin Response Mediator Protein-1 (CRMP-1) (Fig. 1 C).

ii. CRMP-1 is essential for *Listeria* Actin Tail Formation

Since there has been no prior research demonstrating CRMP-1 as part of the actin cytoskeleton network, we first wanted to confirm that we had purified the right factor. We expressed and purified recombinant His-tagged human CRMP-1 in the *E. coli* (Fig. 2

A). The recombinant protein was then used in the same two-step preincubation assay in order to verify its ability to enhance actin assembly. The CRMP-1 preincubation condition showed more actin cloud formation at a fixed time point compared to the control (Fig. 2 B). When we changed the procedure and provide CRMP-1 in the solution with Arp2/3 (rather than preincubated CRMP-1 with the bacteria), we still detected longer actin tails compared to the condition without CRMP-1 (Fig. 3). Therefore, CRMP-1 is a new factor that can enhance actin assembly on *Listeria*. Quantification demonstrated that CRMP-1 provides a dose-dependent effect on actin cloud formation (Fig. 2 C). Using an equal concentration of Arp2/3, 80% more Listeria formed a detectable actin cloud when preincubated with 0.5 μM CRMP-1.

Next, we wanted to assess the importance of CRMP-1 for *Listeria* actin tail formation. I performed an immunodepletion assay using the rabbit polyclonal antibodies our lab generated and successfully depleted 50-70% of endogenous CRMP-1 (Fig. 4 A). CRMP-1 depleted cytosol resulted in fewer and shorter actin comet tails (Fig. 4 B and C). These defects can be rescued by preincubating the *Listeria* with the recombinant CRMP-1. CRMP-1 therefore has an important role for *Listeria* actin tail formation.

We noticed that while preincubation of CRMP-1 can fully rescue the number of bacteria with detectable actin clouds, this rescue procedure can only partially rescue the tail length. *Listeria* actin tail growth is a complex procedure involving in different actin-binding proteins. This result might indicate that while Arp2/3 is essential for initiation of comet tail assembly, actin comet tail elongation might be independent of frequent Arp2/3 mediated actin nucleation reactions. Arp2/3 independent comet tail elongation has been seen before under certain experimental conditions (Brieher et al., 2004). Arp2/3 independent comet tail elongation requires the preincubation of the bacteria with brain cytosol. After the preincubation step, Arp2/3 was then provided to the reaction in order to initiate comet tail assembly. Brieher and colleagues showed that this comet tail will continue grow as long as fascin, an actin bundling protein, was provided to the reaction. The growing of the tail at this stage is Arp2/3-independent. They suspected there were factors bound to the bacterial surface that permit elongation of the tail in the presence of fascin. Yet we still do not know what those factors are. Brieher and colleagues tested if EVL or VASP alone accounted for the elongation activity. EVL is a known *Listeria*-

binding and actin-binding protein that contributes to actin tail formation (Laurent et al., 1999). Preincubating the *Listeria* with EVL or its related homolog alone cannot effectively support actin tail growth in the absence of Arp2/3 (Brieher et al., 2004). Neither can CRMP-1 or the mixture of CRMP-1 plus EVL (Fig. 5). It is possible that CRMP-1 somehow also contribute to the tail elongation in an Arp2/3 independent fashion. Adding back recombinant CRMP-1 cannot rescue the tail length is due to the activity of the recombinant CRMP-1 is not comparable with the endogenous CRMP-1. This possibility will be discussed further in the following paragraph.

We noticed that a higher amount of recombinant CRMP-1 was required to boost actin formation under defined conditions (Fig. 2 C) than in the rescue experiment (Fig. 4). Half maximal induction of actin cloud formation under defined conditions with CRMP-1 and Arp2/3 alone required 100 μg/ml of CRMP-1 while rescuing CRMP-1 depleted extracts only required 10 μg/ml CRMP-1. These differences open the possibility that either post translational modifications or additional cytosolic factors work in conjunction with CRMP-1 to further activate it to stimulate Arp2/3-dependent actin nucleation. CRMP-1 antibodies might pull down not only CRMP-1 but also CRMP-1-associated proteins. Those associated proteins might contribute to *Listeria* actin tail formation as well. One data to support this idea is the observation that recombinant CRMP-1 displays a higher buoyant density after incubating with cytosol for one hour (Fig. 6). Another possibility would be that endogenous CRMP-1 interacts with other CRMP family proteins to form hetero-oligomers (Wang and Strittmatter, 1997), which might result in the formation of a more potent activator of the Arp2/3 complex. Therefore, adding back recombinant CRMP-1 alone could not fully compensate for the loss of other proteins, which leads to less efficient tail formation. In aggregate, the results demonstrated that CRMP-1 is a novel factor for Arp2/3-mediated *Listeria* actin cloud and comet tail formation.

iii. CRMP-1 and CRMP family proteins facilitate Arp2/3-dependent assembly

We want to know the underlying mechanism CRMP-1 uses in this *Listeria* system. The purification procedures we used to identify CRMP-1 implies that it binds to the *Listeria* surface. Researches have shown that ActA is the only protein contributed by

Listeria to the actin assembly reaction (Domann et al., 1992; Kocks et al., 1992; Kocks et al., 1995; Pistor et al., 1994; Smith et al., 1995). CRMP-1 is therefore likely to bind to ActA. I tested this possibility using recombinant ActA and recombinant CRMP-1. ActA-coated beads were incubated with solutions containing various concentrations of CRMP-1. After an incubation period, the beads were pelleted, and the amount of CRMP-1 remaining in solution was quantified by Western blotting. This method is a simple approach suggested by Pollard to obtain the dissociation constant for a protein-protein interaction (Pollard, 2010). Using this method, I found that CRMP-1 binds to ActA-coated beads, with an affinity of 2.5 μM (Fig. 7 A & B).

To test whether CRMP-1 enhances ActA function, we performed pyrene-actin polymerization assays. In this assay, I conjugated pyrene to actin at cysteine residue 374, a residue that is located at the interacting interface between two actin molecules in the filament. This pyrene compound is sensitive to the solution environment. When the pyrene dye is in a hydrophilic environment, which occurs when the actin is in its monomeric state, pyrene fluoresce is quenched. However, when the pyrene compound is buried inside the actin polymer (hydrophobic environment), the fluorescence is no longer quenched and the signal can be detected by a fluorometer. This is a classic approach for monitoring actin polymerization over time.

We did not detect any stimulation of actin assembly by CRMP-1 alone or CRMP-1 in conjunction with ActA (Fig. 7 C). Nor could we detect direct activation of Arp2/3 by CRMP-1 alone (Fig. 7 D). CRMP-1 itself is therefore not a nucleator nor a classic NPF capable of activating Arp2/3 directly. CRMP-1, however, facilitated ActA-activated, Arp2/3-dependent polymerization in a dose-dependent manner (Fig. 7 F). Similar effects can be detected by other CRMP family members. I expressed recombinant CRMPs and DHPase (Figure 8A) and repeated the pyrene assay. The results showed that different CRMPs seem to be able to facilitate this reaction to different extents (Fig. 8 B-D). For example, CRMP-3 seemed to be the most potent for ActA-Arp2/3 reacrion (Figure 8C). We also detected a slight increase in the rate of ActA-Arp2/3 polymerization in the presence of increasing amounts of DHPase (Fig. 8 D). These results reveal that: 1) CRMP family proteins are new factors that contribute to *Listeria* actin comet tail assembly; 2) CRMP family proteins can bind ActA and enhance its ability to activate the Arp2/3

complex; 3) other CRMP family members can contribute to ActA-Arp2/3 dependent actin assembly but they might not be equally potent. The difference is possibly coming from the intrinsic sequence difference among different CRMPs. Further studies are required to verify how CRMP family members contribute differently to Arp2/3 mediated actin assembly.

iv. CRMP-1 increases Arp2/3-dependent branching

Arp2/3 produces branched actin filaments, yet not all Arp2/3 activators increase the density of filament branches (Goley and Welch, 2006; Wagner et al., 2013). To determine whether CRMP-1 increases Arp2/3 dependent branching, I imaged single actin filaments to compare the density of filament branches in the presence of ActA and Arp2/3 alone to that in the presence of added CRMP-1. Our results indicated a greater number of branches in the presence of CRMP-1 than in its absence (Fig. 9 A & B). Many factors that facilitate Arp2/3-dependent actin nucleation and branching are also able to bind to F-actin (Goley and Welch, 2006; Huang et al., 1997). Previous work has shown that CRMP-4, a member of the CRMP family proteins, can bind to F-actin (Rosslenbroich et al., 2005). We used cosedimentation to show that CRMP-1 can also bind F-actin with an apparent affinity of 0.7 μM (Fig. 9 C). CRMP-1 is therefore an F-actin binding protein that is capable of increasing Arp2/3 dependent actin nucleation and Arp2/3 dependent actin filament branching.

II. Localization and Functional Study of CRMP-1 at Cadherin-Mediated Adherens Junction in MDCK Cells

i. CRMP-1 locates at cadherin-mediated cell-cell contacts

To understand the potential role of CRMP-1 in regulating actin dynamics mammalian cells, we first detected the localization of CRMP-1 inside the mammalian cells. Our first goal is to see if CRMP-1 localizes to any actin related structures. We chose to use epithelial MDCK cell since it can form various kinds of actin-dependent structures. MDCK cells can form a structurally and functionally polarized monolayer which has actin filaments distributed at different locations: microvilli at the apical surface, cell-cell interactions at the lateral surface, and cell-substrate interaction at the basal

surface. Among them, research has been interested in understanding the mechanisms that drive the formation of cell-cell contacts, since cell-cell adhesion is an essential determinant in the development of the polarized epithelial sheets.

When we used the CRMP-1 antibodies to perform immunostaining in MDCK monolayers, we detected CRMP-1 at the cell boundary where two cells contact. The CRMP-1 signal overlaps with E-cadherin and actin signal at cell-cell contacts (Fig. 10 A). This localization of CRMP-1 can be observed in the monolayers of different ages: the young monolayer (the 1st day of reaching confluency), the mold monolayer (the 6th day) (Fig. 10 A) and the mid-age monolayer (2nd-3rd day of confluency) (Fig 10 B). Close inspection of CRMP-1, E-cadherin and actin signals along the cell-cell contact reveals that the majority of CRMP-1 signal overlaps with cadherin signals at cell-cell contacts (Fig. 10 B & C). Yet some area (~15-20%) contains CRMP-1 signal without cadherin signals, and vice versa (Fig. 10 C & D). In contrast, every spots that contain CRMP-1 signal show actin signal (Fig. 10 C). Our result demonstrates that CRMP-1 not only localizes to cell-cell contact, but also highly associates with actin filaments at this location.

ii. CRMP-1 is recruited to cell-cell contact at the early stage of the contact re-formation

We wanted to decipher the role of CRMP-1 at this cellular localization. Since CRMP-1 has been shown to facilitate actin polymerization for the *Listeria* actin tail, we speculated CRMP-1 might undergoes a similar mechanism inside the cell. In order to mediate the stabilization of newly formed contact, actin polymerization occurs at adherens junction once two cells contact each other (Vasioukhin et al., 2000). CRMP-1 might have a role in facilitating actin assembly during this process. To test our hypothesis, we first need to know if CRMP-1 contributes to the initiation of cadherin contact zone extension. We used a calcium switch assay to detect the distribution of CRMP-1 and E-cadherin in response to the chelation of extracellular calcium in confluent monolayers of the MDCK cells. Extensive cadherin-based cell-cell contacts were observed before chelating reagent was provided, with CRMP-1 signal locating at the adherens junction (Fig. 11 A, untreated). In the presence of the chelating reagent EGTA, cell-cell contacts were destroyed as expected. Both cadherin and CRMP-1 signals were excluded from the

cellular peripheries (Fig. 11, 0 min). Removal of the chelating reagent induced a rapid recruitment of CRMP-1 to cellular periphery where the two cells meet. While E-cadherin seemed to distribute to cell-cell contact simultaneously with CRMP-1, some contact zones showing CRMP-1 signal contained no E-cadherin signal (Fig. 11, 15 min, yellow arrowhead). At 30 minutes after removal of chelating reagent, both CRMP-1 and E-cadherin signals form a solid line along cell-cell contacts (Fig. 11, 30 min). These results support our hypothesis that CRMP-1 might have a role at the initial stage of junction formation. In addition, the early arrival of CRMP-1 at the new contacts implies that CRMP-1 might help the recruitment of cadherin to the junction, which will be discussed later.

iii. Depletion of CRMP-1 reduces cadherin and F-actin amount at the apical junction

CRMP-1 can facilitate Arp2/3 dependent assembly of *Listeria* actin comet tails. To address if CRMP-1 is also a regulator for actin filament polymerization at cell-cell contacts, we examine the change of the amount of junctional actin in the presence or absence of endogenous CRMP-1. Our first approach was to use phalloidin staining to compare the amount of F-actin in wildtype and CRMP-1 knockdown MDCK monolayers. While using shRNA to deplete CRMP-1 amount inside the cells, we detected a 50% loss of F-actin at the apical region of the cell-cell contacts (Fig. 12 A & B). Surprisingly, the amount of cortical actin (F-actin in the middle of the cell) at the same focal plan was greatly reduced as well. Quantification of the result indicates that depletion of CRMP-1 causes more than 80% loss of the cortical actin intensity at the apical surface (Fig. 12 C). CRMP-1 is therefore important for the global accumulation of F-actin inside the cell. This result suggests that CRMP-1 might modulate actin polymerization in the mammalian cells, as its role in *Listeria monocytogenes* actin tail.

iv. Reduced stress fiber was detected in the CRMP-1 knockdown cells

The reduction in F-actin intensity after phalloidin-staining can also be detected at the basal surface. Wild-type MDCK cells form stress fibers that contribute to focal adhesion assembly that attach cells to the extracellular matrix. We detected a dramatic loss of stress fibers in the basal area of CRMP-1 knockdown cells (Fig. 13 A). While measuring

the actin intensity along the detectable fibers, more than half of the F-actin was lost when CRMP-1 is depleted (Fig. 13 B). While the width of the stress fibers did not seem to change much between scramble and CRMP-1-depleted cells (Fig. 13 C), other morphological characteristics seem to be different. Under fluorescence microscope, each individual stress fiber was displayed as a line composed by many higher-intensity dots. Those dots locate in close proximity to one another (Fig. 13 A, stars). However, those dots are more distant from one another in the CRMP-1 knockdown cells. The formation of the stress fiber in the MDCK cells is not yet clear if it is downstream of Arp2/3 complex or downstream of other cellular nucleator, such as formin. Our initial data here showed that CRMP-1 might regulate basal actin accumulation and the integrity of stress fibers. Further study is required to test whether CRMP-1 has a direct effect on either Arp2/3 or formin mediated assembly of actin stress fibers. It is also possible that the changes in stress fibers we detected here are a downstream consequence of the massive changes in apical actin and cell-cell adhesion. The works from different groups have mentioned a significant crosstalk between apical cadherins and basal integrins. Purturbing the cytoskeleton of one location affects the cytoskeleton of the other locarion (Silvestre et al., 2009; Weber et al., 2011).

v. CRMP-1 knockdown cells share similar many attributes with the Arp2/3 knockdown MDCK cells

In *Listeria* actin comet tails, actin polymerization depends on the Arp2/3 complex. Inside the cell, Arp2/3 complex is also known to be the essential nucleator for the de novo actin polymerization. At cadherin mediated contacts, Arp2/3 activity is essential to efficiently generate actin filaments (Verma et al., 2004). We wondered if the global loss of actin in CRMP-1 knockdown cell can be explained by the change in Arp2/3 activity. We especially interested in the role of CRMP-1 at adherens junctions, since the mechanism of how and what are the regulatory components involved in this Arp2/3 dependent process remain unclear. To test the possibility that CRMP-1 and Arp2/3 contribute to the same pathway, we generated different knockdown cell lines to detect if they share similar morphology. We made two kinds of Arp2/3 knockdown cell lines in parallel with CRMP-1 knockdown cells. We used shRNAs to target Arp3 or p34 subunits of the Arp2/3 complex individually, and stained for phalloidin in confluent monolayers

(Fig. 12 A). The efficiency of our knockdown approaches was verified by immunoblotting of cell extracts (Fig. 12 E). Similar to the results we observed in CRMP-1 knockdown cells, both of the Arp2/3 knockdown cell lines showed loss of F-actin at the junction and in the cortical region. In addition, knockdown of these three different genes (CRMP-1, p34 and Arp3) leads to the same morphology: the apical surface area is enlarged (Fig. 12 D). Therefore, CRMP-1 and Arp2/3 might function in the same pathway to regulate actin polymerization in the MDCK cells and cell morphology. Note that other groups showed that the disturbing the function cortactin, a weak Arp2/3 activator, also caused morphology change in MDCK cells. Those cortactin mutant cells displayed irregular outline; they lost the regular cubical shape of MDCK cell (Han et al., 2014). Our CRMP-1 or Arp2/3 knockdown cells, however, remain the cobblestone shape, even though become flat in z-axis and enlarged in x-y axis.

vi. Arp2/3 might be less active under the CRMP-1-knockdown background

We wonder if there is a decrease in the Arp2/3 amount at the junction under CRMP-1 depleted background. Our speculation came from the observation that 1) the junctional actin amount reduced in CRMP-1 knockdown cells; and 2) CRMP-1 knockdown cells showed similar phenotypes as Arp2/3 knockdowns. To answer this question, we quantified the intensity of Arp2/3 at the junctions. Immunostaining result showed that CRMP-1 knockdown indeed resulted in less accumulation of Arp2/3 at cell-cell contacts (Fig. 14 A). We also observed a decrease of alpha-actinin-4 at this cellular location after CRMP-1 is depleted (Fig. 14 B). Previous study from the lab showed that alpha-actinin-4, an actin-binding protein, has a critical role for Arp2/3-dependent actin assembly at the adherens junction. It is not yet known how alpha-actinin-4 is recruited to the junction. Our result here shows that CRMP-1 might contribute to Arp2/3 recruitment to the junction. The recruitment of alpha-actinin-4 to adherens junction might also be downstream of CRMP-1 function.

More interestingly, even though the amount of Arp2/3 and alpha-actinin-4 both reduced ~40% in the CRMP-1 knockdown cells (Fig. 14 A & B), they show different attributes while comparing their correlation with junctional actin amount (Fig. 14 C & D). Despite that junctional alpha-actinin-4 is reduced in CRMP-1 depleted cells, its correlation to the amount of junctional actin does not change compared to the scramble

condition (Fig. 14 D). In other words, the number of alpha-actinin-4 per actin remains the same in scramble and CRMP-1 depleted cells. This statistic result tell us that the loss of the junctional actin under CRMP-1 depleted condition was probably not due to less alpha-actinin-4 at the loci. In contrast, the correlation between Arp2/3 and junctional actin decreased almost half-fold when CRMP-1 is depleted (Fig. 14 C). The same amount of Arp2/3 in the scramble cells could generate more F-actin. In other words, in order to generate the same amount of junctional actin as wildtype, CRMP-1 knockdown cells would need to recruit more Arp2/3 complex. Arp2/3 complex might be less active without CRMP-1.

vii. CRMP-1 highly associates with cadherin-enriched membrane fraction and contributes to de novo Arp2/3 polymerization in the purified liver membrane system

To better understand if CRMP-1 regulates the amount of F-actin through modulating actin polymerization in mammalian cells, we compared the efficiency of actin polymerization under different conditions using an in vitro membrane system. This membrane was obtained after various homogenizing-buffer washes followed with a serious centrifugation. This procedure allowed us to purify a membrane fraction that is enriched in the adherens junctional complex and is able to perform actin polymerization in an Arp2/3 dependent manner. It has been shown previously that actin polymerization initiates as 0.5-micron dots on this membrane at the loci where junctional proteins and Arp2/3 exist (Tang and Brieher, 2012). With this purified membrane, we can in vitro dissect the components involved in the actin assembly at cadherin-junctional-complex-enriched foci by extracting different factors off the membrane with different solutions. This membrane system also allows us to biochemically reconstitute Arp2/3 dependent actin polymerization by adding back the extractable factors to restore actin assembly.

For example, high-salt treatment on the purified membrane attenuates actin polymerization because essential components for actin assembly were no longer remain on the membrane fraction. It has been shown that adding back alpha-actinin-4 could rescue Arp2/3-dependent polymerization on high-salt stripped membrane. Alpha-actinin-4, a salt-extractable factor, is therefore required for Arp2/3-dependent actin assembly at the junctional complex foci (Tang and Brieher, 2012). Unlike alpha-actininin-4, which

would be stripped off membrane at high-salt condition, a large portion of CRMP-1 remains on the membrane fraction after high-salt treatment (Fig. 15 A). In fact, CRMP-1 could still associate with membrane fraction after sequential high-salt and detergent wash. This implies that CRMP-1 might strongly associate with adherens-complex to help maintain the integrity of junctional complex and/or to regulate the Arp2/3-dependent actin polymerization at cadherin adhesive sites.

To characterize the contribution of CRMP-1 on actin assembly on a molecular basis, we manipulated the activity of the membrane-bound CRMP-1 using CRMP-1 antibodies. These same antibodies have been used to perform immunodepletion experiments before (Fig. 4). We wished to use these antibodies to block the activity of the remaining CRMP-1 on the high-salt stripped membrane. We provided CRMP-1 antibodies and alpha-actinin-4 in the preincubation step. After the preincubation, we compared the efficiency of actin polymerization on the antibody-treated membrane (experimental condition, labeled as CRMP-1 Ab in Fig 15) with preimmune serum-treated membrane (control condition). Alpha-actinin-4 was added because alpha-actinin-4 is required to restore the assembly reaction on the stripped membrane. CRMP-1 antibodies did not affect the binding of alpha-actinin-4 to the membrane (Fig. 15 B); therefore we could rule out the possibility that any change in actin polymerization is due to the lack of alpha-actinin-4 on the membrane. The condition that the membrane was preincubated with CRMP-1 antibodies (experimental condition), even in the presence of alpha-actinin-4, showed attenuation on the formation of Arp2/3-depedent actin polymerization (Fig. 15 C). Arp2/3 dependent actin polymerization would result in high-intensity actin puncta on the membrane. The number of those puncta decreased in the experimental condition (Fig. 15 D). Even though we sometimes observed the 0.5-micron foci on the membranes under the experimental condition, the actin intensity on those foci was relatively lower than the ones under the control condition (Fig. 15 D). Therefore, blocking CRMP-1 directly affects the efficiency of Arp2/3-dependent actin assembly on this in vitro purified membrane system. CRMP-1 is hence a new factor that directly regulates Arp2/3 dependent polymerization at adherens junction.

viii. CRMP-1, rather than using VCA fragment of WAVE, works with EVL to activate Arp2/3 complex

Next, we examined through what mechanism CRMP-1 uses to modulate actin assembly on adherens junction. The molecular basis of CRMP-1 on actin assembly has been characterized in the *Listeria* system: CRMP-1 facilitates ActA-mediated Arp2/3 polymerization. *Listeria* uses ActA protein as a NPF to recruit and activate the Arp2/3 around the bacteria surface. Even though there is no known ActA homolog in the mammalian cells, VCA region of mammalian NPFs has been long considered functionally comparable to *Listeria* ActA (Zalevsky et al., 2001). ActA and VCA share many attributes, including binding and activating the Arp2/3 complex, and binding monomeric actin. At cadherin mediated junction, it has been shown that WAVE-2, a VCA-containing protein, serves as the essential activator for Arp2/3 complex (Verma et al., 2012). A small portion of WAVE-2 remains on our purified membrane after high-salt extraction (Fig. 15 A). It is possible that CRMP-1 collaborates WAVE-2 at cadherin-mediated contacts to control Arp2/3 dependent polymerization. CRMP-1 might function with the known NPF in mammalian cell, just as the mechanism it uses in the *Listeria* system.

We hence test if CRMP-1 can facilitate Arp2/3 polymerization in the presence of VCA peptide, the essential region of WAVE to bind and activate Arp2/3 complex. To our surprise, CRMP-1 can barely enhance VCA-Arp2/3 polymerization in pyrene actin assembly assay (Fig. 16 A). This result cannot explain why blocking CRMP-1 activity weakens de novo Arp2/3 polymerization on the purified membrane (Fig. 15 C & D). Neither can it explain why depletion of CRMP-1 inside the cell could cause such dramatic loss of F-actin at the junction, with a phenotype similar to Arp2/3-depleted cells (Fig. 12 A & B). This discrepancy suggested that even though there has been evidence showing WAVE-2 activates Arp2/3 at adherens junction, CRMP-1 might not go through WAVE-2 to contribute to actin assembly. Instead, CRMP-1 might involve in a non-canonical VCA pathway to build actin filaments at the junction.

We wonder if CRMP-1 works with other proteins that co-exist at the junction to regulate Arp2/3 activity. We mixed CRMP-1 with known junctional proteins, and tested the ability of the mixture to induce Arp2/3-depdent actin polymerization in pyrene actin

polymerization assay. While mixing CRMP-1 and EVL in the reaction, we successfully detected an enhancement on Arp2/3 dependent polymerization while even in the absence of VCA peptide (Fig. 16 B-D). Various biochemical studies have shown that VASP family proteins themselves can facilitate actin assembly due to its weak nucleation activity (Huttelmaier et al., 1999; Schirenbeck et al., 2006) and/or its intrinsic polymerase activity (Bilancia et al., 2014). We did not detected an increase in polymerization rate by EVL alone in our condition. EVL and Arp2/3 alone, or CRMP-1 and EVL, does not seem to nucleates actin assembly either (Fig. 16 B). Actin polymerization only occurs when CRMP-1 and EVL are present in the reaction simultaneously with Arp2/3 complex. If the reaction started with EVL and Arp2/3, there is no induction in Arp2/3 dependent actin assembly. Yet if CRMP-1 was later added into the reaction, the rate of actin assembly suddenly increases (Fig. 16 C, orange curve). This combination (CRMP plus EVL) successfully induces Arp2/3-dependent polymerization in a dose-dependent manner (Fig. 16 D). This reaction would be attenuated in the presence of Arp2/3 inhibitors (Fig. 16 E), further confirming that CRMP-1 and EVL induce actin assembly in an Arp2/3 dependent manner.

Previous studies shows that VASP family proteins can elongate actin filaments. CRMP-1 might be able to facilitate the actin polymerase activity of VASP family protein and hence boost the rate of actin polymerization. We tested this possibility by elongating the actin filaments in the presence of EVL, then adding CRMP-1 into the reaction. The rate of actin polymerization was recorded using the same pyrenyl actin polymerization assays. Our results showed that EVL alone can slightly increase the rate of actin polymerization in a dose-dependent manner. Adding CRMP-1 into the reaction can significantly increase the rate in pyrenyl assays, implying the positive role of CRMP-1 in facilitating EVL-mediated filament elongation (Fig. 16 F & G). Similar effect can be detected using the EVH2 domain, the actin binding domain, of EVL, but not with EVH1 domain (Fig. 16 H). The other two VASP family proteins, VASP (Fig. 16 I) and Mena-EVH2 (Fig. 16 J), can provide the similar trace in the presence of CRMP-1, indicating CRMP-1 can generously enhance the elongation rate of the three VASP family proteins.

In vitro binding assay demonstrates the direct interaction between EVL and CRMP-1. CRMP-1 interacts strongly with beads coated with MBP-EVL, but not with MBP-

peptide alone (control) (Fig. 16 K), with a binding affinity at 2 μm (Fig. 16 L). CRMP-1 seems to be specifically binding to the EVH2 domain of EVL (Fig. 16 M), which is consistent with our kinetic observation that CRMP-1 can boost actin polymerization in the presence of EVH2 domain, yet not EVH1 domain (Fig. 16 H). Therefore, CRMP-1, through binding with EVL, can facilitate EVL or VASP mediated actin polymerization. The two protein complex can also function as a novel Arp2/3 activator.

ix. EVL and CRMP localize to cadherin mediated junction and mediate junctional actin assembly

The discovery of CRMP-1 and EVL as Arp2/3 activators provide a way to explain our in vitro membrane results (Fig. 15) and the phenotypes of CRMP-1 knockdown cells (Fig. 12). CRMP-1 can directly affect actin polymerization by modulating Arp2/3 activity. Even though there are profound researches on Ena/VASP family protein showing that the recruitment of this family protein to cadherin-mediated cell-cell contact is important during junctional formation (Oldenburg et al., 2015; Vasioukhin et al., 2000), no research address the role of the homolog, EVL, as an Arp2/3 activator for this cellular process. We want to confirm the localization of EVL at cell-cell contacts in MDCK cells. Using the EVL antibodies we generated, we successfully detected EVL on adherens junctions of a confluent monolayers of MDCK cell (Fig. 17 A).

We next wanted to know if CRMP-1 and EVL localize to sites of Arp2/3-dependent actin assembly at the junction. Actin assembly at the apical junction of a confluent monolayer can be monitored using latrunculin treatment. Latrunculin is an actin monomer sequester. In the presence of laturncuin, the majority of the actin filaments would be depolymerized. A pool of stable actin, or the latrunculin-resistant puncta, remains along cell-cell contacts at the apical surface. Those latrunculin-resistant puncta have been shown to be the sites that contains Arp2/3 complex. Those puncta can also perform Arp2/3 dependent actin polymerization after the removal of latrunculin (Tang and Brieher, 2012). We probed CRMP-1 and EVL after latrunculin treatment in order to know whether CRMP-1 and EVL locate to those puncta where de novo Arp2/3 polymerization takes place (Fig. 17 B). Our immunostaining results revealed that while the majority of F-actin at cell-cell contact disappeared after laturnculin treatment, there

were remaining actin along the cell-cell contacts in puncta shape. CRMP-1 and EVL signals indeed overlaped with those puncta.

CRMP-1 and EVL have to be present simultaneously to activate Arp2/3 in pure solution (Fig. 16 B). If CRMP-1 and EVL share this pathway inside the cell, then the removal of either one of them should abrogate the activation of Arp2/3 complex and reduce the formation of actin filaments. We knew that depletion of CRMP-1 alone caused loss of junctional actin, to an extend that is as severe as the Arp2/3 depleted cells. We then test if depletion of EVL alone would generate the same result. In a paralleled experiment, we depleted CRMP-1 or EVL individually inside MDCK cells and compared their phenotypes with the control cells transfected with scramble shRNAs. Consistent with the results we obtained earlier, CRMP-1 knockdown cells have reduced actin amount inside the cell. EVL knockdown cells obtained the same phenotype as CRMP-1 knockdown cells (Fig. 17 C). In fact, perturbing EVL function by expressing dominant-negative EVL (EVL-DN) can also reduce F-actin at the junction (Fig. 18). These results support our in vitro kinetic result: CRMP-1 and EVL has to present simultaneously in order to activate Arp2/3-dependent actin polymerization (Fig. 16). The number of actin per cadherin decreased when CRMP-1 or EVL was perturbed, indicating those two proteins contribute to the accumulation of actin amount at this loci (Fig. 17 D).

Interestingly, using immunostaining, we observed the loss of E-cadherin intensity in the knockdown cells. Arp2/3 activity is necessary for efficient formation of E-cadherin adhesive contacts (Yap, 2004). Actin polymerization at cadherin-mediated cell-cell contacts has been thought to stabilize the clustered cadherin receptors. Loss of cadherin at the junction might simply due to the loss of actin assembly in CRMP-1 or EVL depleted cells. Another possible explanation is that CRMP-1 can mediate cadherin clustering on the membrane. We detected CRMP-1 locates early to the cell-cell contacts (Fig. 11). CRMP-1 is also highly associated on the membrane (Fig. 15 A). CRMP-1 might serve as an adaptor protein to recruit cadherin molecules. Moreover, we also detected a loss of the EVL intensity at the junction reduced in the CRMP-1 depleted cells (Fig. 17 D). In vitro result showed that EVL is easier to be extracted off the purified membrane after high-salt treatment compared to CRMP-1 (Fig 15 A). Since CRMP-1 and EVL directly

interact with each other (Fig. 17 K & L), CRMP-1 might be a receptor for EVL to be recruited cadherin-mediated cell-cell junction. This hypothesis needs to be further tested.

x. Depletion of CRMP-1 or EVL decrease cell-cell attachment and reduces the rate of junction formation

Reduced actin and cadherin signal might result in biological defects. Misregulation of the proteins involved in cell-cell contact formation could cause pathological results, such as cancer. Even though the role of cadherin-mediated adherens junction in cancer biology is complex, it has been generally accepted that reduced E-cadherin and the sequentially impaired adherens junction favors the epithelia-mesenchymal transition at least in some cancers (Berx and van Roy, 2009). Emerging evidence showing the relationship of actin CRMP-1 or Ena/VASP proteins on cancer invasion (Ali et al., 2015). In fact, CRMP-1 has been referred to as cancer suppresser gene by different groups (Shih et al., 2001; Steeg, 2001). Our CRMP-1 knockdown cells showed reduced cadherin and actin at the junction might explain why CRMP-1 can suppress tumor progression.

We wanted to confirm that CRMP-1 knockdown indeed repeals the strength of cell-cell adhesion, we used hanging drop experiments so that we can monitor cell clustering without the influence of focal adhesion. We also combine the experiment with trituration approach to test the resistance of the cell aggregates to a shearing force. At the beginning of the hanging drop experiment, both control cells and CRMP-1 knockdown cells were present as single cells or clusters of fewer than ten cells (Fig. 19, 0 hour). In control experiment, the number of cells in large clusters (more than 50 cells) covers 30% of total cells after 2 hours, and to almost 60% at 3-hour time point. In the contrarily, the majority of the cells remains as small clusters in CRMP-1 depleted condition even at 3-hour time point. After 4 hours, 70% of the cells are in large clusters in CRMP-1 depleted condition, while the control condition had already reached 98%. CRMP-1 depleted cells represented a slower rate on the formation of cell-cell contact.

Control cells showed better resistance to trituration than CRMP-1 depleted cells. Before trituration, the control cells at 3 hour and the CRMP-1 depleted cells at 4 hour shares similar cluster profile: 60-70% of the cells are in large clusters (more than 50 cells); around 25% of the cells are in middle clusters (11-50 cells). After trituration, those

large clusters were all broken down to smaller size in CRMP-1 depleted cells, while around 50% of the control cells remains in large clusters. In agreement with our hang-drop result, we noticed that the cells in the CRMP-1 knockdown monolayer are easier to be washed apart from each other (Fig. 20). These results showing that CRMP-1 depleted cells form slower and weaker cell-cell adhesion than the control cells, probably resulting from fewer F-actin at cell-cell contact (Fig. 12).

III. Localization and Functional Study of CRMP-1 in Lamellipodia

i. CRMP-1 locates to the leading edge of protrusive structures in MDCK cell

Our study on the confluent MDCK monolayers reveals the role of CRMP-1 for Arp2/3-dependent actin polymerization at E-cadherin-mediated cell-cell contacts (Chapter 3, II). When we used immunostaining to probe CRMP-1 in non-confluent MDCK cells, we detect CRMP-1 signal at the leading edge of the lamellipodia, an Arp2/3 dependent structure (Fig. 21 A & B). It has been believed that when MDCK cells are plated at low confluency, they make protrusions that would facilitate the formation of cell-cell contacts (Ehrlich et al., 2002; Yamazaki et al., 2007). When we performed spreading assay to induce MDCK cells to form protrusions, both the endogenous CRMP-1 and exogenous GFP-CRMP-1 colocalize with F-actin at the edge of the protrusive structures (Fig. 21 A & B), implying that CRMP-1 might contribute to actin assembly at this cellular location. Note that when we used TCA fixation to probe DHPase, a highly identical protein to the CRMP family, we observed that DHPase signal slightly enhanced at the leading edge of a single spreading cell (Fig. 21 C). Since the primary sequence of the CRMP family proteins are highly identical to the DHPase's, the whole CRMP family might share this same cellular localization. In addition, the DHPase-like domain in CRMP-1, or other CRMPs, might be essential for the recruitment of CRMP-1 (CRMPs) to the lamellipodia. These hypotheses need to be tested in the future.

ii. CRMP-1 is essential for cell spreading in an Arp2/3-dependent manner

To determine if CRMP-1-dependent protrusion is necessary for cell spreading, we compared the rate of cell spreading in CRMP-1 knockdown cells to the scramble condition. While 70% of the cells transfected with a scrambled shRNA extended

protrusions and spread on collagen within one hour, only 20% of the CRMP-1-depleted cells spread. The CRMP-1 depleted cells that did spread failed to make protrusion with classic characteristics of lamellipodia: a smooth edge with an enriched actin band at the leading edge. Depletion of CRMP-1 caused a loss of F-actin signal inside the cells: CRMP-1 knockdown cells does not have an enriched F-actin band at the edge of the protrusive structure. Comparing to the scramble cells, the intensive F-actin signal in the middle of the cell body is absent as well. In contrast, overexpression of GFP-CRMP-1 increased the percentage of spreading with increase in F-actin signal at the front edge of the protrusions (Fig. 22 B) and throughout the whole cell (Fig. 22. A). These spreading results demonstrate that there is a positive correlation between the amount of CRMP-1 and the amount of F-actin inside the cell.

Since the formation of F-actin at this cellular location is Arp2/3 dependent, and since CRMP-1 modulate Arp2/3 activity in the *Listeria* actin tail (Chapter 3.I) and at adherens junction (Chapter 3.II), we wanted to know if CRMP-1 and Arp2/3 involve in the same pathway to control lamellipodia formation. Previous results have shown that Arp2/3 activity is not required for fibroblasts to spread on fibronectin (Suraneni et al., 2012). We do not know if this result can be applied to epithelial MDCK cell spreading. To test if Arp2/3 is necessary for epithelial cells to spread on substrate, we first inhibited Arp2/3 activity using small molecules (Nolen et al., 2009). Addition of 100 nm of Arp2/3 inhibitors blocked cell spreading (Fig. 22). While using shRNAs to deplete either the p34 subunit or the Arp3 subunit of the Arp2/3 complex, the percentage of cell spreading reduced ~70%-80%, as the result we observed from CRMP-1 depleted cells (Fig. 22 B). Thus, spreading of MDCK cells on collagen is an Arp2/3 dependent process that requires CRMP-1.

iii. CRMP-1 contributes to F-actin accumulation at the leading edge of lamellipodia of a wounded cell

To test if the observations in spreading assay (Fig. 22) reveal the ability of the cells to form protrusions, we investigated the effect of perturbing CRMP-1 for making protrusions in response to the wound. Epithelial cells can close wounds by extending protrusive lamellipodia into the open area (Fenteany et al., 2000). Those lamellipodia are characterized by a band of concentrated F-actin at the leading edge (Fig. 23 A, no

inhibitors' condition). We confirmed that this lamellipodia is indeed Arp2/3-dependent, since Arp2/3 inhibitors abolish its formation after wounding (Fig. 23C).

Next, we want to decipher if manipulating the amount of CRMP-1 inside the cell would affect the amount of F-actin at the leading edge. We depleted CRMP-1 inside the cell and wounded the cell on the 2nd day of confluency. The cells were allowed to recover for one hour after the wounding procedure. We stained for Arp2/3 complex with the antibody against p34 subunit of the Arp2/3 complex. We also used phalloidin to stain for stable F-actin. Depleting cells of CRMP-1 decreased both the amount of F-actin and the amount of Arp2/3 at the leading edge (Fig. 23 B & C). In contrast, over-expressing CRMP-1 induced a greater fraction of cells to form lamellipodia. The protrusions in the CRMP-1-overexpressing background were enriched in F-actin and Arp2/3 relative to control cells (Fig. 23 C). Note that CRMP-1-depleted cells made smaller protrusions compared to the scramble cells; CRMP-1-overexpression cells made bigger protrusions. Those results were consistent with our observation in the single spreading cell (Fig. 22). Hence, CRMP-1 contributes to the formation of Arp2/3-dependent protrusions during single-cell and confluent-cell stages.

iv. No obvious change in microtubule organization was detected in CRMP-1-depleted or –overexpressing cells

Interactions between the various CRMP family members and the cytoskeletons are complicated. CRMP-2 binds to tubulin dimers to accelerate microtubule assembly while CRMP-4 has been shown to bundle actin filaments (Fukata et al., 2002; Khazaei et al., 2014). We wonder if manipulating CRMP-1 amount in the MDCK cell would alter the microtubule organization inside the cell. In other words, the effect of CRMP-1on lamellipodia formation (Fig. 22 and Fig. 23 B & C) might be the downstream effect of CRMP-microtubule pathway, since microtubule cytoskeleton also has a role in cell protrusions (Ballestrem et al., 2000; Wadsworth, 1999; Waterman-Storer and Salmon, 1997; Wittmann and Waterman-Storer, 2001).

To investigate microtubule structures in response to our experimental conditions, we performed microtubule staining in the wounded monolayers. Our preliminary data shows that we did not see an obvious, gross alteration in microtubule organization among the three different genetic backgrounds: scramble cells, CRMP-1-depleted and CRMP-1-

overexpressing cells (Fig. 24). Therefore, while genetically down- or up- regulation of the CRMP-1 provides a dramatic change in actin cytoskeleton, its effect on microtubule is minor or maybe neglectable. Note that our immunostaining results, which were obtained from fixed samples, could not address if there were changes in microtubule dynamics when we manipulated CRMP-1 amount inside the cell. Further study needs to be done to answer this question.

v. Semaphorin 3A does not attenuate the formation of the protrusive structures in MDCK cells

There are profound researches on CRMP family proteins and Sema3A signaling in neuronal cells (see Chapter 1.V). Yet role of Sema3A in epithelial cell morphology or in regulating actin cytoskeleton remain obscure. MDCK cells express Sema3A receptor, Plexin (William M. Brieher, private conversations). We would like to test the possibility whether the spreading phenotype or the formation of the protrusive structures in the MDCK cells is Semaphorin-dependent.

We expressed exogenous Sema3A in HEK 293 cells. In control cells, we transfected empty vectors. The supernatant from these two conditions were collected and applied to MDCK cells under different experimental setups: freshly trypsinized MDCK cell undergoing spreading on collagen, or wounded MDCK cells undergoing recovery (Fig. III.5 A). In neuronal cells, Sema3A is a repulsive cue. CRMP family proteins contribute to growth cone collapse as a downstream effector for Sema3A signaling. If Sema3A also functions as a repulsive cue for the epithelial cells, then we should detect a defect of forming protrusive structures in the Sema3A-treated conditions. If the change in cell morphology after Sema-3A treatment phenocopies either CRMP-1 knockdown or CRMP-1 overexpressing cells, it would reveal the possibility that CRMP-1 works downstream of Sema3A in regulating epithelial cell morphology. Qualitative results showed that no significant change in the formation of protrusions in either experimental setup. Single cells could still spread and form protrusive structures (Fig. 25 B). In wounded monolayer, Sema3A-treated condition did not abrogate the lamellipodia formation at the wounded edge (Fig. 25 C). These preliminary results could not verify what role Sema3A has in epithelial MDCK cells, nor can it help distinguish if CRMP-1 works downstream of Sema3A signaling in this cell type. We did not know the amount of

Sema3A was expressed by HEK 293 cells in this data set, either. More experiments need to be done in order to determine the contribution of Sema3A in MDCK cells.

vi. CRMP-1 contributes to the stability of the protrusive edge

To better understand the role of CRMP-1 in Arp2/3 dependent cell protrusion, we acquired 5-minutes time-lapse movies of the leading edges after wounding (Fig. 26). We compared the behavior of leading edges between control cells and the cells depleted or over-expressing CRMP-1. Behavior of the leading edge was quantified by analyzing kymographs drawn from the time-lapse sequences (Fig. 26 A & B). Depletion of CRMP-1 had little effect on the average rate of lamellipodial advance compared to wild-type cells. Leading edges of control cells and cells depleted of CRMP-1 both advanced at an average rate less than 0.2 microns/minute (Fig. 26 C). However details within the kymographs showed that leading edges of CRMP-1 depleted cells were unstable and retracted frequently. While CRMP-1 depleted cells might occasionally advance rapidly, this movement was offset by frequent, fast retractions of the leading edge. In contrast, cells over-expressing CRMP-1 extended protrusions at a faster average rate of 0.87 microns/minute. In addition, leading edges of CRMP-1 over-expressing cells were stable and rarely retracted. Cortactin is another factor that is already known to facilitate Arp2/3 dependent actin nucleation (Weaver et al., 2001). Perturbing cortactin function has the same effect on lamellipodia dynamics as depleting CRMP-1 (Bryce et al., 2005). The results then are consistent with the hypothesis that CRMP-1 promotes the assembly and stability of Arp2/3 dependent lamellipodia.

vii. CRMP-1 contributes to the directionality in wounded monolayers

We next asked if CRMP-1 dependent changes in F-actin content altered cell migration. We pursued this question by comparing cell migration behavior during the 60 minute following wounding as a function of CRMP-1 (Fig. 27 A). The three different cells (Scramble; CRMP-1 knockdown and CRMP-1-overexpressing cells) display distinct migratory characteristics. Control cells moved into the wound slowly yet maintained their directionality. In contrast, protrusions in CRMP-1-depleted cells advanced more rapidly yet lost directionality (Fig. 27 B & C). The movement of the leading edge of CRMP-1-

overexpressing cells maintained their directionality while migrating faster (Fig. 27 C). Therefore, CRMP-1 not only controls the amount of F-actin in lamellipodia to produce a persistently advancing leading edge but also controls the directionality of cell migration.

In two-dimensional migration, such as our wound healing experiment, the movement of the cell sheet is considered to be the combination of exploration of new space, the initiation of substrate adhesion, the influence from the contraction force inside a cell, and the coordination of cell-cell adhesion with the adjacent cell. In both CRMP-1 depleted and CRMP-1 overexpressed cells, an increased migration rate of the leading edge were detected during wound healing process. This result revealed that tuning the amount of CRMP-1 inside cell would affect the balance among the criteria listed above. Our current work showed the novel role of CRMP in regulating Arp2/3 related actin structures, especially in lamellipodia formation. Yet it did not rule out that CRMP-1 might also have a role in other actin structures, which are dependent or independent of Arp2/3 complex. For instance, CRMP-1 might regulate the strength of focal adhesion (Kawahara et al., 2013) or cell-cell adhesion, on which cell migration is interdependent.

CRMP-1 might also function upstream of myosin to regulate cell migration. CRMP-2, one of the CRMP family proteins, has been shown to have an inhibitory role for ROCKII, which indirectly regulates myosin activity and cell migration (Yoneda et al., 2012). Our result is not able to elucidate precisely why increase and decrease CRMP-1 amount would trigger faster cell migration in wound healing experiment. Yet similar result can be found on CRMP-2 studies. Cell migration of SW620 cells was reduced while cells were transfected with one of the isoform of CRMP-2 (Yoneda et al., 2012).

CHAPTER 4: DISCUSSION

Previous researches imply the unknown factors remain to be discovered for *Listeria* actin tail formation (Brieher et al., 2004; Welch et al., 1997). We followed the protocol described by Brieher and colleagues (Brieher et al., 2004), and successfully identified CRMP-1 is such a factor that facilitates Arp2/3-dependent actin assembly on *Listeria* (Fig. 1 & 2). In vitro biochemical assays revealed the molecular mechanism of which CRMP-1 used to enhance Arp2/3 activity. CRMP-1 works with *Listeria* ActA and enhances ActA-mediated Arp2/3 polymerization. We verified that CRMP-1 can interact with ActA (Fig. 4). In other words, ActA might very likely to be the receptor on *Listeria* surface that recruits CRMP-1. This explains why CRMP-1 was able to be identified from brain cytosol by our 2-step preincubation assay (Fig. 1). Inside the cell, Ena/VASP family proteins are also able to bind to ActA. It has been known that the proline-rich domain of ActA is the ligand for EVH1 domain of Ena/VASP family (Laurent et al., 1999; Niebuhr et al., 1997). We have not yet dissect which domain CRMP-1 uses to bind to ActA. The ActA binding sequence for CRMP-1 also remains unverified as well. Now we show CRMP-1 and EVL, an Ena/VASP family protein, can activate Arp2/3 complex in the absence of the known NPF (Fig. 16). It would be interesting to know if the CRMP-1 binding site on ActA is in close proximity of the EVL binding site. Since CRMP-1 and EVL interact with each other (Fig. 16), recruitment of either one of them should sequentially locate the other one to the *Listeria* surface. Under this condition, Arp2/3 complex can be activated on the *Listeria* surface through two mechanism: *Listeria* ActA, and CRMP-1+EVL.

Our discovery of CRMP-1 as a novel factor for actin assembly opens a new field of study on how this new factor can work conjunction with other known actin-binding protein to modulate *Listeria* actin tail dynamics. However, our identification of CRMP-1 cannot fully explain the full mechanism *Listeria* uses to build the actin tail. There might still be more factors that need to be identified. Brieher and colleague showed that brain cytosol contains factors that can facilitate the growth of *Listeria* actin tail in an Arp2/3-independent manner (Brieher et al., 2004). The CRMP-1 function in our assay seems to be purely Arp2/3-depndent. While repeating the experimental procedure described by

Brieher, we did not detect an enhancement of Arp2/3-independent tail growth in the presence of CRMP-1 or CRMP-1 + EVL (Fig. 3 B). This missing factor might possibly be a small molecule, since it stays active after heating treatment and organic-solvent treatment (William M. Brieher, private conversations). Now we know CRMP-1 contributes to actin tail formation. We also know CRMP-1 is a protein that is highly identical with DHPase regarding to their primary sequences and tertiary structures. DHPase can metabolize pyrimidine. It would be intriguing to know if the small molecule pyrimidine is the missing factor, which work through CRMP-1 to promot Arp2/3-independent tail elongation. It would be worth testing if CRMP-1 can bind to pyrimidine, and whether the activity of CRMP-1 on *Listeria* actin tail formation would change upon this binding. Maybe CRMP-1 can contribute to Arp2/3-independent tail growth in the presence of pyrimidine.

CRMP-1 is one member of a family of five related proteins (Fukada et al., 2000; Hamajima et al., 1996; Wang and Strittmatter, 1996). We detected CRMPs can facilitate ActA-Arp2/3 reaction to different extends (Fig. 5). For example, CRMP-3 has a powerful effect; yet CRMP-2 does not seem to potentiate this reaction. CRMP family protein can form hetero-tetramer (Deo et al., 2004; Wang and Strittmatter, 1997). Researches showed CRMP might functionally antagonize to one another (see Chapter 1.V.iii). It is possible that the CRMP family proteins cooperate all together. They tune their ability of facilitating actin assembly through making hetero-oligomer with different combinations.

This study also provides the first-hand evidence on CRMP-1 functioning in regulating the F-actin amount inside mammalian cells. This phenomena was detected in two different cellular locations, at the cadherin-mediated cell-cell contacts (Fig. 12) and at the leading edge of lamellipodia (Fig. 10). Both of the structures are Arp2/3-dependent. WAVE-2 and N-WASP, the canonical Arp2/3 NPF that contains VCA/VVCA peptide, have been shown to activate Arp2/3 at these two cellular localizations, respectively. Yet we failed to detect the ability of CRMP-1 to enhance actin polymerization in a VCA- or VVCA-dependent manner (Fig. 16). We envisage that CRMP-1 works conjunction with EVL to activate Arp2/3 complex at this two cellular locations. Consistent with our speculation, this two proteins have to be present simultaneously in order to activate Arp2/3 complex in pure solution (Fig. 16). Perturbing the function of either one of them,

by knockdown approach or by dominant-negative construct, would reduce F-actin amount at those cellular locations (Fig. 17, 22 & 23). The phenotype of CRMP-1 knockdown and/or EVL knockdown MDCK cells perfectly photocopy the Arp2/3 knockdown cells (Fig. 12 & 17). In addition, blocking CRMP-1 activity alone on the purified membrane abrogates de novo Arp2/3 dependent actin assembly (Fig. 15). Those results demonstrated that CRMP-1 and EVL are important factors for actin assembly in the mammalian system. Our results also reveal a whole new pathway to regulate Arp2/3 activity inside the cell.

While disturbing CRMP-1, EVL or Arp2/3 inside the cultured MDCK cells, we observed interesting changes in morphology. Perturbing other factors that contribute junctional actin assembly could also change cell morphology, yet not the same as the knockdown cells we show here. Cortactin, for example, is a protein that binds to WAVE-2 and Arp2/3 to modulate actin assembly at adherens junction. Perturbing cortactin function would change cell morphology: irregular outlines and long cellular extensions (Han et al., 2014). CRMP-1 knockdown cells, however, maintain regular cobblestone morphology characteristic as wildtype MDCK cells, even though the F-actin amount is reduced (Fig. 12). It would be interested to know why interfering different pathways of activating Arp2/3 complex could cause different dissertations of epithelial cell morphology. It is possible that the actin network initiated through WAVE-2 or CRMP-1/EVL is structurally distinct or functionally different. From a molecular basis, cortactin enhances Arp2/3-driven actin polymerization through a canonical WASp/WAVE-dependent pathway; whereas CRMP-1 works with EVL to activate Arp2/3. It is possible that the two pathways response to different upstream signals and/or build different actin networks which then contribute to the organization of different cell morphology. Another interesting feature of our knockdown cells is that CRMP-1 knockdown cells displayed enlarged apical surface area with overall shorter in height (thinner in z-axis) (Fig. 12). This phenotype can be explained by different aspects.

First, apical surface of epithelial cells has been shown to be constricted by actomyosin network at the medioapical surface (Martin et al., 2009). The missing actin network under CRMP-1 knockdown condition is possibly as part of the actomyosin meshwork. As a consequence, insufficient amount of actin-mysoin network fails to

coalesce myosin and contract the meshwork in order to generate force to "close" the apical surface. Secondly, during epithelial cell polarization and maturation, it has been believed the stable cell-cell contact is required prior to junction maturation and cubical morphology development. The weaker and easer dissociated adhesion under CRMP-1 depleted conditions (Fig. 19 & 20) implying the cell-cell contacts might fail to or might be less efficient to reach its ultimate stable stage to support the sequential maturation steps. The acquisition of the full polarity takes place while neighboring cells would compact towards each other. Yet CRMP-1 knockdown cells showed loosely organized cells even under confluent condition (Fig. 12), which provides another explanation to why those cells fail to form a tall cubical shape.

Live cell-imaging of CRMP-1 knockdown cells reveals its erratic migration during wound closure (Fig. 27). During wound closure, the whole sheet of cells behind the wounded edge undergoes collective migration, which is a process that a group of cells moves in concert without separating from each other. Since cell-cell contacts is one of the factors that contributes to cells moving collectively, and since cell-substrate adhesion also plays a role during cell migration, we suspected that the cell sheet formed by CRMP-1-depleted cells become more motile due to: 1) reduced spreading ability to provide sufficient surface area (Fig. 22) in order to connect to the substrate, and 2) reduced cell-cell adhesion (Fig. 19 & 20) to constrain the shifting.

The CRMP family is implicated in altering cell motility in response to regulatory signals (Goshima et al., 1995; Hedgecock et al., 1985; Inagaki et al., 2001). CRMP-2, for example, is necessary for neuronal growth collapse in response to Semaphorin 3A (Goshima et al., 1995). My result on Sema3A and MDCK morphology is very preliminary (Fig. 25). Many control needs to be done in order to clarify if Sema3A can regulate MDCK cell biology. If future experiments demonstrate Sema3A can alter MDCK morphology, then our results here provide a mechanism for understanding how the CRMP proteins might alter cell motility in response to migration guidance: through regulating Arp2/3-dependent actin assembly.

CHAPTER 5: REFERENCES

Akin, O., and R.D. Mullins. 2008. Capping protein increases the rate of actin-based motility by promoting filament nucleation by the Arp2/3 complex. *Cell*. 133:841-851.

Alabed, Y.Z., M. Pool, S. Ong Tone, and A.E. Fournier. 2007. Identification of CRMP4 as a convergent regulator of axon outgrowth inhibition. *J. Neurosci.* 27:1702-1711.

Alabed, Y.Z., M. Pool, S. Ong Tone, C. Sutherland, and A.E. Fournier. 2010. GSK3 beta regulates myelin-dependent axon outgrowth inhibition through CRMP4. *J. Neurosci.* 30:5635-5643.

Ali, M., L.K. Rogers, and G.M. Pitari. 2015. Serine phosphorylation of vasodilator-stimulated phosphoprotein (VASP) regulates colon cancer cell survival and apoptosis. *Life Sci.* 123:1-8.

Arimura, N., N. Inagaki, K. Chihara, C. Menager, N. Nakamura, M. Amano, A. Iwamatsu, Y. Goshima, and K. Kaibuchi. 2000. Phosphorylation of collapsin response mediator protein-2 by Rho-kinase. Evidence for two separate signaling pathways for growth cone collapse. *J. Biol. Chem.* 275:23973-23980.

Arimura, N., C. Menager, Y. Kawano, T. Yoshimura, S. Kawabata, A. Hattori, Y. Fukata, M. Amano, Y. Goshima, M. Inagaki, N. Morone, J. Usukura, and K. Kaibuchi. 2005. Phosphorylation by Rho kinase regulates CRMP-2 activity in growth cones. *Mol. Cell. Biol.* 25:9973-9984.

Ballestrem, C., B. Wehrle-Haller, B. Hinz, and B.A. Imhof. 2000. Actin-dependent lamellipodia formation and microtubule-dependent tail retraction control-directed cell migration. *Molecular biology of the cell*. 11:2999-3012.

Berx, G., and F. van Roy. 2009. Involvement of members of the cadherin superfamily in cancer. *Cold Spring Harbor perspectives in biology*. 1:a003129.

Bilancia, C.G., J.D. Winkelman, D. Tsygankov, S.H. Nowotarski, J.A. Sees, K. Comber, I. Evans, V. Lakhani, W. Wood, T.C. Elston, D.R. Kovar, and M. Peifer. 2014. Enabled negatively regulates diaphanous-driven actin dynamics in vitro and in vivo. *Dev. Cell*. 28:394-408.

Borisy, G.G., and T.M. Svitkina. 2000. Actin machinery: pushing the envelope. *Curr. Opin. Cell Biol.* 12:104-112.

Bretin, S., V. Rogemond, P. Marin, M. Maus, Y. Torrens, J. Honnorat, J. Glowinski, J. Premont, and C. Gauchy. 2006. Calpain product of WT-CRMP2 reduces the amount of surface NR2B NMDA receptor subunit. *J. Neurochem.* 98:1252-1265.

Brieher, W.M., M. Coughlin, and T.J. Mitchison. 2004. Fascin-mediated propulsion of Listeria monocytogenes independent of frequent nucleation by the Arp2/3 complex. *J. Cell Biol.* 165:233-242.

Brot, S., V. Rogemond, V. Perrot, N. Chounlamountri, C. Auger, J. Honnorat, and M. Moradi-Ameli. 2010. CRMP5 interacts with tubulin to inhibit neurite outgrowth, thereby modulating the function of CRMP2. *J. Neurosci.* 30:10639-10654.

Brown, M., T. Jacobs, B. Eickholt, G. Ferrari, M. Teo, C. Monfries, R.Z. Qi, T. Leung, L. Lim, and C. Hall. 2004. Alpha2-chimaerin, cyclin-dependent Kinase 5/p35, and

its target collapsin response mediator protein-2 are essential components in semaphorin 3A-induced growth-cone collapse. *J. Neurosci.* 24:8994-9004.
Bryan, J., and L.M. Coluccio. 1985. Kinetic analysis of F-actin depolymerization in the presence of platelet gelsolin and gelsolin-actin complexes. *J. Cell Biol.* 101:1236-1244.
Bryce, N.S., E.S. Clark, J.L. Leysath, J.D. Currie, D.J. Webb, and A.M. Weaver. 2005. Cortactin promotes cell motility by enhancing lamellipodial persistence. *Curr. Biol.* 15:1276-1285.
Buckley, C.D., J. Tan, K.L. Anderson, D. Hanein, N. Volkmann, W.I. Weis, W.J. Nelson, and A.R. Dunn. 2014. Cell adhesion. The minimal cadherin-catenin complex binds to actin filaments under force. *Science*. 346:1254211.
Buel, G.R., J. Rush, and B.A. Ballif. 2010. Fyn promotes phosphorylation of collapsin response mediator protein 1 at tyrosine 504, a novel, isoform-specific regulatory site. *J. Cell. Biochem.* 111:20-28.
Byk, T., T. Dobransky, C. Cifuentes-Diaz, and A. Sobel. 1996. Identification and molecular characterization of Unc-33-like phosphoprotein (Ulip), a putative mammalian homolog of the axonal guidance-associated unc-33 gene product. *J. Neurosci.* 16:688-701.
Byk, T., S. Ozon, and A. Sobel. 1998. The Ulip family phosphoproteins--common and specific properties. *Eur. J. Biochem.* 254:14-24.
Chae, Y.C., S. Lee, K. Heo, S.H. Ha, Y. Jung, J.H. Kim, Y. Ihara, P.G. Suh, and S.H. Ryu. 2009. Collapsin response mediator protein-2 regulates neurite formation by modulating tubulin GTPase activity. *Cell. Signal.* 21:1818-1826.
Christofori, G., and H. Semb. 1999. The role of the cell-adhesion molecule E-cadherin as a tumour-suppressor gene. *Trends Biochem. Sci.* 24:73-76.
Chung, M.A., J.E. Lee, J.Y. Lee, M.J. Ko, S.T. Lee, and H.J. Kim. 2005. Alteration of collapsin response mediator protein-2 expression in focal ischemic rat brain. *Neuroreport*. 16:1647-1653.
Cole, A.R., M.P. Soutar, M. Rembutsu, L. van Aalten, C.J. Hastie, H. McLauchlan, M. Peggie, M. Balastik, K.P. Lu, and C. Sutherland. 2008. Relative resistance of Cdk5-phosphorylated CRMP2 to dephosphorylation. *J. Biol. Chem.* 283:18227-18237.
Cole, R.N., and G.W. Hart. 1999. Glycosylation sites flank phosphorylation sites on synapsin I: O-linked N-acetylglucosamine residues are localized within domains mediating synapsin I interactions. *J. Neurochem.* 73:418-428.
Cole, R.N., and G.W. Hart. 2001. Cytosolic O-glycosylation is abundant in nerve terminals. *J. Neurochem.* 79:1080-1089.
Cossart, P. 2000. Actin-based motility of pathogens: the Arp2/3 complex is a central player. *Cell. Microbiol.* 2:195-205.
David, V., E. Gouin, M.V. Troys, A. Grogan, A.W. Segal, C. Ampe, and P. Cossart. 1998. Identification of cofilin, coronin, Rac and capZ in actin tails using a Listeria affinity approach. *J. Cell Sci.* 111 (Pt 19):2877-2884.
Deo, R.C., E.F. Schmidt, A. Elhabazi, H. Togashi, S.K. Burley, and S.M. Strittmatter. 2004. Structural bases for CRMP function in plexin-dependent semaphorin3A signaling. *EMBO J.* 23:9-22.

Domann, E., J. Wehland, M. Rohde, S. Pistor, M. Hartl, W. Goebel, M. Leimeister-Wachter, M. Wuenscher, and T. Chakraborty. 1992. A novel bacterial virulence gene in Listeria monocytogenes required for host cell microfilament interaction with homology to the proline-rich region of vinculin. *EMBO J.* 11:1981-1990.

Drees, F., S. Pokutta, S. Yamada, W.J. Nelson, and W.I. Weis. 2005. Alpha-catenin is a molecular switch that binds E-cadherin-beta-catenin and regulates actin-filament assembly. *Cell*. 123:903-915.

Eden, S., R. Rohatgi, A.V. Podtelejnikov, M. Mann, and M.W. Kirschner. 2002. Mechanism of regulation of WAVE1-induced actin nucleation by Rac1 and Nck. *Nature*. 418:790-793.

Ehrlich, J.S., M.D. Hansen, and W.J. Nelson. 2002. Spatio-temporal regulation of Rac1 localization and lamellipodia dynamics during epithelial cell-cell adhesion. *Dev. Cell*. 3:259-270.

Fenteany, G., P.A. Janmey, and T.P. Stossel. 2000. Signaling pathways and cell mechanics involved in wound closure by epithelial cell sheets. *Curr. Biol.* 10:831-838.

Fujii, T., A.H. Iwane, T. Yanagida, and K. Namba. 2010. Direct visualization of secondary structures of F-actin by electron cryomicroscopy. *Nature*. 467:724-728.

Fukada, M., I. Watakabe, J. Yuasa-Kawada, H. Kawachi, A. Kuroiwa, Y. Matsuda, and M. Noda. 2000. Molecular characterization of CRMP5, a novel member of the collapsin response mediator protein family. *J. Biol. Chem.* 275:37957-37965.

Fukata, Y., T.J. Itoh, T. Kimura, C. Menager, T. Nishimura, T. Shiromizu, H. Watanabe, N. Inagaki, A. Iwamatsu, H. Hotani, and K. Kaibuchi. 2002. CRMP-2 binds to tubulin heterodimers to promote microtubule assembly. *Nat. Cell Biol.* 4:583-591.

Gaetano, C., T. Matsuo, and C.J. Thiele. 1997. Identification and characterization of a retinoic acid-regulated human homologue of the unc-33-like phosphoprotein gene (hUlip) from neuroblastoma cells. *J. Biol. Chem.* 272:12195-12201.

Goley, E.D., S.E. Rodenbusch, A.C. Martin, and M.D. Welch. 2004. Critical conformational changes in the Arp2/3 complex are induced by nucleotide and nucleation promoting factor. *Mol. Cell*. 16:269-279.

Goley, E.D., and M.D. Welch. 2006. The ARP2/3 complex: an actin nucleator comes of age. *Nat. Rev. Mol. Cell Biol.* 7:713-726.

Goshima, Y., F. Nakamura, P. Strittmatter, and S.M. Strittmatter. 1995. Collapsin-induced growth cone collapse mediated by an intracellular protein related to UNC-33. *Nature*. 376:509-514.

Gu, Y., and Y. Ihara. 2000. Evidence that collapsin response mediator protein-2 is involved in the dynamics of microtubules. *J. Biol. Chem.* 275:17917-17920.

Hagmann, J., M. Grob, and M.M. Burger. 1992. The cytoskeletal protein talin is O-glycosylated. *J. Biol. Chem.* 267:14424-14428.

Hamajima, N., M. Kouwaki, P. Vreken, K. Matsuda, S. Sumi, M. Imaeda, S. Ohba, K. Kidouchi, M. Nonaka, M. Sasaki, N. Tamaki, Y. Endo, R. De Abreu, J. Rotteveel, A. van Kuilenburg, A. van Gennip, H. Togari, and Y. Wada. 1998. Dihydropyrimidinase deficiency: structural organization, chromosomal localization, and mutation analysis of the human dihydropyrimidinase gene. *Am. J. Hum. Genet.* 63:717-726.

Hamajima, N., K. Matsuda, S. Sakata, N. Tamaki, M. Sasaki, and M. Nonaka. 1996. A novel gene family defined by human dihydropyrimidinase and three related proteins with differential tissue distribution. *Gene*. 180:157-163.

Han, S.P., Y. Gambin, G.A. Gomez, S. Verma, N. Giles, M. Michael, S.K. Wu, Z. Guo, W. Johnston, E. Sierecki, R.G. Parton, K. Alexandrov, and A.S. Yap. 2014. Cortactin scaffolds Arp2/3 and WAVE2 at the epithelial zonula adherens. *J. Biol. Chem.* 289:7764-7775.

Hart, G.W. 1997. Dynamic O-linked glycosylation of nuclear and cytoskeletal proteins. *Annu. Rev. Biochem.* 66:315-335.

Hedgecock, E.M., J.G. Culotti, J.N. Thomson, and L.A. Perkins. 1985. Axonal guidance mutants of Caenorhabditis elegans identified by filling sensory neurons with fluorescein dyes. *Dev. Biol.* 111:158-170.

Higurashi, M., M. Iketani, K. Takei, N. Yamashita, R. Aoki, N. Kawahara, and Y. Goshima. 2012. Localized role of CRMP1 and CRMP2 in neurite outgrowth and growth cone steering. *Dev Neurobiol*. 72:1528-1540.

Honda, K., T. Yamada, R. Endo, Y. Ino, M. Gotoh, H. Tsuda, Y. Yamada, H. Chiba, and S. Hirohashi. 1998. Actinin-4, a novel actin-bundling protein associated with cell motility and cancer invasion. *J. Cell Biol.* 140:1383-1393.

Horiuchi, M., O. El Far, and H. Betz. 2000. Ulip6, a novel unc-33 and dihydropyrimidinase related protein highly expressed in developing rat brain. *FEBS Lett.* 480:283-286.

Hotta, A., R. Inatome, J. Yuasa-Kawada, Q. Qin, H. Yamamura, and S. Yanagi. 2005. Critical role of collapsin response mediator protein-associated molecule CRAM for filopodia and growth cone development in neurons. *Molecular biology of the cell*. 16:32-39.

Hou, S.T., S.X. Jiang, A. Desbois, D. Huang, J. Kelly, L. Tessier, L. Karchewski, and J. Kappler. 2006. Calpain-cleaved collapsin response mediator protein-3 induces neuronal death after glutamate toxicity and cerebral ischemia. *J. Neurosci.* 26:2241-2249.

Huang, C., Y. Ni, T. Wang, Y. Gao, C.C. Haudenschild, and X. Zhan. 1997. Down-regulation of the filamentous actin cross-linking activity of cortactin by Src-mediated tyrosine phosphorylation. *J. Biol. Chem.* 272:13911-13915.

Hung, R.J., U. Yazdani, J. Yoon, H. Wu, T. Yang, N. Gupta, Z. Huang, W.J. van Berkel, and J.R. Terman. 2010. Mical links semaphorins to F-actin disassembly. *Nature*. 463:823-827.

Huttelmaier, S., B. Harbeck, O. Steffens, T. Messerschmidt, S. Illenberger, and B.M. Jockusch. 1999. Characterization of the actin binding properties of the vasodilator-stimulated phosphoprotein VASP. *FEBS Lett.* 451:68-74.

Inagaki, N., K. Chihara, N. Arimura, C. Menager, Y. Kawano, N. Matsuo, T. Nishimura, M. Amano, and K. Kaibuchi. 2001. CRMP-2 induces axons in cultured hippocampal neurons. *Nat. Neurosci.* 4:781-782.

Inatome, R., T. Tsujimura, T. Hitomi, N. Mitsui, P. Hermann, S. Kuroda, H. Yamamura, and S. Yanagi. 2000. Identification of CRAM, a novel unc-33 gene family protein that associates with CRMP3 and protein-tyrosine kinase(s) in the developing rat brain. *J. Biol. Chem.* 275:27291-27302.

Ivanov, A.I., D. Hunt, M. Utech, A. Nusrat, and C.A. Parkos. 2005. Differential roles for actin polymerization and a myosin II motor in assembly of the epithelial apical junctional complex. *Molecular biology of the cell*. 16:2636-2650.

Jiang, S.X., J. Kappler, B. Zurakowski, A. Desbois, A. Aylsworth, and S.T. Hou. 2007. Calpain cleavage of collapsin response mediator proteins in ischemic mouse brain. *Eur. J. Neurosci.* 26:801-809.

Jou, T.S., D.B. Stewart, J. Stappert, W.J. Nelson, and J.A. Marrs. 1995. Genetic and biochemical dissection of protein linkages in the cadherin-catenin complex. *Proceedings of the National Academy of Sciences of the United States of America*. 92:5067-5071.

Kane, R.E. 1975. Preparation and purification of polymerized actin from sea urchin egg extracts. *J. Cell Biol.* 66:305-315.

Kawahara, T., N. Hotta, Y. Ozawa, S. Kato, K. Kano, Y. Yokoyama, M. Nagino, T. Takahashi, and K. Yanagisawa. 2013. Quantitative proteomic profiling identifies DPYSL3 as pancreatic ductal adenocarcinoma-associated molecule that regulates cell adhesion and migration by stabilization of focal adhesion complex. *PloS one*. 8:e79654.

Kemler, R. 1993. From cadherins to catenins: cytoplasmic protein interactions and regulation of cell adhesion. *Trends Genet.* 9:317-321.

Khazaei, M.R., M.P. Girouard, R. Alchini, S. Ong Tone, T. Shimada, S. Bechstedt, M. Cowan, D. Guillet, P.W. Wiseman, G. Brouhard, J.F. Cloutier, and A.E. Fournier. 2014. Collapsin Response Mediator Protein 4 regulates growth cone dynamics through the actin and microtubule cytoskeleton. *J. Biol. Chem.*

Kimura, T., H. Watanabe, A. Iwamatsu, and K. Kaibuchi. 2005. Tubulin and CRMP-2 complex is transported via Kinesin-1. *J. Neurochem.* 93:1371-1382.

Kocks, C., E. Gouin, M. Tabouret, P. Berche, H. Ohayon, and P. Cossart. 1992. L. monocytogenes-induced actin assembly requires the actA gene product, a surface protein. *Cell*. 68:521-531.

Kocks, C., J.B. Marchand, E. Gouin, H. d'Hauteville, P.J. Sansonetti, M.F. Carlier, and P. Cossart. 1995. The unrelated surface proteins ActA of Listeria monocytogenes and IcsA of Shigella flexneri are sufficient to confer actin-based motility on Listeria innocua and Escherichia coli respectively. *Mol. Microbiol.* 18:413-423.

Kovacs, E.M., M. Goodwin, R.G. Ali, A.D. Paterson, and A.S. Yap. 2002. Cadherin-directed actin assembly: E-cadherin physically associates with the Arp2/3 complex to direct actin assembly in nascent adhesive contacts. *Curr. Biol.* 12:379-382.

Kovacs, E.M., S. Verma, R.G. Ali, A. Ratheesh, N.A. Hamilton, A. Akhmanova, and A.S. Yap. 2011. N-WASP regulates the epithelial junctional actin cytoskeleton through a non-canonical post-nucleation pathway. *Nat. Cell Biol.* 13:934-943.

Kovacs, E.M., and A.S. Yap. 2002. The web and the rock: cell adhesion and the ARP2/3 complex. *Dev. Cell*. 3:760-761.

Kowara, R., Q. Chen, M. Milliken, and B. Chakravarthy. 2005. Calpain-mediated truncation of dihydropyrimidinase-like 3 protein (DPYSL3) in response to NMDA and H2O2 toxicity. *J. Neurochem.* 95:466-474.

Laurent, V., T.P. Loisel, B. Harbeck, A. Wehman, L. Grobe, B.M. Jockusch, J. Wehland, F.B. Gertler, and M.F. Carlier. 1999. Role of proteins of the Ena/VASP family in actin-based motility of Listeria monocytogenes. *J. Cell Biol.* 144:1245-1258.

Lin, P.C., P.M. Chan, C. Hall, and E. Manser. 2011. Collapsin response mediator proteins (CRMPs) are a new class of microtubule-associated protein (MAP) that selectively interacts with assembled microtubules via a taxol-sensitive binding interaction. *J. Biol. Chem.* 286:41466-41478.

Majava, V., N. Loytynoja, W.Q. Chen, G. Lubec, and P. Kursula. 2008. Crystal and solution structure, stability and post-translational modifications of collapsin response mediator protein 2. *FEBS J.* 275:4583-4596.

Martin, A.C., M. Kaschube, and E.F. Wieschaus. 2009. Pulsed contractions of an actin-myosin network drive apical constriction. *Nature*. 457:495-499.

Minturn, J.E., H.J. Fryer, D.H. Geschwind, and S. Hockfield. 1995a. TOAD-64, a gene expressed early in neuronal differentiation in the rat, is related to unc-33, a C. elegans gene involved in axon outgrowth. *J. Neurosci.* 15:6757-6766.

Minturn, J.E., D.H. Geschwind, H.J. Fryer, and S. Hockfield. 1995b. Early postmitotic neurons transiently express TOAD-64, a neural specific protein. *J. Comp. Neurol.* 355:369-379.

Morris, D.H., J. Dubnau, J.H. Park, and J.M. Rawls, Jr. 2012. Divergent functions through alternative splicing: the Drosophila CRMP gene in pyrimidine metabolism, brain, and behavior. *Genetics*. 191:1227-1238.

Mullins, R.D., J.A. Heuser, and T.D. Pollard. 1998. The interaction of Arp2/3 complex with actin: nucleation, high affinity pointed end capping, and formation of branching networks of filaments. *Proceedings of the National Academy of Sciences of the United States of America*. 95:6181-6186.

Nakagawa, H., H. Miki, M. Ito, K. Ohashi, T. Takenawa, and S. Miyamoto. 2001. N-WASP, WAVE and Mena play different roles in the organization of actin cytoskeleton in lamellipodia. *J. Cell Sci.* 114:1555-1565.

Nakamura, F., K. Kumeta, T. Hida, T. Isono, Y. Nakayama, E. Kuramata-Matsuoka, N. Yamashita, Y. Uchida, K. Ogura, K. Gengyo-Ando, S. Mitani, T. Ogino, and Y. Goshima. 2014. Amino- and carboxyl-terminal domains of Filamin-A interact with CRMP1 to mediate Sema3A signalling. *Nature communications*. 5:5325.

Niebuhr, K., F. Ebel, R. Frank, M. Reinhard, E. Domann, U.D. Carl, U. Walter, F.B. Gertler, J. Wehland, and T. Chakraborty. 1997. A novel proline-rich motif present in ActA of Listeria monocytogenes and cytoskeletal proteins is the ligand for the EVH1 domain, a protein module present in the Ena/VASP family. *EMBO J.* 16:5433-5444.

Nishimura, T., Y. Fukata, K. Kato, T. Yamaguchi, Y. Matsuura, H. Kamiguchi, and K. Kaibuchi. 2003. CRMP-2 regulates polarized Numb-mediated endocytosis for axon growth. *Nat. Cell Biol.* 5:819-826.

Nolen, B.J., N. Tomasevic, A. Russell, D.W. Pierce, Z. Jia, C.D. McCormick, J. Hartman, R. Sakowicz, and T.D. Pollard. 2009. Characterization of two classes of small molecule inhibitors of Arp2/3 complex. *Nature*. 460:1031-1034.

Oldenburg, J., G. van der Krogt, F. Twiss, A. Bongaarts, Y. Habani, J.A. Slotman, A. Houtsmuller, S. Huveneers, and J. de Rooij. 2015. VASP, zyxin and TES are

tension-dependent members of Focal Adherens Junctions independent of the alpha-catenin-vinculin module. *Scientific reports*. 5:17225.

Oliemuller, E., R. Pelaez, S. Garasa, M.J. Pajares, J. Agorreta, R. Pio, L.M. Montuenga, A. Teijeira, S. Llanos, and A. Rouzaut. 2013. Phosphorylated tubulin adaptor protein CRMP-2 as prognostic marker and candidate therapeutic target for NSCLC. *Int. J. Cancer*. 132:1986-1995.

Pan, S.H., Y.C. Chao, P.F. Hung, H.Y. Chen, S.C. Yang, Y.L. Chang, C.T. Wu, C.C. Chang, W.L. Wang, W.K. Chan, Y.Y. Wu, T.F. Che, L.K. Wang, C.Y. Lin, Y.C. Lee, M.L. Kuo, C.H. Lee, J.J. Chen, T.M. Hong, and P.C. Yang. 2011. The ability of LCRMP-1 to promote cancer invasion by enhancing filopodia formation is antagonized by CRMP-1. *J. Clin. Invest.* 121:3189-3205.

Pistor, S., T. Chakraborty, K. Niebuhr, E. Domann, and J. Wehland. 1994. The ActA protein of Listeria monocytogenes acts as a nucleator inducing reorganization of the actin cytoskeleton. *EMBO J.* 13:758-763.

Pollard, T.D. 2010. A guide to simple and informative binding assays. *Molecular biology of the cell*. 21:4061-4067.

Pollard, T.D., and C.C. Beltzner. 2002. Structure and function of the Arp2/3 complex. *Curr. Opin. Struct. Biol.* 12:768-774.

Pollard, T.D., and G.G. Borisy. 2003. Cellular motility driven by assembly and disassembly of actin filaments. *Cell*. 112:453-465.

Ponnusamy, R., and B. Lohkamp. 2013. Insights into the oligomerization of CRMPs: crystal structure of human collapsin response mediator protein 5. *J. Neurochem.*

Quinn, C.C., E. Chen, T.G. Kinjo, G. Kelly, A.W. Bell, R.C. Elliott, P.S. McPherson, and S. Hockfield. 2003. TUC-4b, a novel TUC family variant, regulates neurite outgrowth and associates with vesicles in the growth cone. *J. Neurosci.* 23:2815-2823.

Quinn, C.C., G.E. Gray, and S. Hockfield. 1999. A family of proteins implicated in axon guidance and outgrowth. *J. Neurobiol.* 41:158-164.

Reinhard, M., M. Halbrugge, U. Scheer, C. Wiegand, B.M. Jockusch, and U. Walter. 1992. The 46/50 kDa phosphoprotein VASP purified from human platelets is a novel protein associated with actin filaments and focal contacts. *EMBO J.* 11:2063-2070.

Rohatgi, R., L. Ma, H. Miki, M. Lopez, T. Kirchhausen, T. Takenawa, and M.W. Kirschner. 1999. The interaction between N-WASP and the Arp2/3 complex links Cdc42-dependent signals to actin assembly. *Cell*. 97:221-231.

Rosenblatt, J., B.J. Agnew, H. Abe, J.R. Bamburg, and T.J. Mitchison. 1997. Xenopus actin depolymerizing factor/cofilin (XAC) is responsible for the turnover of actin filaments in Listeria monocytogenes tails. *J. Cell Biol.* 136:1323-1332.

Rosslenbroich, V., L. Dai, S.L. Baader, A.A. Noegel, V. Gieselmann, and J. Kappler. 2005. Collapsin response mediator protein-4 regulates F-actin bundling. *Exp. Cell Res.* 310:434-444.

Rouiller, I., X.P. Xu, K.J. Amann, C. Egile, S. Nickell, D. Nicastro, R. Li, T.D. Pollard, N. Volkmann, and D. Hanein. 2008. The structural basis of actin filament branching by the Arp2/3 complex. *J. Cell Biol.* 180:887-895.

Sanger, J.M., J.W. Sanger, and F.S. Southwick. 1992. Host cell actin assembly is necessary and likely to provide the propulsive force for intracellular movement of Listeria monocytogenes. *Infect. Immun.* 60:3609-3619.

Schindelin, J., I. Arganda-Carreras, E. Frise, V. Kaynig, M. Longair, T. Pietzsch, S. Preibisch, C. Rueden, S. Saalfeld, B. Schmid, J.Y. Tinevez, D.J. White, V. Hartenstein, K. Eliceiri, P. Tomancak, and A. Cardona. 2012. Fiji: an open-source platform for biological-image analysis. *Nat. Methods*. 9:676-682.

Schirenbeck, A., R. Arasada, T. Bretschneider, T.E. Stradal, M. Schleicher, and J. Faix. 2006. The bundling activity of vasodilator-stimulated phosphoprotein is required for filopodium formation. *Proceedings of the National Academy of Sciences of the United States of America*. 103:7694-7699.

Schmidt, E.F., S.O. Shim, and S.M. Strittmatter. 2008. Release of MICAL autoinhibition by semaphorin-plexin signaling promotes interaction with collapsin response mediator protein. *J. Neurosci.* 28:2287-2297.

Shih, J.Y., Y.C. Lee, S.C. Yang, T.M. Hong, C.Y. Huang, and P.C. Yang. 2003. Collapsin response mediator protein-1: a novel invasion-suppressor gene. *Clin. Exp. Metastasis*. 20:69-76.

Shih, J.Y., S.C. Yang, T.M. Hong, A. Yuan, J.J. Chen, C.J. Yu, Y.L. Chang, Y.C. Lee, K. Peck, C.W. Wu, and P.C. Yang. 2001. Collapsin response mediator protein-1 and the invasion and metastasis of cancer cells. *J. Natl. Cancer Inst.* 93:1392-1400.

Shizuta, Y., H. Shizuta, M. Gallo, P. Davies, and I. Pastan. 1976. Purification and properties of filamin, and actin binding protein from chicken gizzard. *J. Biol. Chem.* 251:6562-6567.

Siddiqui, S.S., and J.G. Culotti. 1991. Examination of neurons in wild type and mutants of Caenorhabditis elegans using antibodies to horseradish peroxidase. *J. Neurogenet.* 7:193-211.

Silvestre, J., P.J. Kenis, and D.E. Leckband. 2009. Cadherin and integrin regulation of epithelial cell migration. *Langmuir : the ACS journal of surfaces and colloids*. 25:10092-10099.

Siman, R., D. Bozyczko-Coyne, M.J. Savage, and J.M. Roberts-Lewis. 1996. The calcium-activated protease calpain I and ischemia-induced neurodegeneration. *Advances in neurology*. 71:167-174; discussion 174-165.

Skoble, J., V. Auerbuch, E.D. Goley, M.D. Welch, and D.A. Portnoy. 2001. Pivotal role of VASP in Arp2/3 complex-mediated actin nucleation, actin branch-formation, and Listeria monocytogenes motility. *J. Cell Biol.* 155:89-100.

Smith, G.A., D.A. Portnoy, and J.A. Theriot. 1995. Asymmetric distribution of the Listeria monocytogenes ActA protein is required and sufficient to direct actin-based motility. *Mol. Microbiol.* 17:945-951.

Smith, P.D., M.P. Mount, R. Shree, S. Callaghan, R.S. Slack, H. Anisman, I. Vincent, X. Wang, Z. Mao, and D.S. Park. 2006. Calpain-regulated p35/cdk5 plays a central role in dopaminergic neuron death through modulation of the transcription factor myocyte enhancer factor 2. *J. Neurosci.* 26:440-447.

Steeg, P.S. 2001. Collapsin response mediator protein-1: a lung cancer invasion suppressor gene with nerve. *J. Natl. Cancer Inst.* 93:1364-1365.

Stenmark, P., D. Ogg, S. Flodin, A. Flores, T. Kotenyova, T. Nyman, P. Nordlund, and P. Kursula. 2007. The structure of human collapsin response mediator protein 2, a regulator of axonal growth. *J. Neurochem.* 101:906-917.

Suei, S., R. Seyan, P. Noguera, J. Manzi, J. Plastino, and L. Kreplak. 2011. The mechanical role of VASP in an Arp2/3-complex-based motility assay. *J. Mol. Biol.* 413:573-583.

Suraneni, P., B. Rubinstein, J.R. Unruh, M. Durnin, D. Hanein, and R. Li. 2012. The Arp2/3 complex is required for lamellipodia extension and directional fibroblast cell migration. *J. Cell Biol.* 197:239-251.

Svitkina, T.M., and G.G. Borisy. 1999. Arp2/3 complex and actin depolymerizing factor/cofilin in dendritic organization and treadmilling of actin filament array in lamellipodia. *J. Cell Biol.* 145:1009-1026.

Svitkina, T.M., E.A. Bulanova, O.Y. Chaga, D.M. Vignjevic, S. Kojima, J.M. Vasiliev, and G.G. Borisy. 2003. Mechanism of filopodia initiation by reorganization of a dendritic network. *J. Cell Biol.* 160:409-421.

Svitkina, T.M., A.B. Verkhovsky, K.M. McQuade, and G.G. Borisy. 1997. Analysis of the actin-myosin II system in fish epidermal keratocytes: mechanism of cell body translocation. *J. Cell Biol.* 139:397-415.

Tahimic, C.G., N. Tomimatsu, R. Nishigaki, A. Fukuhara, T. Toda, K. Kaibuchi, G. Shiota, M. Oshimura, and A. Kurimasa. 2006. Evidence for a role of Collapsin response mediator protein-2 in signaling pathways that regulate the proliferation of non-neuronal cells. *Biochem. Biophys. Res. Commun.* 340:1244-1250.

Takeichi, M. 1993. Cadherins in cancer: implications for invasion and metastasis. *Curr. Opin. Cell Biol.* 5:806-811.

Takemoto, T., Y. Sasaki, N. Hamajima, Y. Goshima, M. Nonaka, and H. Kimura. 2000. Cloning and characterization of the Caenorhabditis elegans CeCRMP/DHP-1 and -2; common ancestors of CRMP and dihydropyrimidinase? *Gene*. 261:259-267.

Tang, V.W., and W.M. Brieher. 2012. alpha-Actinin-4/FSGS1 is required for Arp2/3-dependent actin assembly at the adherens junction. *J. Cell Biol.* 196:115-130.

Terman, J.R., T. Mao, R.J. Pasterkamp, H.H. Yu, and A.L. Kolodkin. 2002. MICALs, a family of conserved flavoprotein oxidoreductases, function in plexin-mediated axonal repulsion. *Cell*. 109:887-900.

Theriot, J.A., T.J. Mitchison, L.G. Tilney, and D.A. Portnoy. 1992. The rate of actin-based motility of intracellular Listeria monocytogenes equals the rate of actin polymerization. *Nature*. 357:257-260.

Tilney, L.G., and D.A. Portnoy. 1989. Actin filaments and the growth, movement, and spread of the intracellular bacterial parasite, Listeria monocytogenes. *J. Cell Biol.* 109:1597-1608.

Uchida, N., Y. Honjo, K.R. Johnson, M.J. Wheelock, and M. Takeichi. 1996. The catenin/cadherin adhesion system is localized in synaptic junctions bordering transmitter release zones. *J. Cell Biol.* 135:767-779.

Uchida, Y., T. Ohshima, Y. Sasaki, H. Suzuki, S. Yanai, N. Yamashita, F. Nakamura, K. Takei, Y. Ihara, K. Mikoshiba, P. Kolattukudy, J. Honnorat, and Y. Goshima. 2005. Semaphorin3A signalling is mediated via sequential Cdk5 and GSK3beta phosphorylation of CRMP2: implication of common phosphorylating mechanism underlying axon guidance and Alzheimer's disease. *Genes Cells*. 10:165-179.

Van Troys, M., A. Lambrechts, V. David, H. Demol, M. Puype, J. Pizarro-Cerda, K. Gevaert, P. Cossart, and J. Vandekerckhove. 2008. The actin propulsive machinery: the proteome of Listeria monocytogenes tails. *Biochem. Biophys. Res. Commun.* 375:194-199.

Varrin-Doyer, M., P. Vincent, S. Cavagna, N. Auvergnon, N. Noraz, V. Rogemond, J. Honnorat, M. Moradi-Ameli, and P. Giraudon. 2009. Phosphorylation of collapsin response mediator protein 2 on Tyr-479 regulates CXCL12-induced T lymphocyte migration. *J. Biol. Chem.* 284:13265-13276.

Vasioukhin, V., C. Bauer, M. Yin, and E. Fuchs. 2000. Directed actin polymerization is the driving force for epithelial cell-cell adhesion. *Cell*. 100:209-219.

Verma, S., S.P. Han, M. Michael, G.A. Gomez, Z. Yang, R.D. Teasdale, A. Ratheesh, E.M. Kovacs, R.G. Ali, and A.S. Yap. 2012. A WAVE2-Arp2/3 actin nucleator apparatus supports junctional tension at the epithelial zonula adherens. *Molecular biology of the cell*. 23:4601-4610.

Verma, S., A.M. Shewan, J.A. Scott, F.M. Helwani, N.R. den Elzen, H. Miki, T. Takenawa, and A.S. Yap. 2004. Arp2/3 activity is necessary for efficient formation of E-cadherin adhesive contacts. *J. Biol. Chem.* 279:34062-34070.

Veyrac, A., S. Reibel, J. Sacquet, M. Mutin, J.P. Camdessanche, P. Kolattukudy, J. Honnorat, and F. Jourdan. 2011. CRMP5 regulates generation and survival of newborn neurons in olfactory and hippocampal neurogenic areas of the adult mouse brain. *PloS one*. 6:e23721.

Vincent, P., Y. Collette, R. Marignier, C. Vuaillat, V. Rogemond, N. Davoust, C. Malcus, S. Cavagna, A. Gessain, I. Machuca-Gayet, M.F. Belin, T. Quach, and P. Giraudon. 2005. A role for the neuronal protein collapsin response mediator protein 2 in T lymphocyte polarization and migration. *J. Immunol.* 175:7650-7660.

Wadsworth, P. 1999. Microinjection of mitotic cells. *Methods in cell biology*. 61:219-231.

Wagner, A.R., Q. Luan, S.L. Liu, and B.J. Nolen. 2013. Dip1 defines a class of Arp2/3 complex activators that function without preformed actin filaments. *Curr. Biol.* 23:1990-1998.

Wang, L.H., and S.M. Strittmatter. 1996. A family of rat CRMP genes is differentially expressed in the nervous system. *J. Neurosci.* 16:6197-6207.

Wang, L.H., and S.M. Strittmatter. 1997. Brain CRMP forms heterotetramers similar to liver dihydropyrimidinase. *J. Neurochem.* 69:2261-2269.

Waterman-Storer, C.M., and E.D. Salmon. 1997. Actomyosin-based retrograde flow of microtubules in the lamella of migrating epithelial cells influences microtubule dynamic instability and turnover and is associated with microtubule breakage and treadmilling. *J. Cell Biol.* 139:417-434.

Weaver, A.M., A.V. Karginov, A.W. Kinley, S.A. Weed, Y. Li, J.T. Parsons, and J.A. Cooper. 2001. Cortactin promotes and stabilizes Arp2/3-induced actin filament network formation. *Curr. Biol.* 11:370-374.

Weber, G.F., M.A. Bjerke, and D.W. DeSimone. 2011. Integrins and cadherins join forces to form adhesive networks. *J. Cell Sci.* 124:1183-1193.

Welch, M.D., A. Iwamatsu, and T.J. Mitchison. 1997. Actin polymerization is induced by Arp2/3 protein complex at the surface of Listeria monocytogenes. *Nature*. 385:265-269.

Welch, M.D., and M. Way. 2013. Arp2/3-mediated actin-based motility: a tail of pathogen abuse. *Cell Host Microbe*. 14:242-255.

Wittmann, T., and C.M. Waterman-Storer. 2001. Cell motility: can Rho GTPases and microtubules point the way? *J. Cell Sci.* 114:3795-3803.

Yamada, S., S. Pokutta, F. Drees, W.I. Weis, and W.J. Nelson. 2005. Deconstructing the cadherin-catenin-actin complex. *Cell*. 123:889-901.

Yamashita, N., A. Morita, Y. Uchida, F. Nakamura, H. Usui, T. Ohshima, M. Taniguchi, J. Honnorat, N. Thomasset, K. Takei, T. Takahashi, P. Kolattukudy, and Y. Goshima. 2007. Regulation of spine development by semaphorin3A through cyclin-dependent kinase 5 phosphorylation of collapsin response mediator protein 1. *J. Neurosci.* 27:12546-12554.

Yamashita, N., T. Ohshima, F. Nakamura, P. Kolattukudy, J. Honnorat, K. Mikoshiba, and Y. Goshima. 2012. Phosphorylation of CRMP2 (collapsin response mediator protein 2) is involved in proper dendritic field organization. *J. Neurosci.* 32:1360-1365.

Yamazaki, D., T. Oikawa, and T. Takenawa. 2007. Rac-WAVE-mediated actin reorganization is required for organization and maintenance of cell-cell adhesion. *J. Cell Sci.* 120:86-100.

Yang, C., and T. Svitkina. 2011a. Filopodia initiation: focus on the Arp2/3 complex and formins. *Cell adhesion & migration*. 5:402-408.

Yang, C., and T. Svitkina. 2011b. Visualizing branched actin filaments in lamellipodia by electron tomography. *Nat. Cell Biol.* 13:1012-1013; author reply 1013-1014.

Yoneda, A., M. Morgan-Fisher, R. Wait, J.R. Couchman, and U.M. Wewer. 2012. A collapsin response mediator protein 2 isoform controls myosin II-mediated cell migration and matrix assembly by trapping ROCK II. *Mol. Cell. Biol.* 32:1788-1804.

Yonemura, S., M. Itoh, A. Nagafuchi, and S. Tsukita. 1995. Cell-to-cell adherens junction formation and actin filament organization: similarities and differences between non-polarized fibroblasts and polarized epithelial cells. *J. Cell Sci.* 108 (Pt 1):127-142.

Yoshimura, T., Y. Kawano, N. Arimura, S. Kawabata, A. Kikuchi, and K. Kaibuchi. 2005. GSK-3beta regulates phosphorylation of CRMP-2 and neuronal polarity. *Cell*. 120:137-149.

Yuasa-Kawada, J., R. Suzuki, F. Kano, T. Ohkawara, M. Murata, and M. Noda. 2003. Axonal morphogenesis controlled by antagonistic roles of two CRMP subtypes in microtubule organization. *Eur. J. Neurosci.* 17:2329-2343.

Zalevsky, J., I. Grigorova, and R.D. Mullins. 2001. Activation of the Arp2/3 complex by the Listeria acta protein. Acta binds two actin monomers and three subunits of the Arp2/3 complex. *J. Biol. Chem.* 276:3468-3475.

Zencheck, W.D., H. Xiao, B.J. Nolen, R.H. Angeletti, T.D. Pollard, and S.C. Almo. 2009. Nucleotide- and activator-dependent structural and dynamic changes of arp2/3 complex monitored by hydrogen/deuterium exchange and mass spectrometry. *J. Mol. Biol.* 390:414-427.

Zhou, F.Q., and C.S. Cohan. 2001. Growth cone collapse through coincident loss of actin bundles and leading edge actin without actin depolymerization. *J. Cell Biol.* 153:1071-1084.

Zhu, L.Q., H.Y. Zheng, C.X. Peng, D. Liu, H.L. Li, Q. Wang, and J.Z. Wang. 2010. Protein phosphatase 2A facilitates axonogenesis by dephosphorylating CRMP2. *J. Neurosci.* 30:3839-3848.

CHAPTER 6: FIGURES

- Data published in Yu-Kemp and Brieher, *Journal of Biological Chemistry* (2016): Fig. 1, 2, 4, 7 and 9.
- Data used in manuscript for submission to *Journal of Cell Biology*: Fig. 10 A, 10 B, 12, 14, 15 A, 15 C, 15 D, 16 (except K), 17 A, 17 C, 17 D (partial), 23 C (partial). *see Appendix A.*

Figure 1

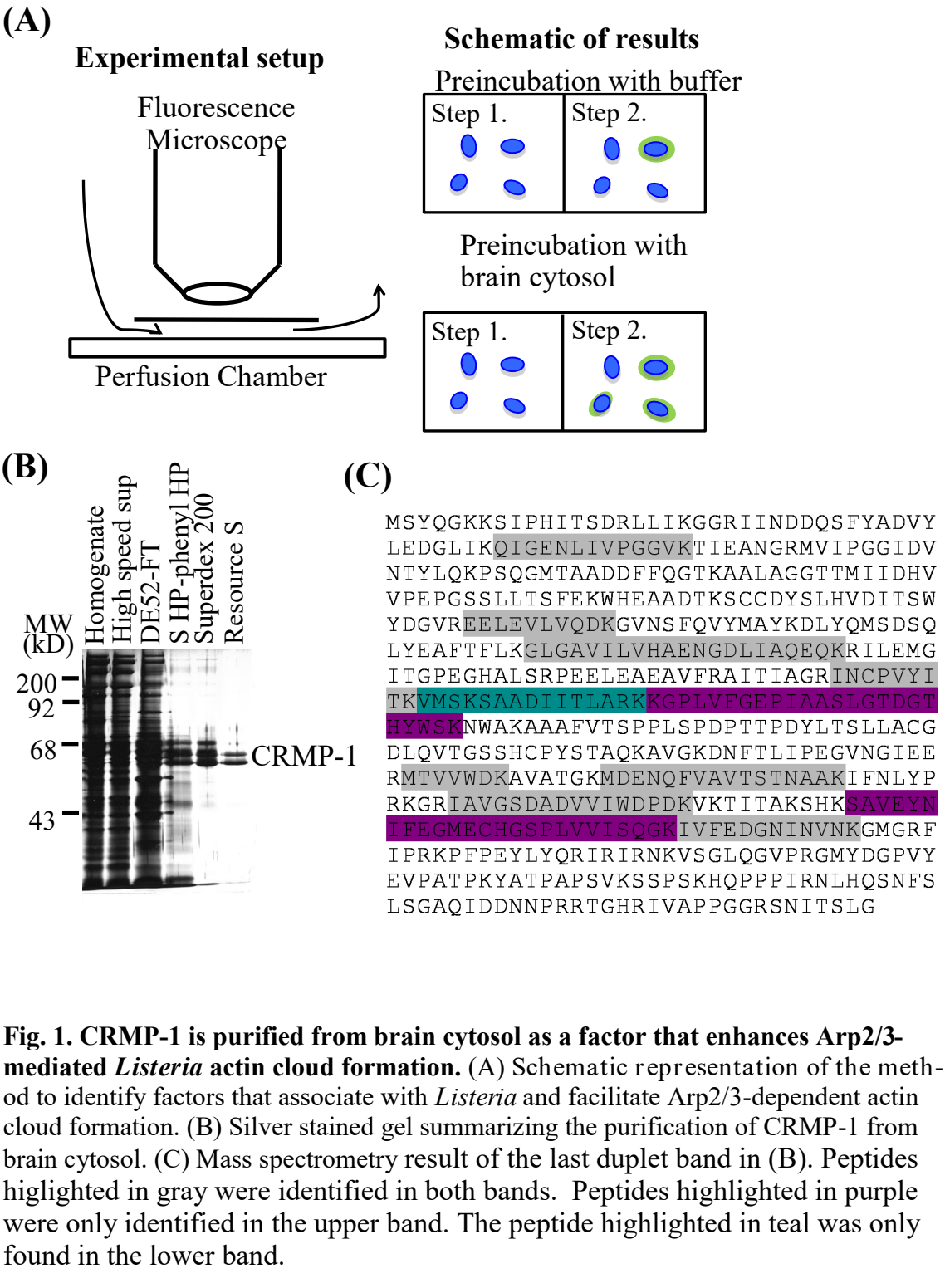

Fig. 1. CRMP-1 is purified from brain cytosol as a factor that enhances Arp2/3-mediated *Listeria* actin cloud formation. (A) Schematic representation of the method to identify factors that associate with *Listeria* and facilitate Arp2/3-dependent actin cloud formation. (B) Silver stained gel summarizing the purification of CRMP-1 from brain cytosol. (C) Mass spectrometry result of the last duplet band in (B). Peptides higlighted in gray were identified in both bands. Peptides highlighted in purple were only identified in the upper band. The peptide highlighted in teal was only found in the lower band.

Images: courtesy of William M. Brieher.

Figure 2

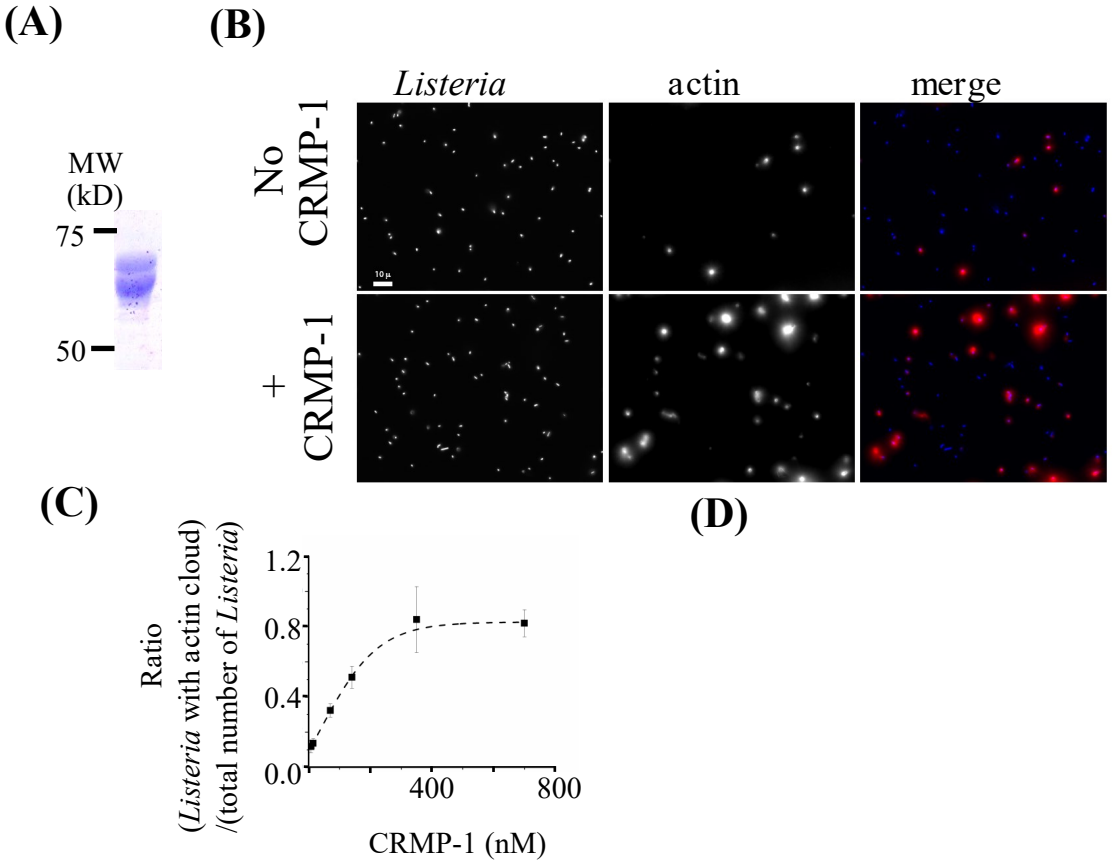

Fig. 2. Preincubation of CRMP-1 with *Listeria* can boost *Listeria* actin cloud formation. (A) Coomassie gel with purified recombinant His-tagged human CRMP-1. (B) Recombinant CRMP-1 potentiates Arp2/3-dependent cloud formation. Field of *Listeria* preincubated with buffer (top), or with recombinant CRMP-1 (bottom), using the method described in Fig. 1. *Listeria* were labeled with DAPI and pseudo-colored in bule. FITC-labeled actin was pseudo-colored in red. (C) Dose-dependent effect of CRMP-1 on *Listeria* actin cloud formation. Scale bar: 20 μ m.

Image (B): courtesy of William M. Brieher.

Figure 3

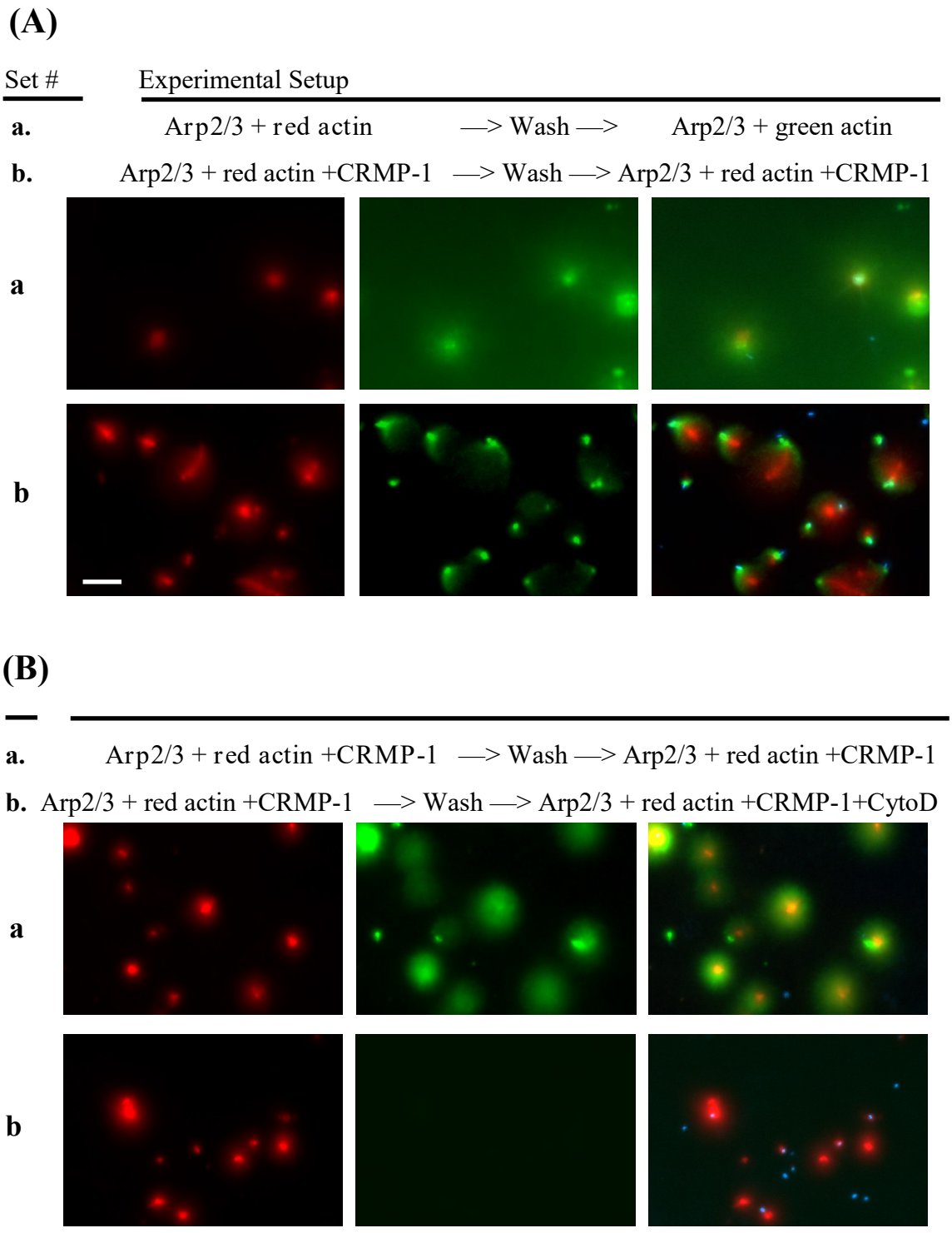

Fig. 3. CRMP-1 successfully facilitates actin tail formation when CRMP-1 is provided in reaction buffer, without preincubation with the *Listeria*. (A) *Listeria* grew longer actin tails in the presence of CRMP-1. (B) Cyto D blocks actin polymerization on *Listeria* even in the presence of CRMP-1 and Arp2/3. Scale bars are 20 μ m.

Figure 4

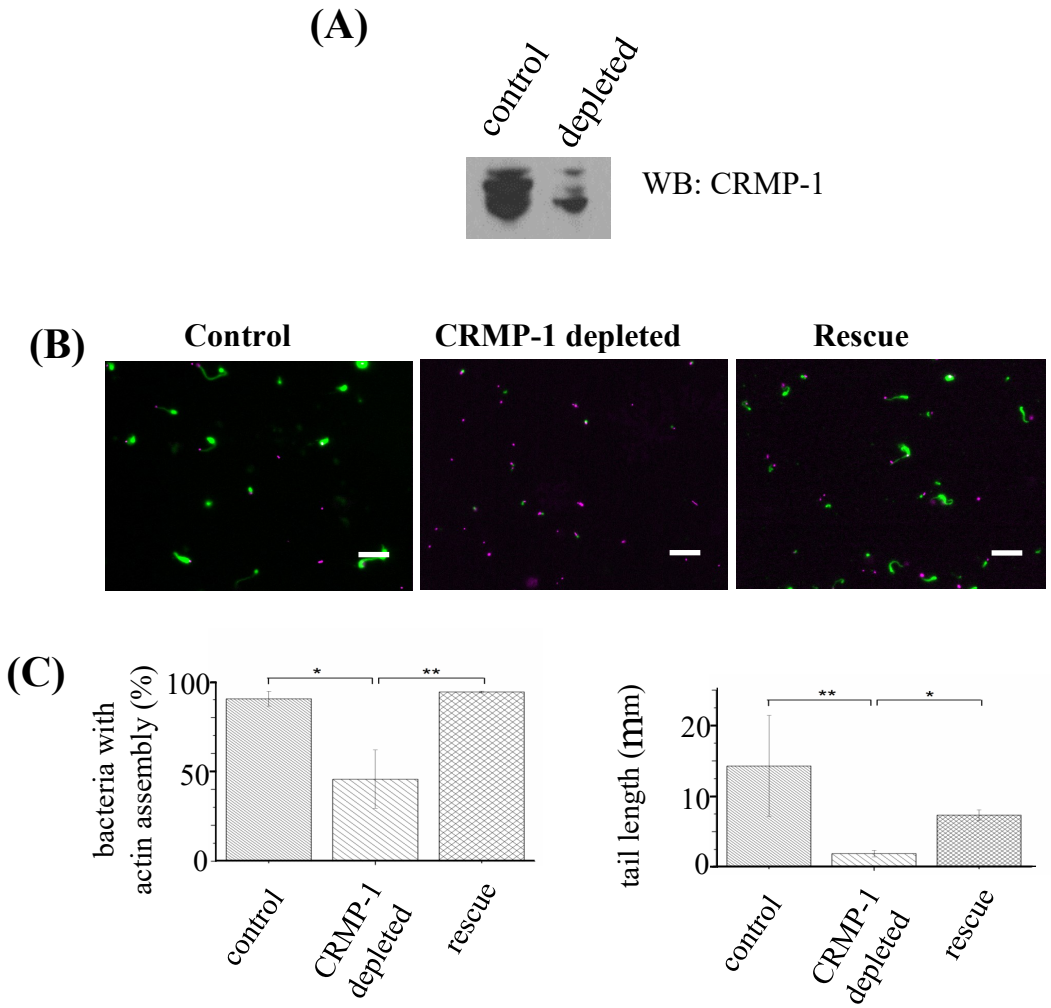

Fig. 4. CRMP-1 is essential for *Listeria* actin cloud formation. (A) Western blot (WB)against CRMP-1 indicating the amount of endogenous CRMP in brain cytosol and the efficiency of the immunodepletion. (B) Immunodepleting CRMP-1 from brain cytosol decreases actin tail formation. Blue: DAPI-labeled *Listeria*; green: fluorescent-labeled actin. (C) Quantifications of (B). Scale bar: 20 μ m.

Figure 5

(A)

Experimental Condition	Step 1 Preincubation	Step 2 Initial Nucleation	Step 3 Elongation/Nucleation
a.	EVL	Arp2/3 + dim actin	Arp2/3 + bright actin
b.	EVL	Arp2/3 + dim actin	bright actin

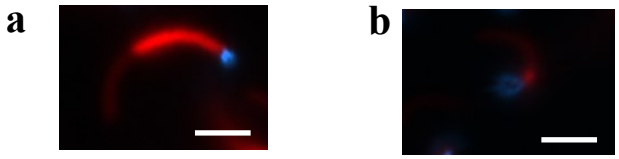

(B)

Experimental Condition	Step 1 Preincubation	Step 2 Initial Nucleation	Step 3 Elongation/Nucleation
a.	EVL	Arp2/3 + red actin	green actin
b.	CRMP-1	Arp2/3 + red actin	green actin
c.	CRMP-1 + EVL	Arp2/3 + red actin	green actin

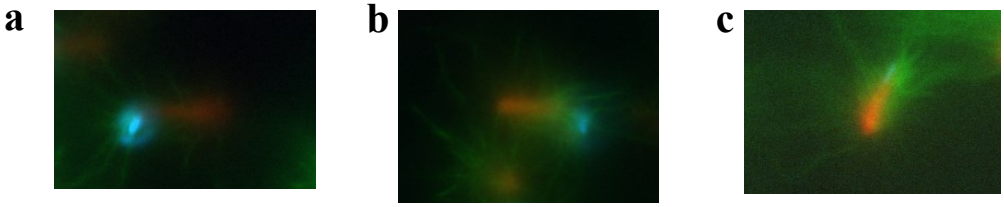

Fig. 5. CRMP-1 does not support Arp2/3-independent actin tail growth in a preincubation assay. (A) Three step preincubation assay shows that continuous supply of Arp2/3 is essential for effective tail growth. *Listeria* was preincubated with 125 nM EVL in step 1. To initiate the actin tail, the preincubation solution was replaced with Arp2/3 and dim actin (step 2). To test the role of Arp2/3 for tail elongation, the nucleating solution was replaced with a solution containing bright actin in the presence (condition a) or absence (condition b) of Arp2/3 (step 3). Red: actin (dim or bright); blue: *Listeria.* (B) CRMP-1 cannot elongate tail in the absence of Arp2/3 complex. In step 1, *Listeria* was preincubated with 125 nM EVL, 125 nM CRMP-1, or CRMP-1 plus EVL (step 1). To initiate the actin tail was initiated by replacing the preincubation solution with Arp2/3 and the red actin (step 2). For the elongation the actin tail, green actin was provided after the removal of the nucleation solution (step 3). Red and green: actin; blue: *Listeria.* Scale bar: 5 μ M.

Figure 6

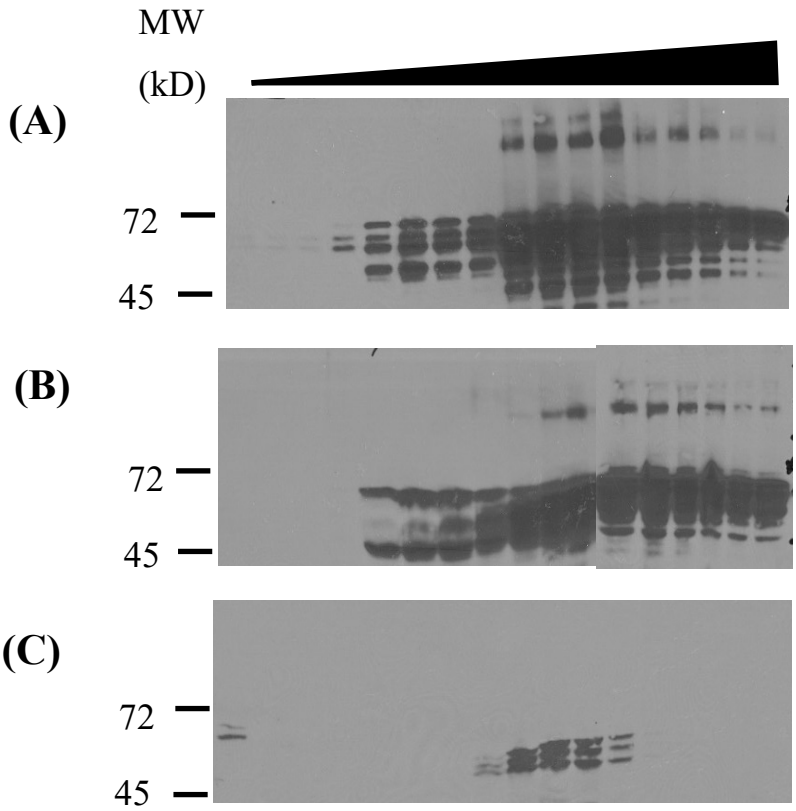

Fig. 6. Recombinant CRMP-1 shifts to a higher buoyant density fraction in brain extract. (A)-(C) Western blotting against CRMP-1 in the fractions from sucrose gradient. Left to right: low sucrose concentration to high sucrose concentration. (A) The distribution profile of recombinant CRMP-1 alone. (B) The distribution profile of recombinant CRMP-1 after incubating one hour in brain extract. Note that we lost CRMP-1 signal in low-sucrose-gradient fractions. (C) The distribution profile of endogenous CRMP -1 in brain extract.

Figure 7

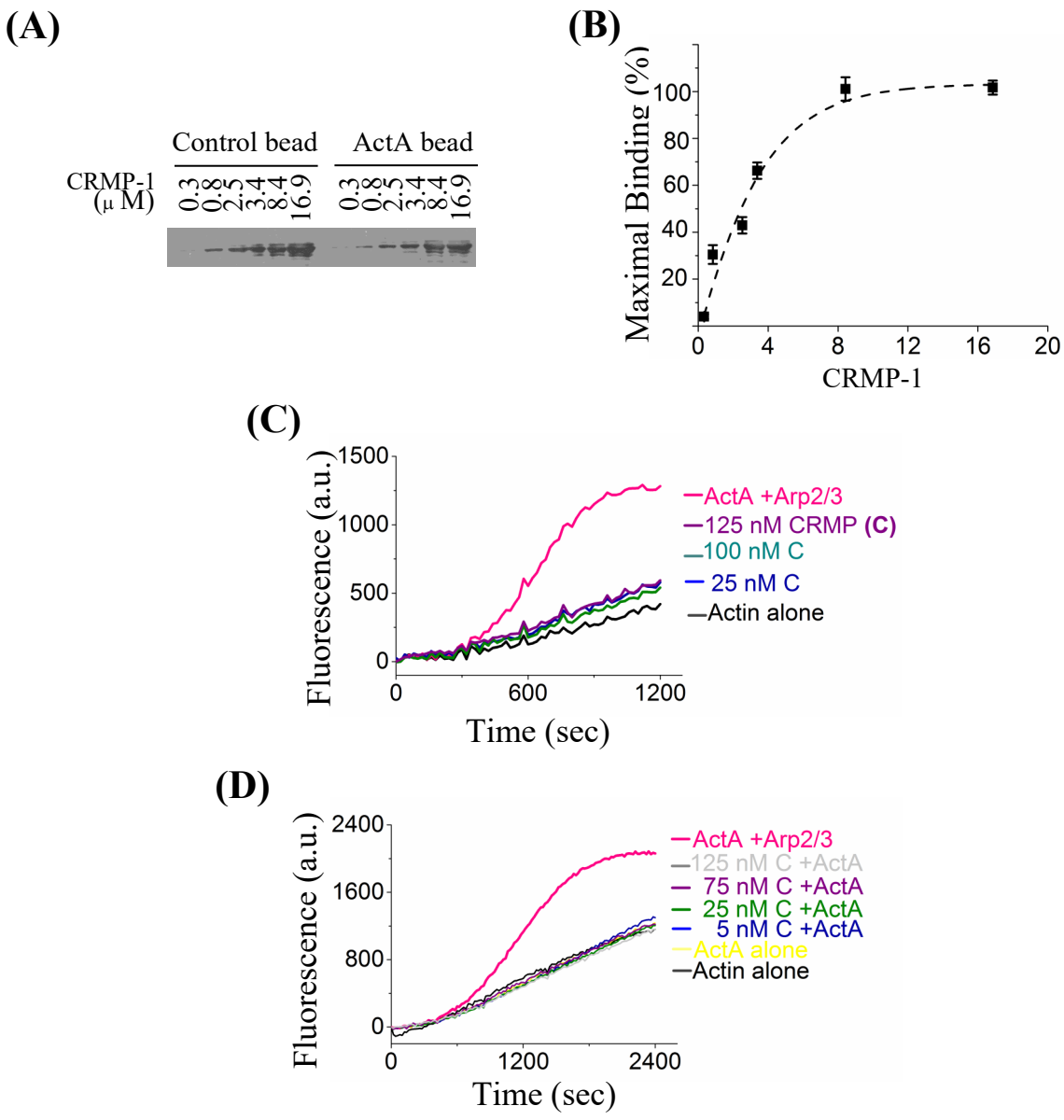
(A)
Control bead
ActA bead
CRMP-1 (μ M)
0.3
0.8
2.5
3.4
8.4
16.9
(B)
Maximal Binding (%)
CRMP-1
(C)
Fluorescence (a.u.)
Time (sec)
ActA +Arp2/3
125 nM CRMP (C)
100 nM C
25 nM C
Actin alone
(D)
Fluorescence (a.u.)
Time (sec)
ActA +Arp2/3
125 nM C +ActA
75 nM C +ActA
25 nM C +ActA
5 nM C +ActA
ActA alone
Actin alone

Figure 7 (cont.)

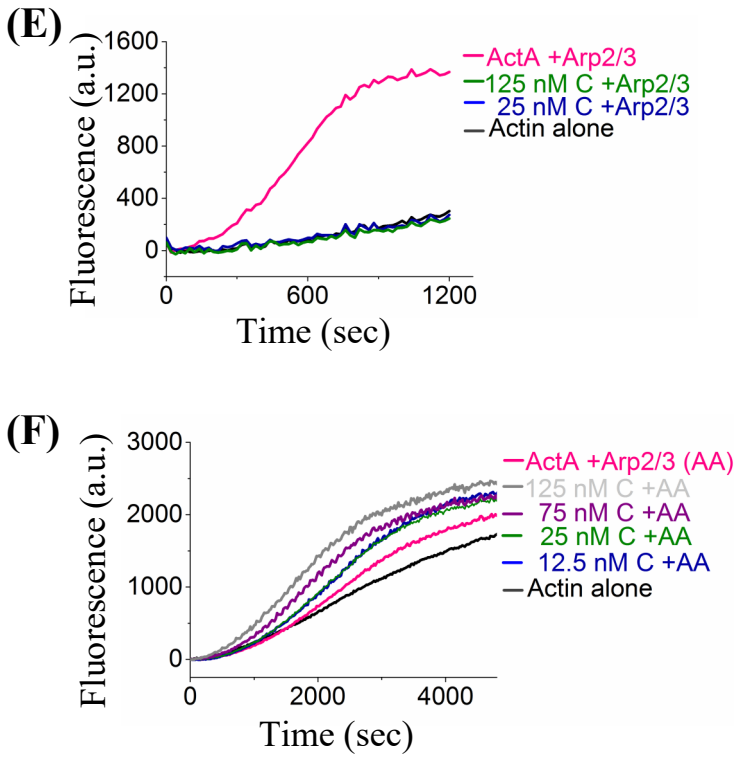

Fig. 7. CRMP-1 facilitates ActA-Arp2/3 mediated actin polymerization. (A) & (B) CRMP-1 binds to ActA. (A) The image is a representative result from western blotting against CRMP-1. It shows the amount of CRMP-1 remaining in the supernatants after co-sedimentation with control or ActA beads. The initial amount of CRMP-1 provided to each reaction was labeled on the top of each panel. (B) The binding curve was generated from the average of three experiments. Error bars are the mean values $\pm$ s.d. The affinity of CRMP-1 for ActA is 2.5 μ M. The gel is a representative western blot of the binding assay. (C)-(F): Pyrene assembly assay testing the role of CRMP-1 in actin polymerization: (A) CRMP-1 alone; (B) CRMP-1 and ActA; (C) CRMP-1 and Arp2/3; (D) CRMP-1 with Arp2/3 and ActA. In different testing conditions, we used the curve of ActA-Arp2/3 polymerization as a positive control. The curve of actin alone is the negative control. a.u., arbitrary units.

Figure 8

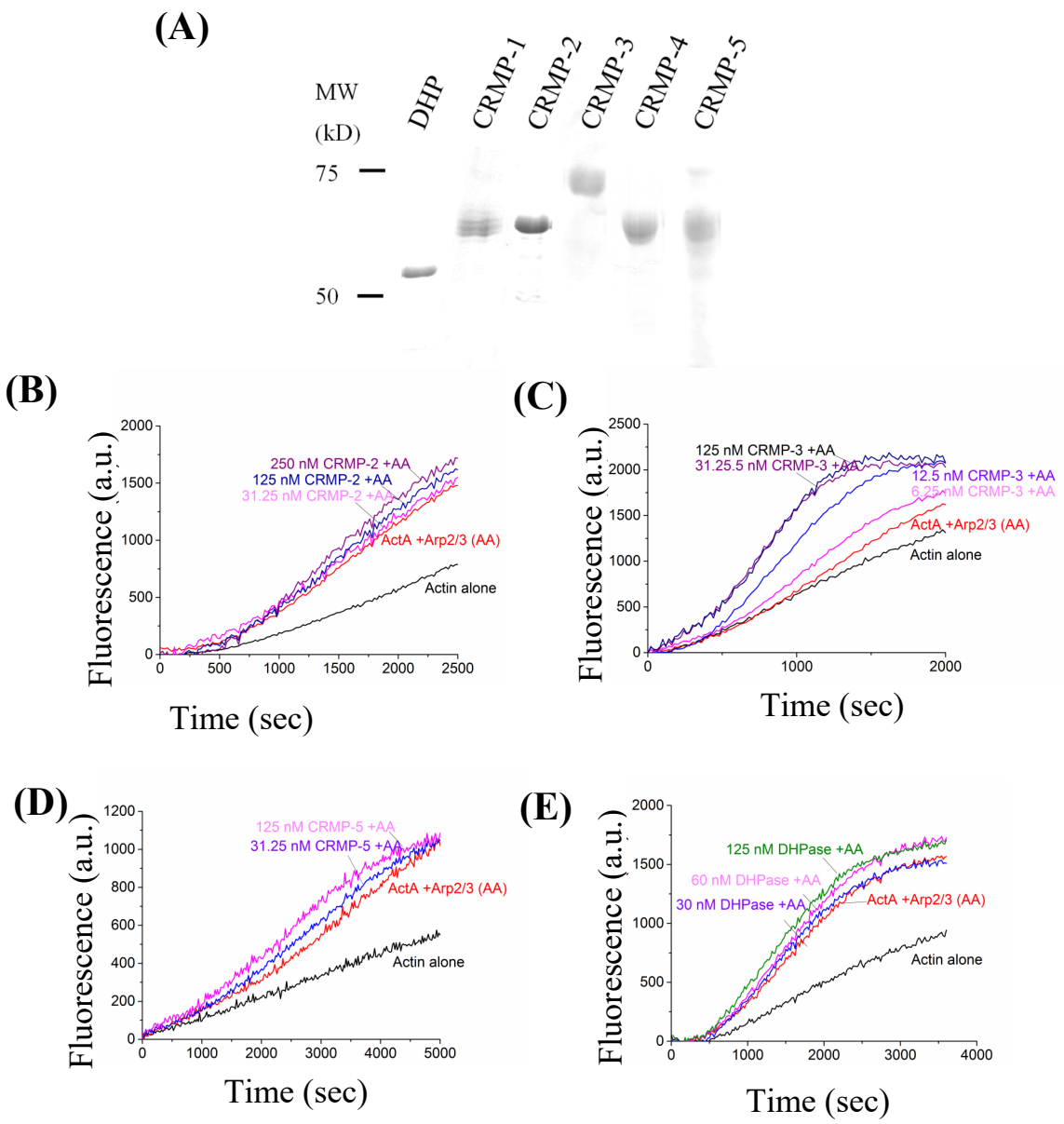

Fig. 8. CRMP family members and DHPase enhance ActA-Arp2/3 polymerization differently. (A) Commassie gel showing the purified recombinant DHPase and different CRMP homologs. (B)-(E) Pyrene assembly assay testing the role of different CRMPs and DHPase in ActA-Arp2/3 actin polymerization: (B) CRMP-2; (C) CRMP-3; (D) CRMP-5; (E) DHPase.

Figure 9

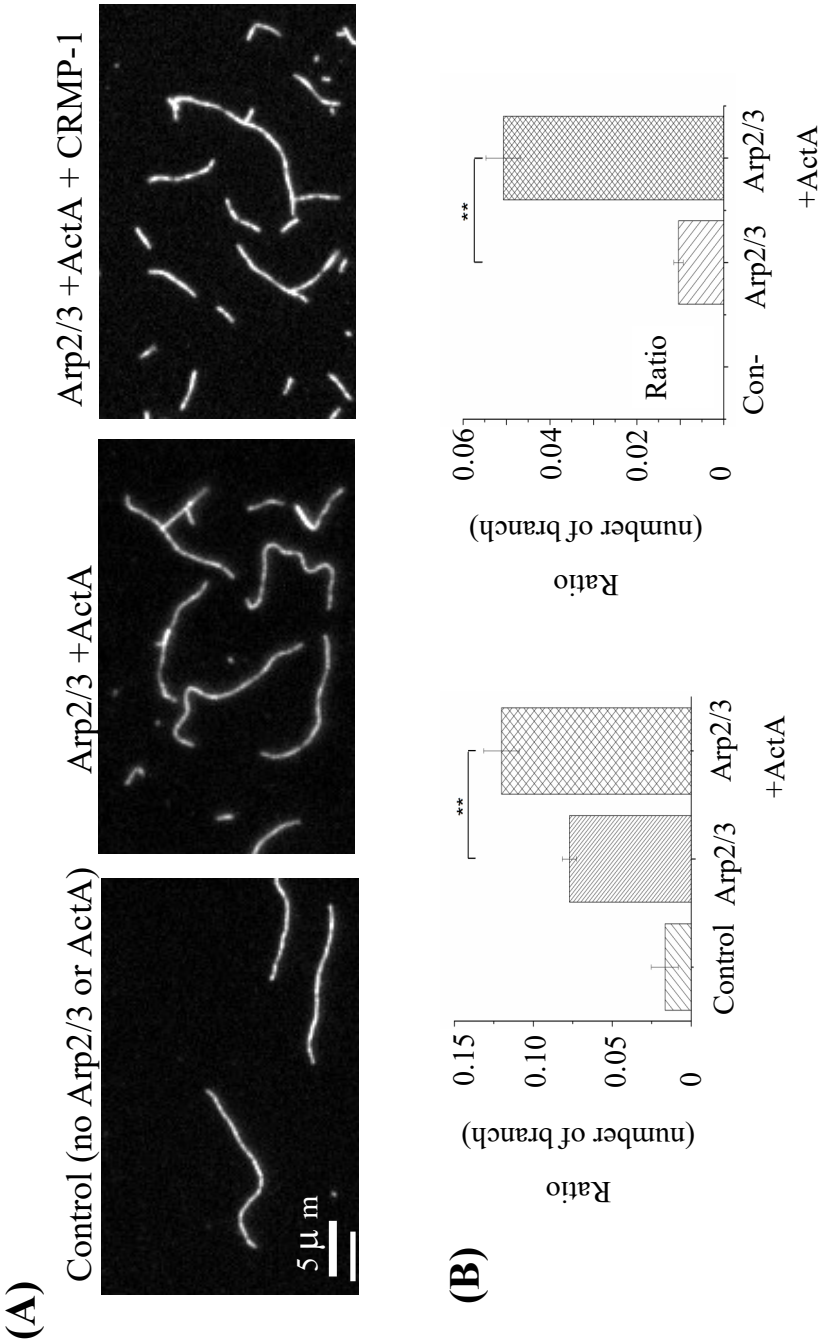
(A)
Control (no Arp2/3 or ActA)
Arp2/3 +ActA
Arp2/3 +ActA + CRMP-1
5 μ m
(B)
Ratio
(number of branch)
0.15
0.10
0.05
0
Control
Arp2/3
Arp2/3 +ActA
**
Ratio
(number of branch)
0.06
0.04
0.02
0
Ratio
Con-
Arp2/3
Arp2/3 +ActA
**

Figure 9 (cont.)

Fig. 9. CRMP-1 is purified from brain cytosol as a factor that enhances Arp2/3-mediated *Listeria* actin cloud formation. (A) Actin branching assay with CRMP-1, ActA and Arp2/3. (B) Quantification results of (A) demonstrate that more branched filaments are detected in the presence CRMP-1. Quantifications were done by three independent experiments (n=3). Bars show the mean values± s.d. * $p<0.05$. ** $p<0.01$. (C) Co-sendimentation assay and a representative coomassie-stained gel demonstrating that CRMP-1 binds F-actin. The value above the lanes indicates the initial amount of CRMP -1 provided in each reaction. The pellets after centrifugation are labeled as P on top of each panel; the supernatants are labeled as S. Points on the graph are the mean values ± s.d.

Figure 10

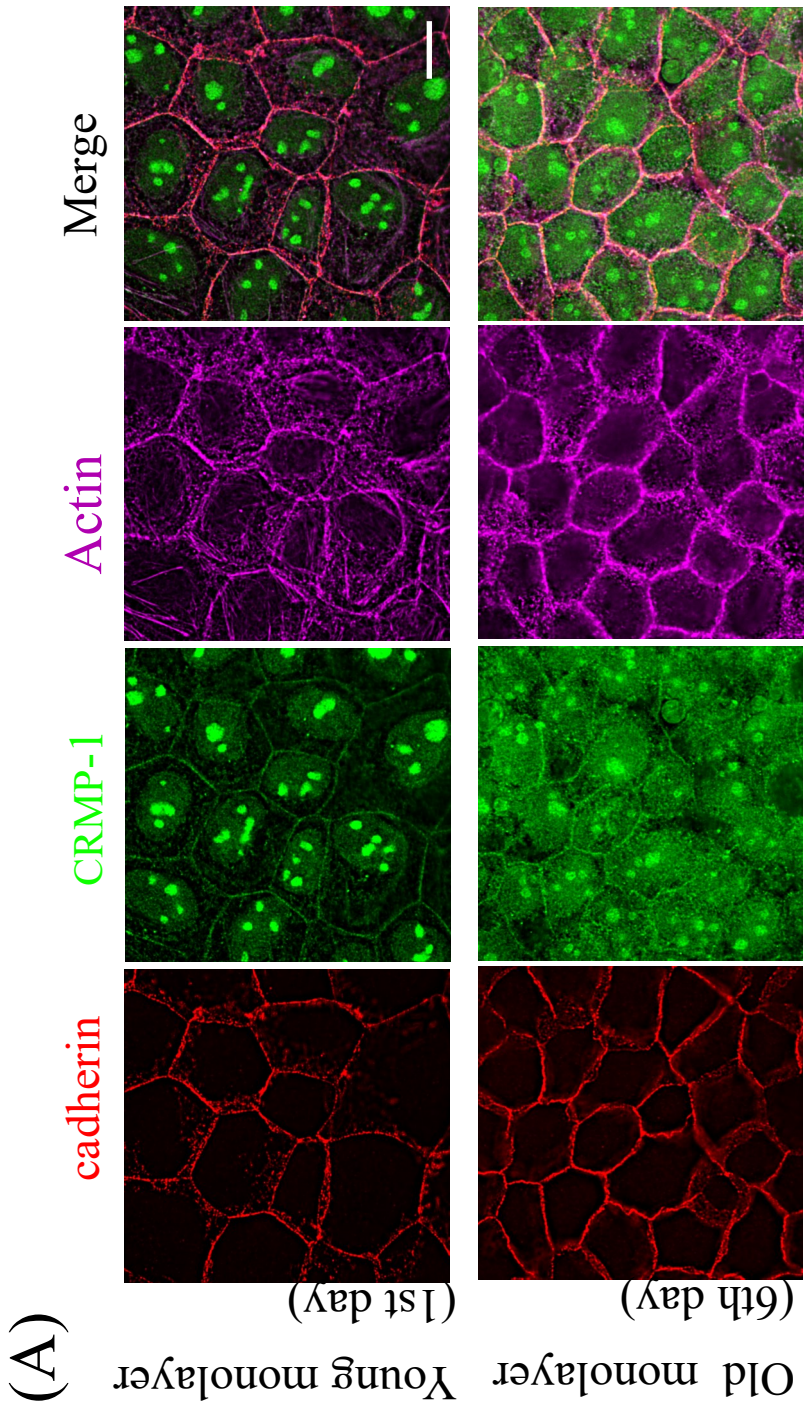
(A)
Young monolayer
(1st day)
Old monolayer
(6th day)
cadherin
CRMP-1
Actin
Merge

Figure 10 (cont.)

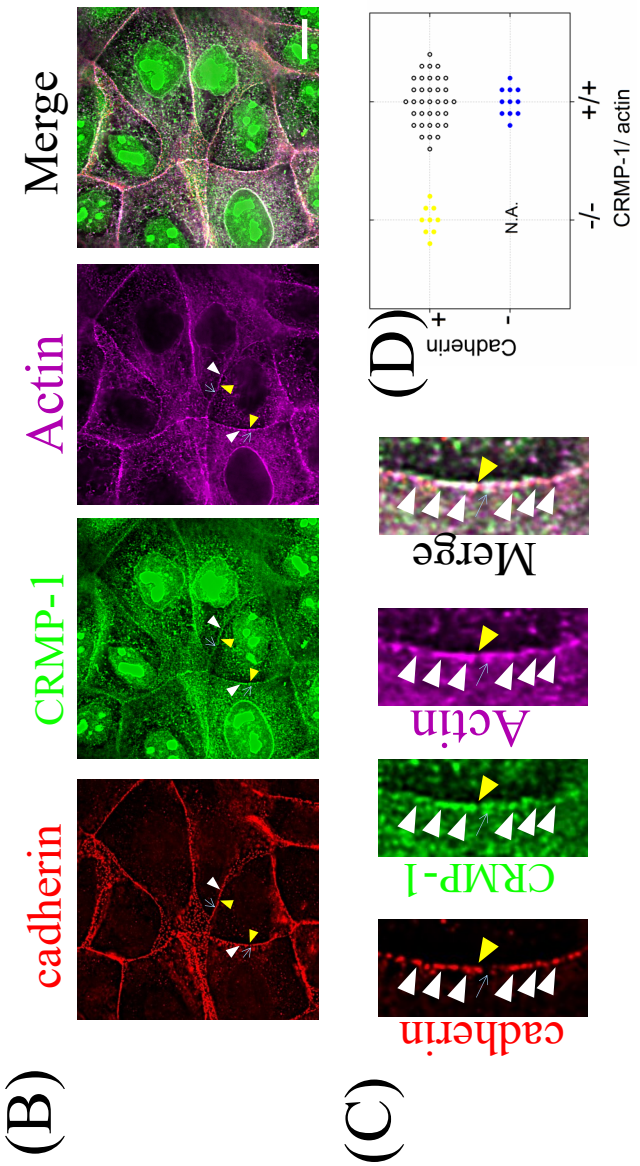

Figure 10. CRMP-1 signal locates to cadherin-mediate cell-cell contacts. (A) & (B) The apical view of a confluent monolayer of MDCK cells showing that CRMP-1 localizes to cadherin mediated cell-cell contacts. CRMP-1 signal at this location can be detected in both young monolayer (1st day of confluency) (A, upper panel), the old monolayer (6th day of confluency) (A, lower panel) and the mid-age monolayer (3rd day of confluency) (B). (C) A close view of (B) showing that CRMP-1 signal overlapped with actin signal and the majority of cadherin signal along cell-cell contacts. White arrowheads point at the region that E-cadherin, CRMP-1 and actin are colocalized. Yellow arrowhead indicates the spot that has E-cadherin yet not CRMP-1 nor actin; blue arrow indicates the spot that contains no E-cadherin but has CRMP-1 and actin. (D) Quantifications of (C). White arrow points out the area that CRMP-1 signal overlaps with E-cadherin signal. Yellow arrowhead indicates the sites that have CRMP-1 but no cadherin. Scale bar: 10 μ m.

Figure 11

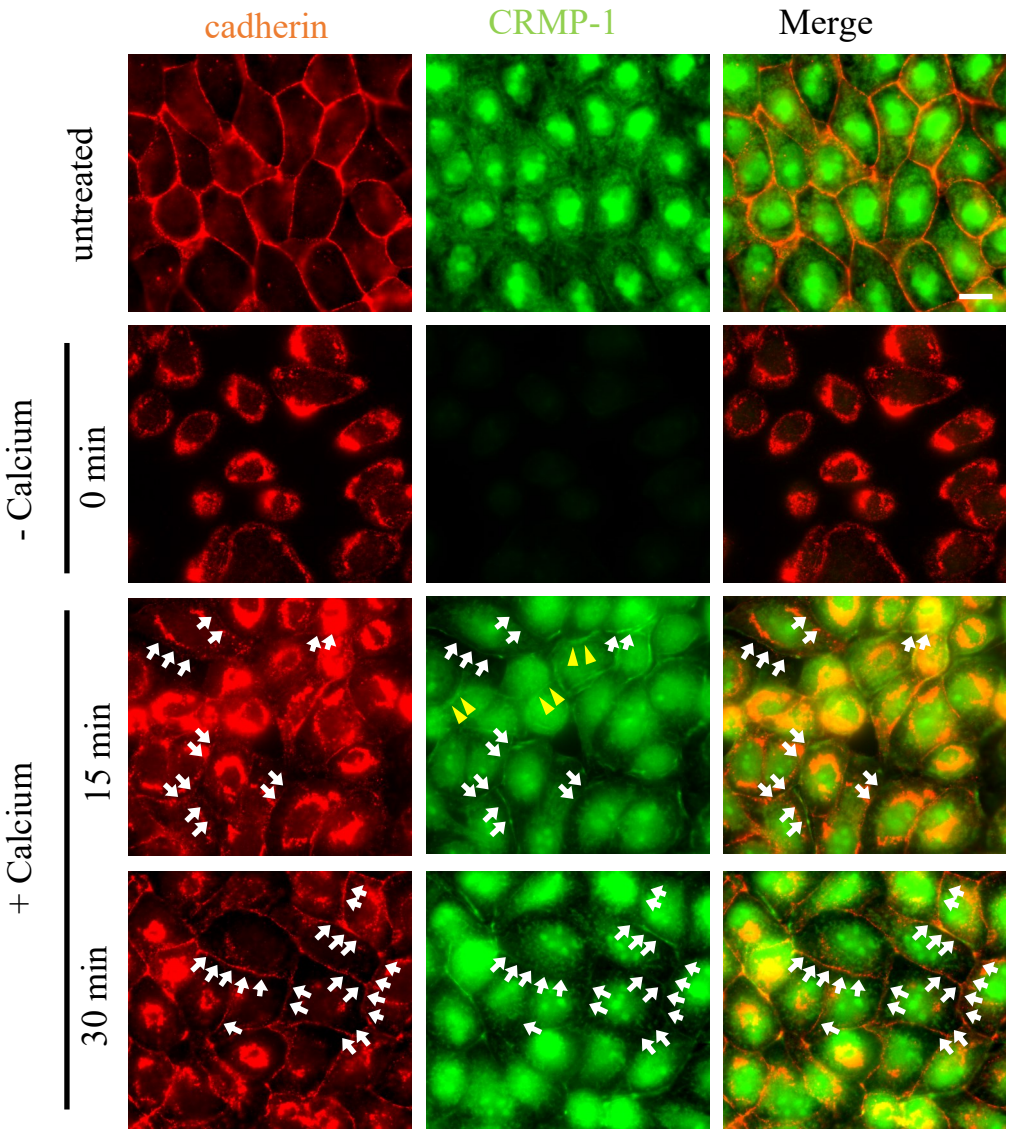

Fig. 11. CRMP-1 locates to cell-cell periphery during cell-cell contact formation. Calcium switch experiment indicating CRMP-1 signal appears at cell boundary while cell-cell contact starts to form. Scale bar: 10 μ m.

Figure 12

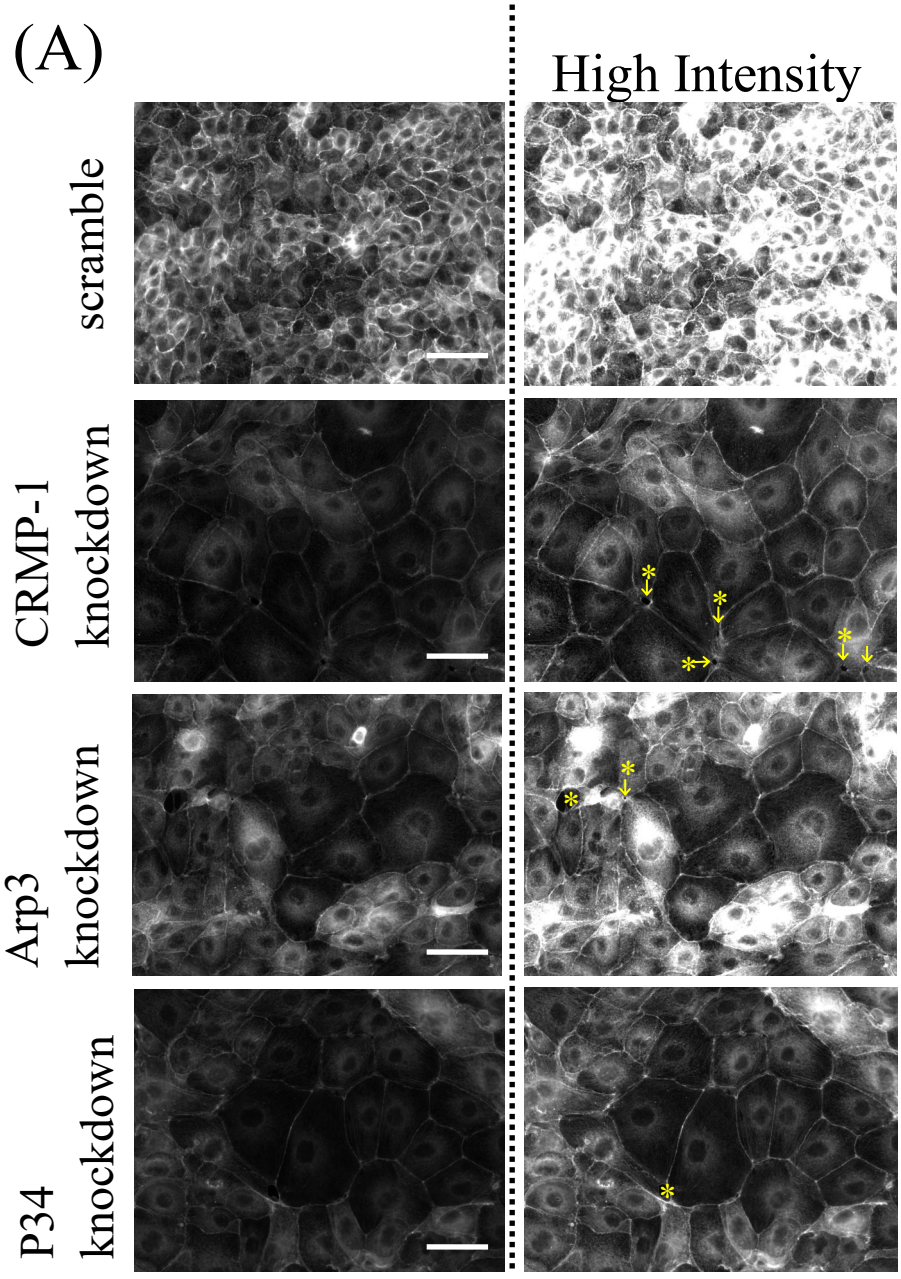
(A)
High Intensity
scramble
CRMP-1 knockdown
Arp3 knockdown
P34 knockdown

Figure 12 (cont.)

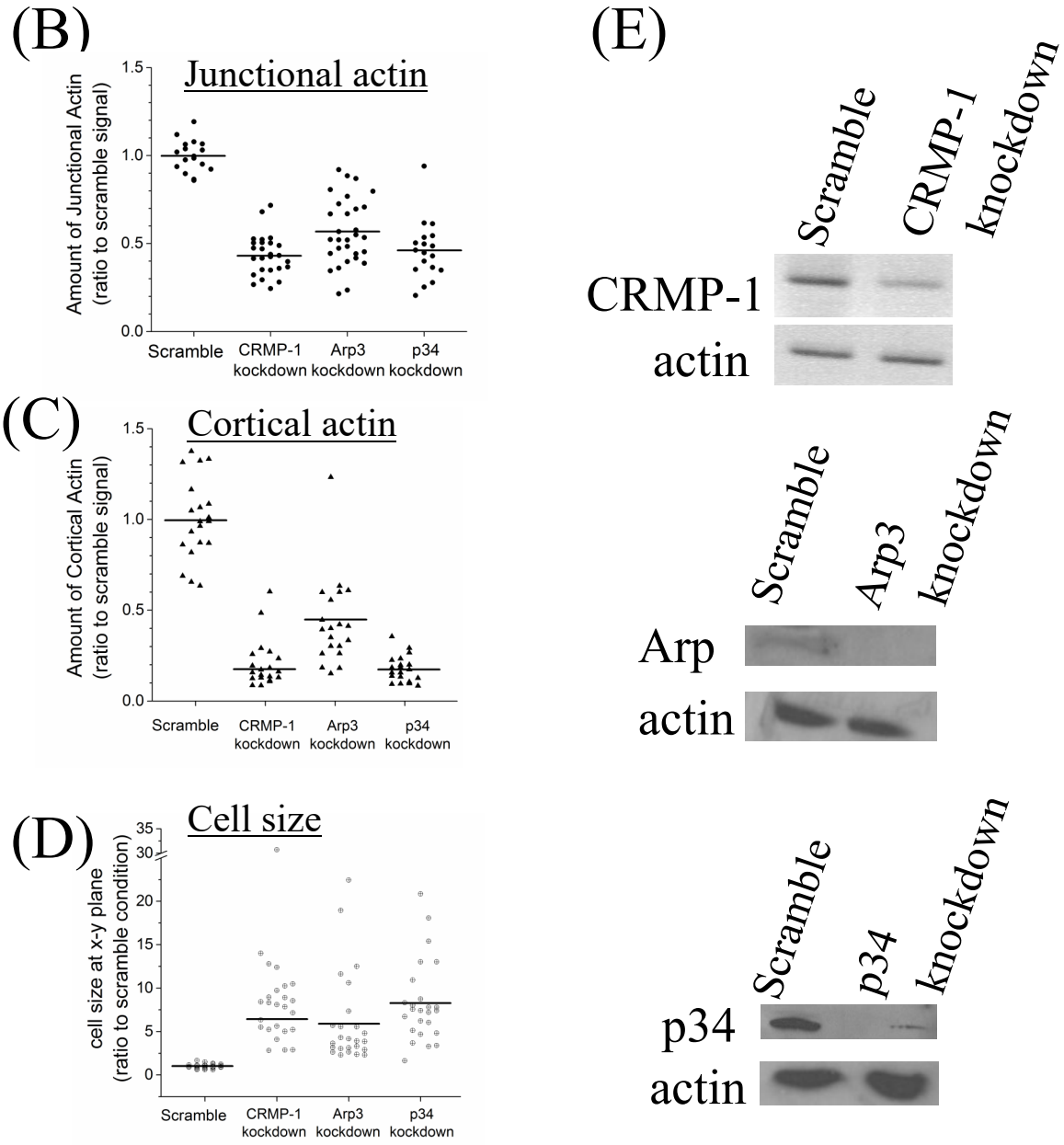

Figure 12. Perturbing CRMP-1 or Arp2/3 function results in the loss of cortical actin and junctional actin. (A) Actin staining for confluent MDCK monolayers of control cells (scramble) and the knockdown cells (CRMP-1 knockdown, Arp3 knockdown or p34 knockdown). Scale bar: 50 μ m. (B)-(D) Quantification of (A). The amount of junctional actin (B) and cortical actin (C) decrease in the knockdown cells. For quantification, n=20. (D) Cell size on x-y plane. In this set of measurement, scramble cells have average size around 282 μ m^2, which was standardized to 1 in the y-axis. 25 cells were measured in each condition. (E) Western blotting indicates the knockdown efficiency.

Figure 13

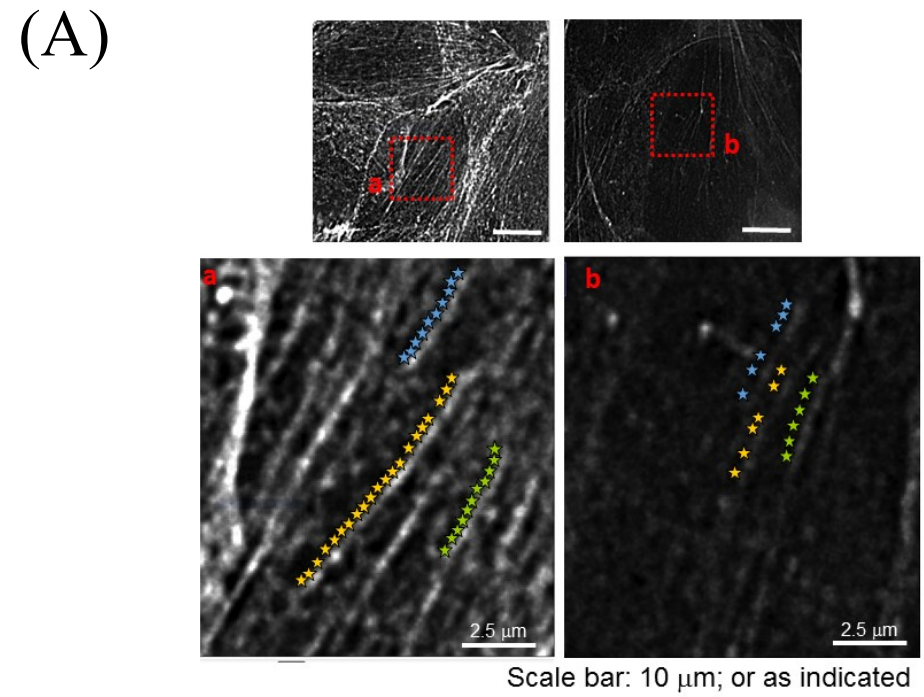

Fig. 13. Perturbing CRMP-1 function results in the loss of stress fiber at the basal surface. (A) Phalloidin staining showing the loss of stress fiber at the basal surface in CRMP-1 depleted condition. Stars: the loci of high-intensity actin alone the stress fiber. Scale bar: 10 μ m, or as indicated. (B) & (C) Quantifications. (B) Reduced actin signal along the stress fibers in CRMP-1-depleted cells. (C) No significant change in the width of the stress fiber in CRMP-1 depleted cells.

Figure 14

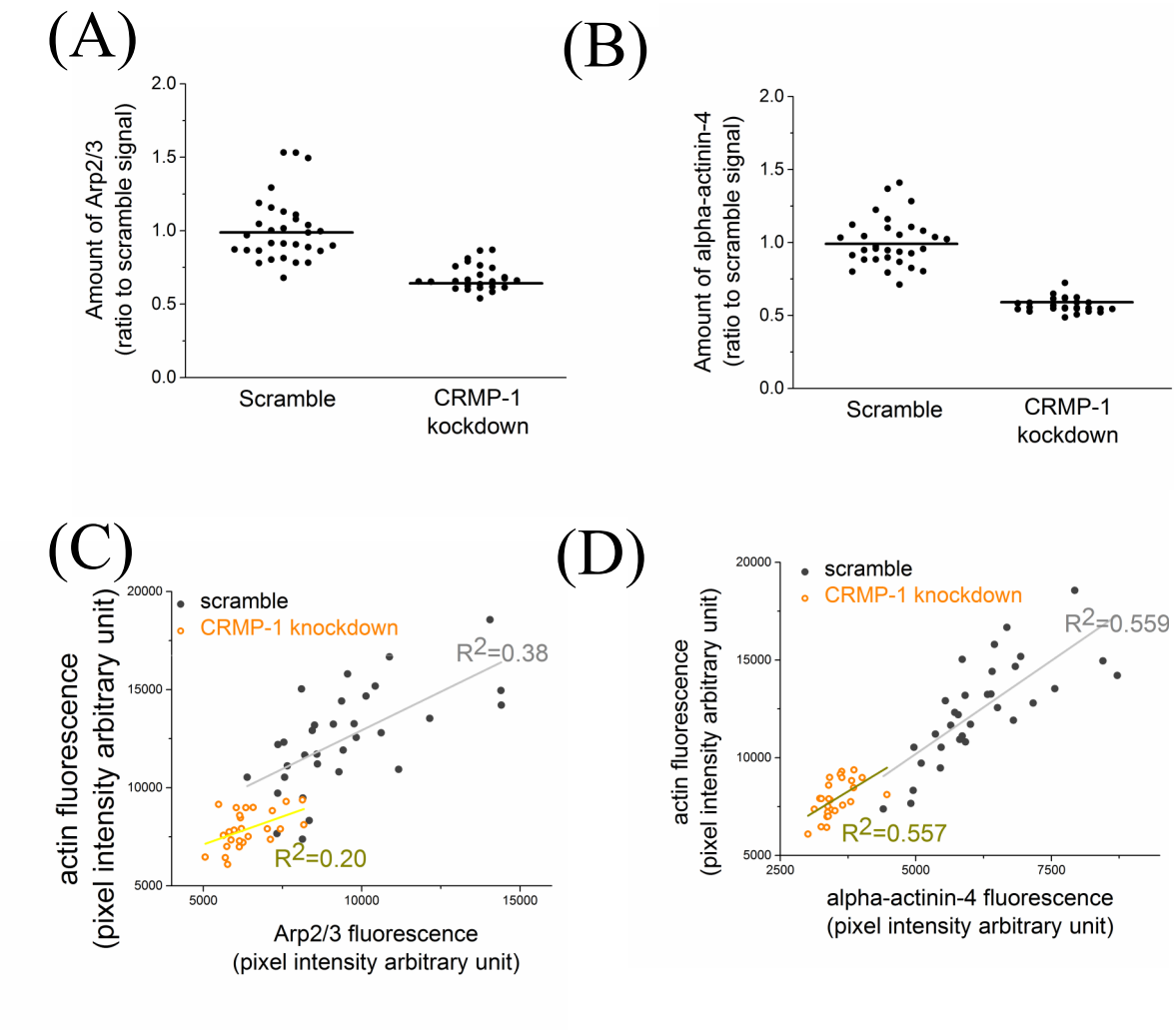

Fig. 14. Arp2/3 might be less active in CRMP-1 depleted cells. (A) & (B) Quantifications of the amount of Arp2/3 (A) and alpha-actinin-4 (B) at cell-cell contact in scramble or CRMP-1-depleted cells. The quantification was done by analyzing the images acquired under fluorescence microscope after immunostaining of Arp2/3 and alpha -actinin-4. Depletion of CRMP-1 results in a decreased amount of Arp2/3 and alpha-actinin-4 at the junction. (C) & (D) Correlation of Arp2/3 (C) and alpha-actinin-4 (D) to actin. The correlation of actin to Arp2/3 changes in CRMP-1 knockdown background: less Arp2/3 per actin in the CRMP-1 depleted junction. Yet the correlation of actin to alpha-actinin-4 remains the same.

Fig. 15

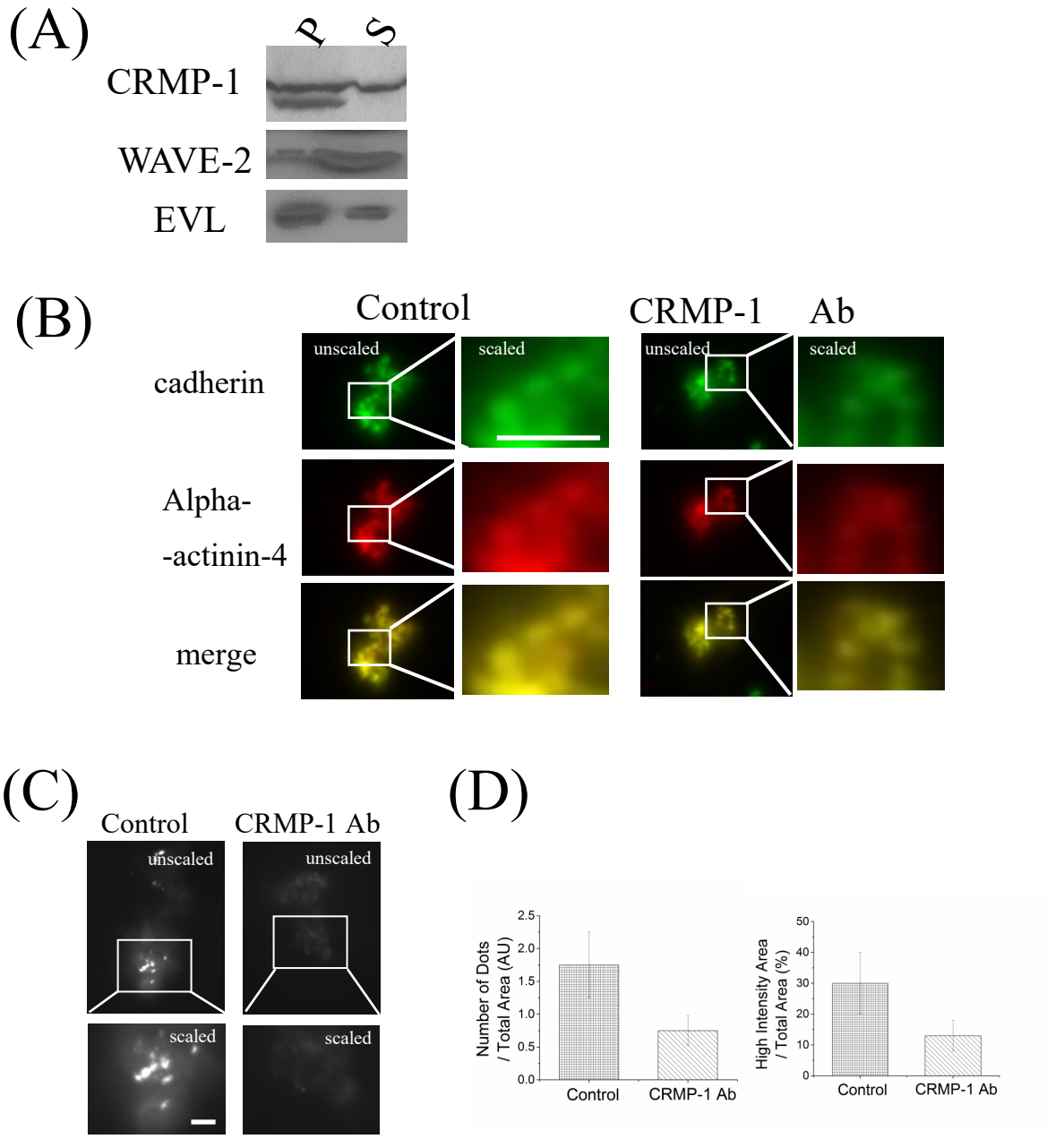

Fig. 15. CRMP-1 controls actin assembly on adherens-complex-enriched membrane. (A) Immunobloting of CRMP-1 indicates CRMP-1 associates with purified liver membrane fraction. The membrane were treated with high-salt solution prior to centrifugation. Lane P: pellet; lane S: supernatant. (B) CRMP-1 antibodies (CRMP-1 Ab) do not block the recruitment of alpha-actinin-4 to the high-salt stripped membrane. (C) Actin formation at junctional-protein-enriched membrane is regulated by CRMP-1. CRMP-1 antibodies inhibited actin polymerization on the stripped membrane. Left: control. The images show the signal from fluorescent actin. Scale bar: 2 μ m. (D) Quantifications of (C).

Figure 16

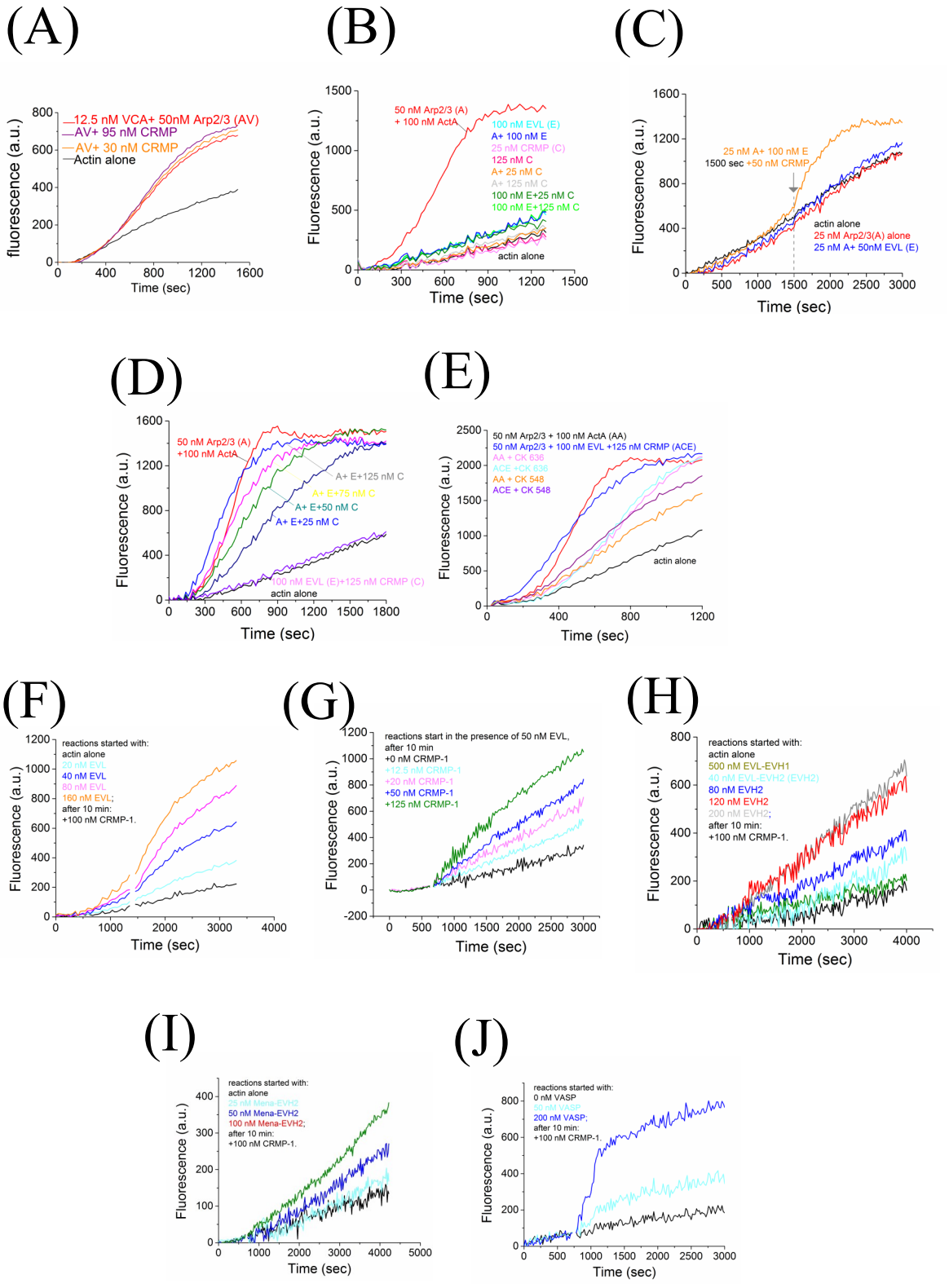
(A)
12.5 nM VCA+ 50nM Arp2/3 (AV)
AV+ 95 nM CRMP
AV+ 30 nM CRMP
Actin alone
fluorescence (a.u.)
Time (sec)
(B)
50 nM Arp2/3 (A)
+ 100 nM ActA
100 nM EVL (E)
A+ 100 nM E
25 nM CRMP (C)
125 nM C
A+ 25 nM C
A+ 125 nM C
100 nM E+25 nM C
100 nM E+125 nM C
actin alone
Fluorescence (a.u.)
Time (sec)
(C)
25 nM A+ 100 nM E
1500 sec +50 nM CRMP
actin alone
25 nM Arp2/3(A) alone
25 nM A+ 50nM EVL (E)
Fluorescence (a.u.)
Time (sec)
(D)
50 nM Arp2/3 (A)
+100 nM ActA
A+ E+125 nM C
A+ E+75 nM C
A+ E+50 nM C
A+ E+25 nM C
100 nM EVL (E)+125 nM CRMP (C)
actin alone
Fluorescence (a.u.)
Time (sec)
(E)
50 nM Arp2/3 + 100 nM ActA (AA)
50 nM Arp2/3 + 100 nM EVL +125 nM CRMP (ACE)
AA + CK 636
ACE +CK 636
AA + CK 548
ACE + CK 548
actin alone
Fluorescence (a.u.)
Time (sec)
(F)
reactions started with:
actin alone
20 nM EVL
40 nM EVL
80 nM EVL
160 nM EVL;
after 10 min:
+100 nM CRMP-1.
Fluorescence (a.u.)
Time (sec)
(G)
reactions start in the presence of 50 nM EVL,
after 10 min
+0 nM CRMP-1
+12.5 nM CRMP-1
+20 nM CRMP-1
+50 nM CRMP-1
+125 nM CRMP-1
Fluorescence (a.u.)
Time (sec)
(H)
reactions started with:
actin alone
500 nM EVL-EVH1
40 nM EVL-EVH2 (EVH2)
80 nM EVH2
120 nM EVH2
200 nM EVH2;
after 10 min:
+100 nM CRMP-1.
Fluorescence (a.u.)
Time (sec)
(I)
reactions started with:
actin alone
50 nM Mena-EVH2
100 nM Mena-EVH2;
after 10 min:
+100 nM CRMP-1.
Fluorescence (a.u.)
Time (sec)
(J)
reactions started with:
0 nM VASP
50 nM VASP
200 nM VASP;
after 10 min:
+100 nM CRMP-1.
Fluorescence (a.u.)
Time (sec)

Figure 16 (cont.)

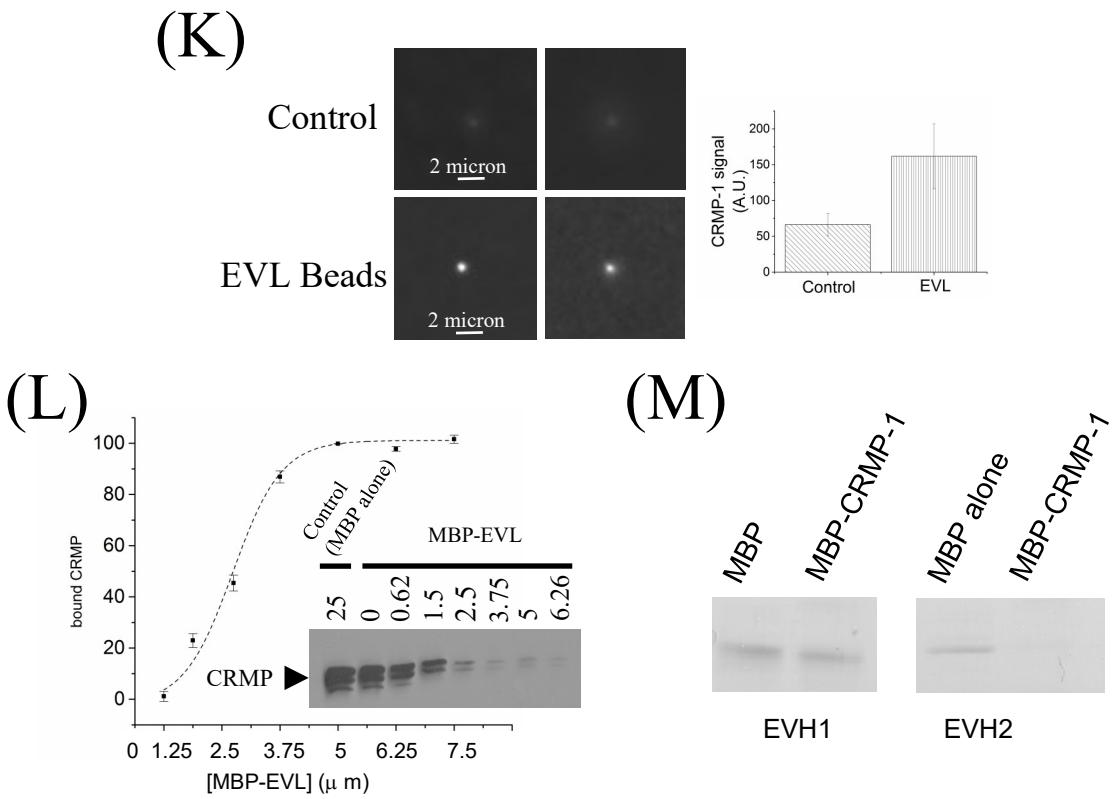

Fig. 16. CRMP-1 activates Arp2/3 complex in the presence of EVL. (A) CRMP-1 does not facilitate VCA-mediated Arp2/3 polymerization. (B) CRMP-1 alone, or EVL alone does not nucleate actin, nor activate Arp2/3 complex. (C) Simultaneous presence of CRMP-1 and EVL can activate Arp2/3 complex. (D) CRMP-1 and EVL activate Arp2/3 polymerization in a dose-dependent manner. (E) Arp2/3 inhibitors, CK636 and CK 548, inhibit CRMP-1-EVL-activated Arp2/3 polymerization. (F) & (G) CRMP-1 facilitates EVL-mediated actin elongation. (H) EVL truncations behave different in this assay. EVH2 domain of EVL works with CRMP-1 to enhance actin polymerization, but not EVH1 domain. (I) & (J) VASP family proteins, VASP (I) and Mena-EVH2 (J) can work with CRMP-1 to increase the rate of actin polymerization. (K) CRMP-1 can interact with EVL. Left panel: representative images showing higher intensity of CRMP-1 signal in EVL-coated beads. Scale bar: 2 mm. Right panel: quantifications. (L) CRMP-1 binds to MBP-EVL in a dose-dependent manner. Right panel: western blotting of CRMP-1 in the supernatants showing CRMP-1 depletion after incubating with different amount of EVL. Numbers above each lane indicate total protein concentration on the beads. (Concentration: EVL was calculated as tetramer; MBP alone was calculated as monomer). (M) EVH2 of EVL interacts with MBP-tagged CRMP-1, but EVH1 domain does not. The coomassie staining shows the amount of EVL truncates remaining in the supernatant after incubating with the immobilized MBP or MBP-tagged CRMP-1. Note: (A)—(J): CRMP-1 concentration was calculated as tetramer; EVL/VASP family proteins were calculated as monomer. (L) EVL concentration was indicated as tetramer.

Figure 17

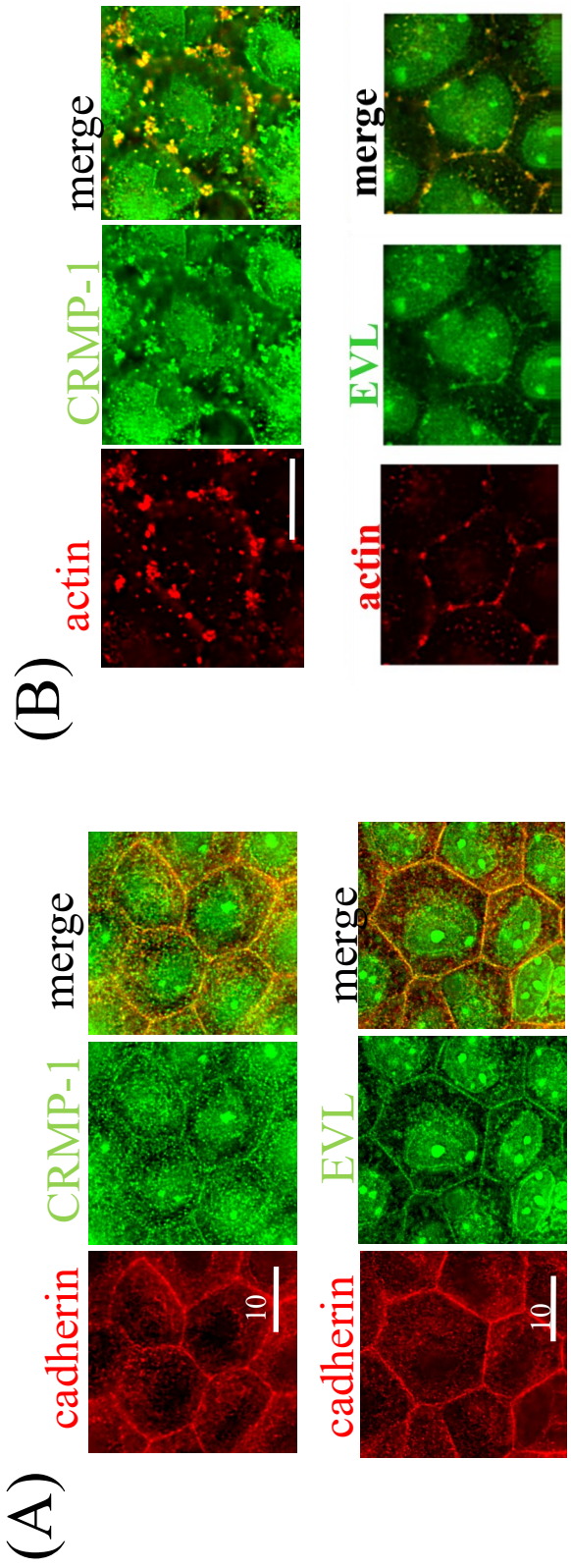
(B)
actin
CRMP-1
merge
EVL
actin
merge
(A)
cadherin
CRMP-1
merge
10
cadherin
EVL
merge
10

Figure 17 (cont.)

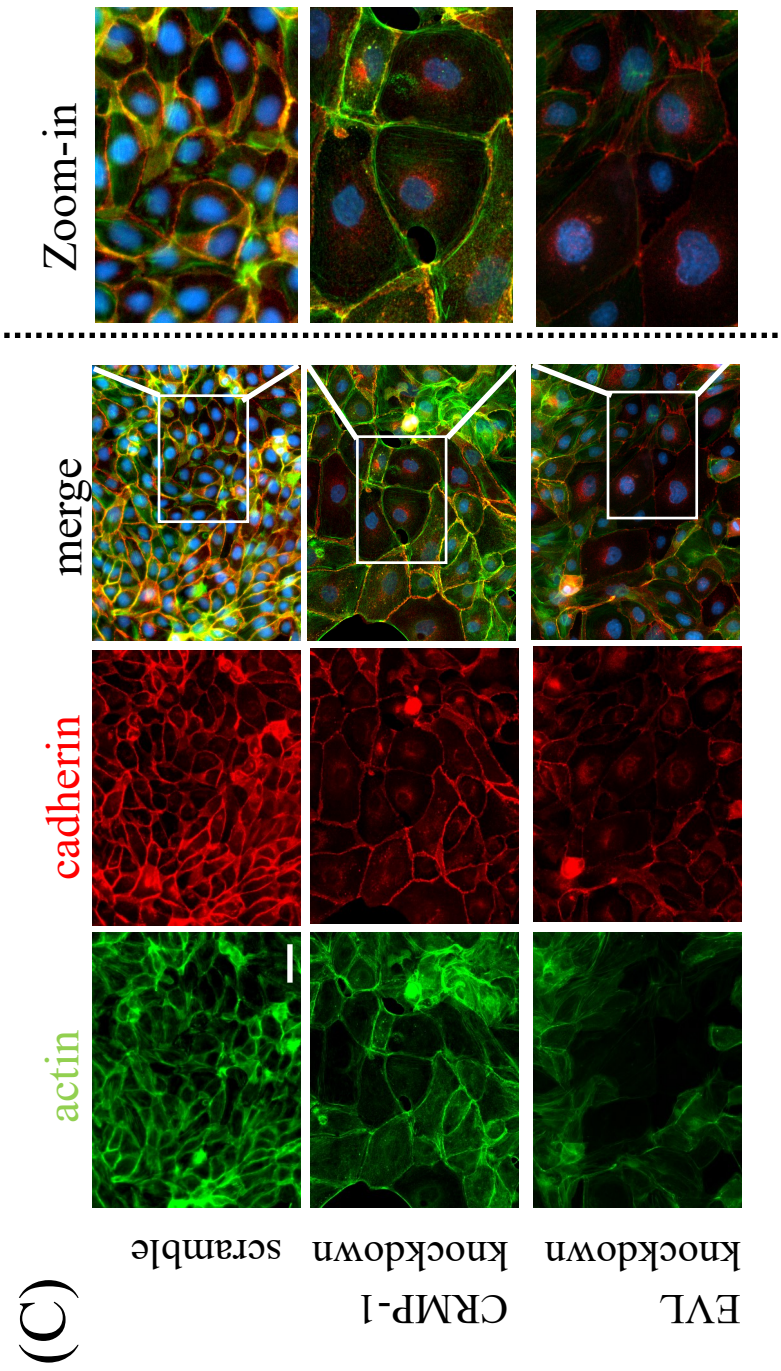

Figure 17 (cont.)

Fig. 17. CRMP-1 and EVL regulates the amount of actin at cadherin mediated cell-cell contacts. (A) CRMP-1 and EVL locates to adherens junction. Red: cadherin; green: CRMP-1 or EVL. Scale bar: 10 μ m. (B) CRMP-1 and EVL remain at latrunculin-resistant puncta, where de novo Arp2/3 polymerization occurs. Red: actin; green: CRMP-1 or EVL. Scale bar: 10 μ m. (C) Knockdown either CRMP-1 or EVL reduces actin and cadherin signals at cell-cell contact. Scale bar: 50 μ m. (D) Quantifications of (C).

Figure 18

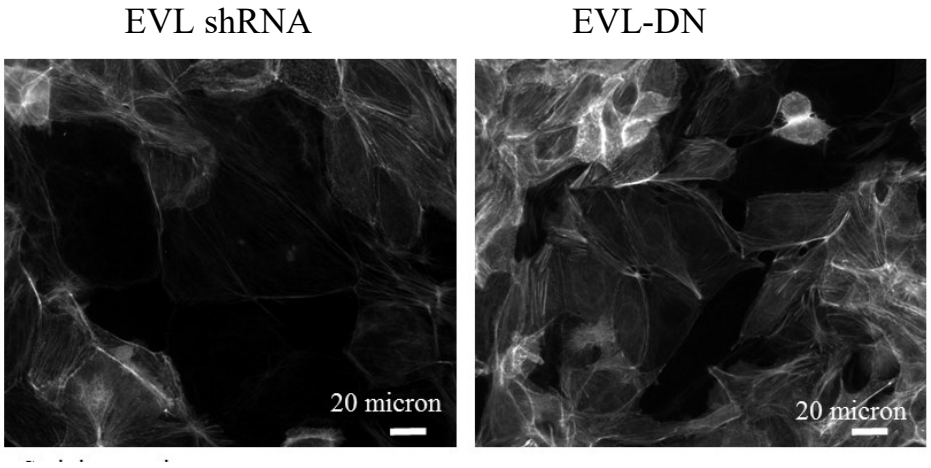

Fig. 18. Perturbing EVL function by shRNA or EVL dominant-negative constructs (EVL-DN) provides similar phenotype. Actin staining shows the reduced F-actin amount in both conditions. Scale bar: 20 μ m.

Figure 19

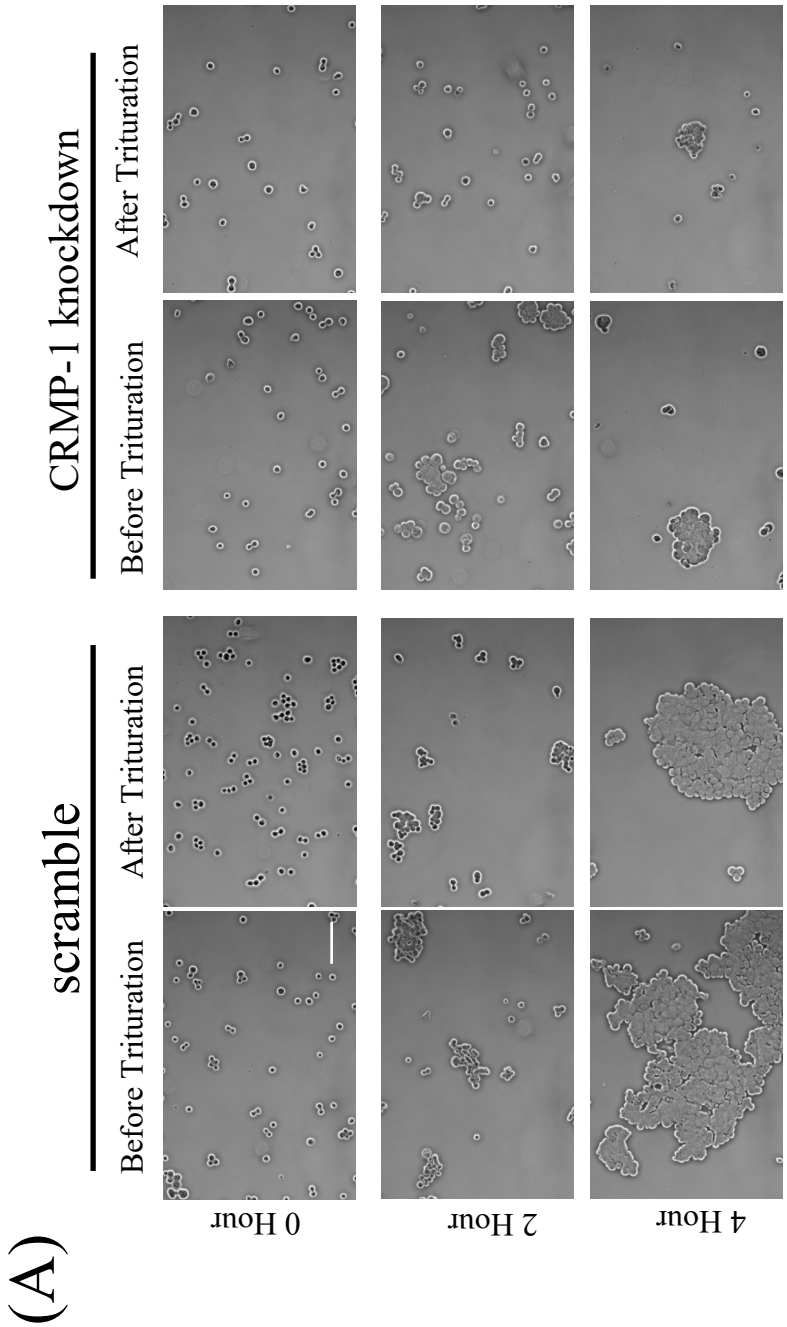
(A)
scramble
CRMP-1 knockdown
Before Trituration
After Trituration
Before Trituration
After Trituration
0 Hour
2 Hour
4 Hour

Figure 19 (cont.)

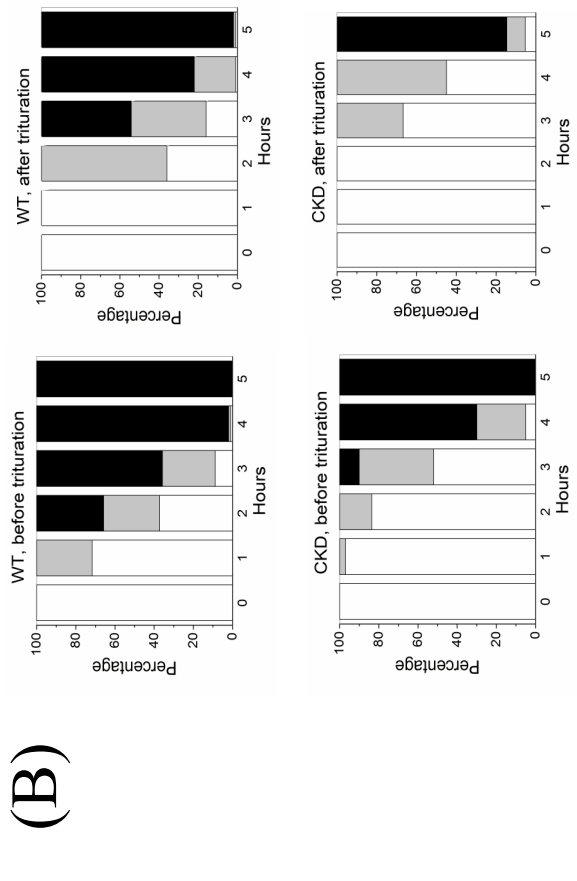

Fig. 19. CRMP-1 contributes to stable cell contact formation. (A) The representative images of the hang-drop experiments. Images are collected at 0, 2 hr and 4 hr, before and after trituration. Scale bar: 100 μ m. (B) Quantifications of (A). Hanging drop experiment demonstrates CRMP-1 knockdown cells display a delay in stable cell-cell contact formation. The stacked column represent the percentage of cells in clusters as 0-10 cells (white), 11-50 cells (gray) or >50 cells (black).

Figure 20

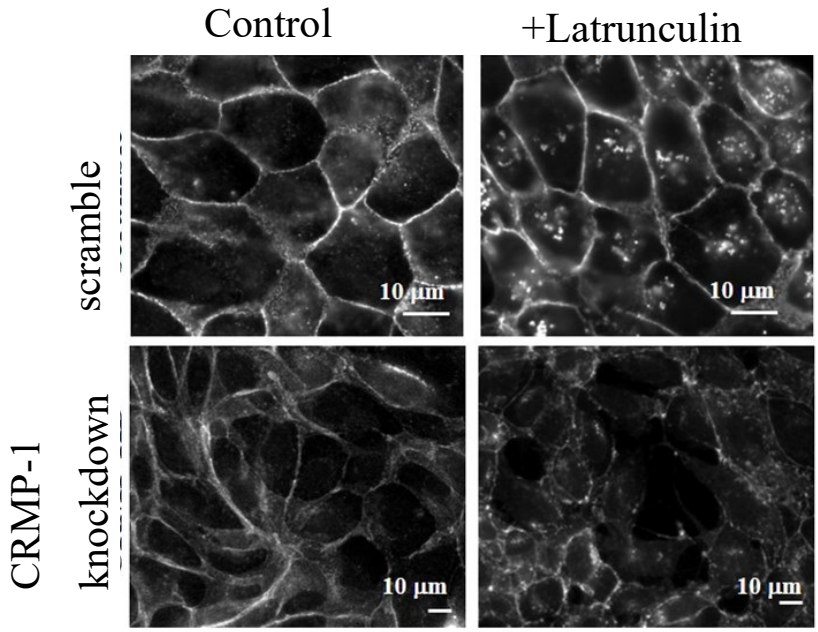

Fig. 20. CRMP-1 depleted monolayers fail to maintain integrity after latrunculin treatment. E-cadherin staining for the monolayers of CRMP-1 knockdown or control cells under different conditions. The loss of the CRMP-1 knockdown cells after lantruculin treatment implies the weaker cell adhesion under the knockdown background

Figure 21

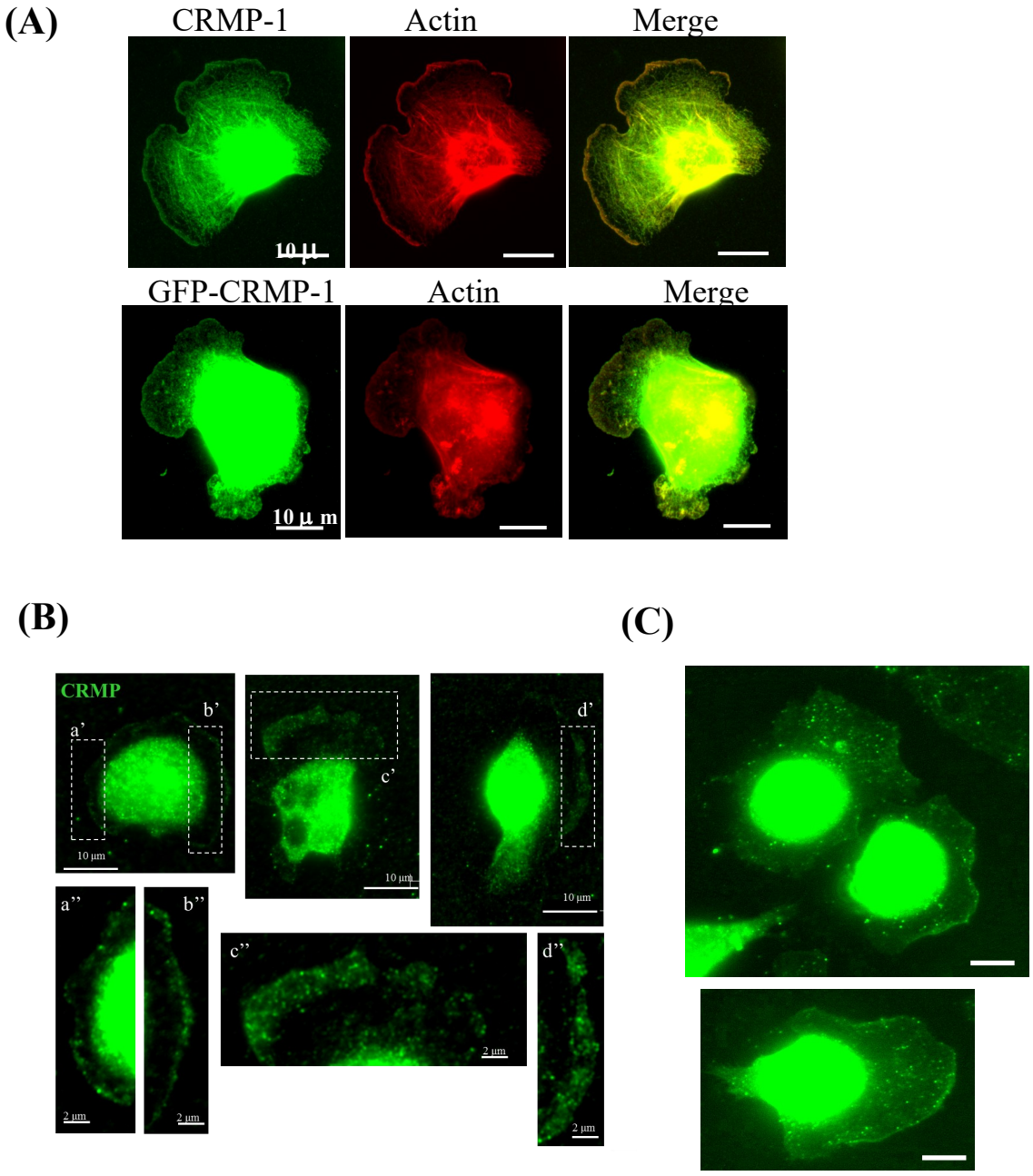

Fig. 21. CRMP-1 localizes at the leading edge of lamellipodia. (A) Immunostaining of CRMP-1 shows that CRMP-1 localizes to lamellipodia. Its signal colocalized with actin signal at the leading edge. Fixation method: formaldehyde fixation. (B) GFP-CRMP-1 localizes to lamellipodia. (C) Immunostaining of CRMP-1 at lamellipodia. Fixation method: TCA fixation. (D) TCA fixation and immunostaining indicates that DHPase can be detected in the leading edge. Scale bar: 10 µ m, unless indicated.

Figure 22

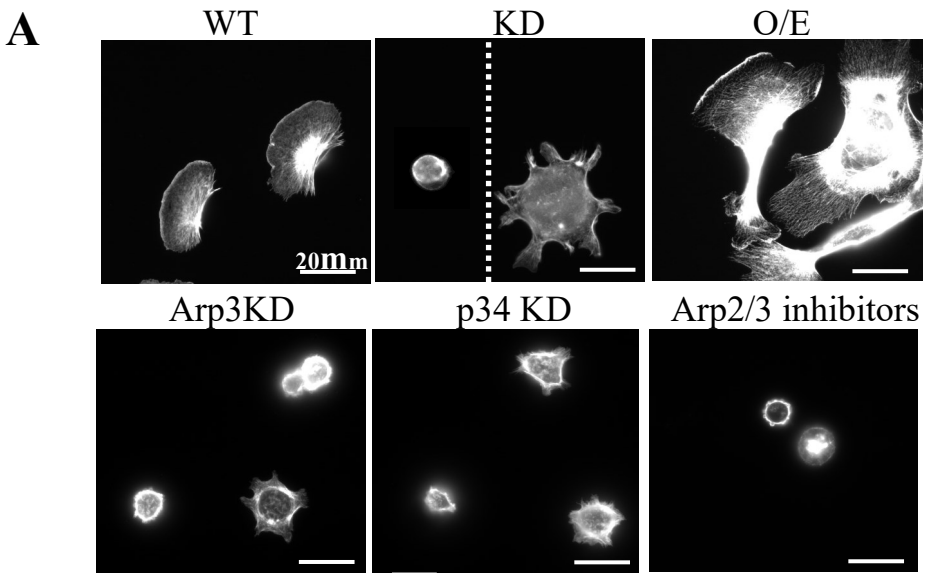

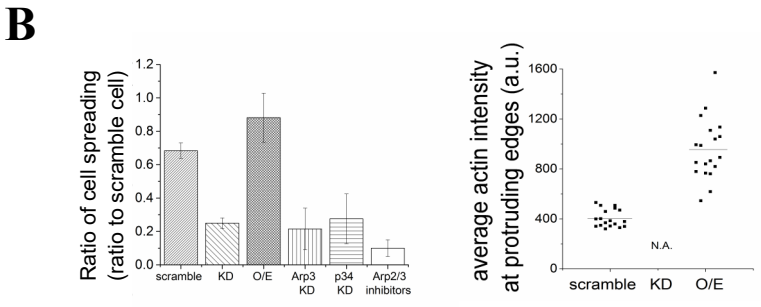

Fig. 22. CRMP-1 regulates actin polymerization during cell spreading. (A) Perturbing CRMP-1 or Arp2/3 disrupts cell spreading on collagen. Images show phalloidin staining of actin in spreading cells. (B) Quantification of results from (A). Cells depleted of CRMP-1 are not included in the quantification for actin intensity since they do not make protrusions.

Figure 23

(A)

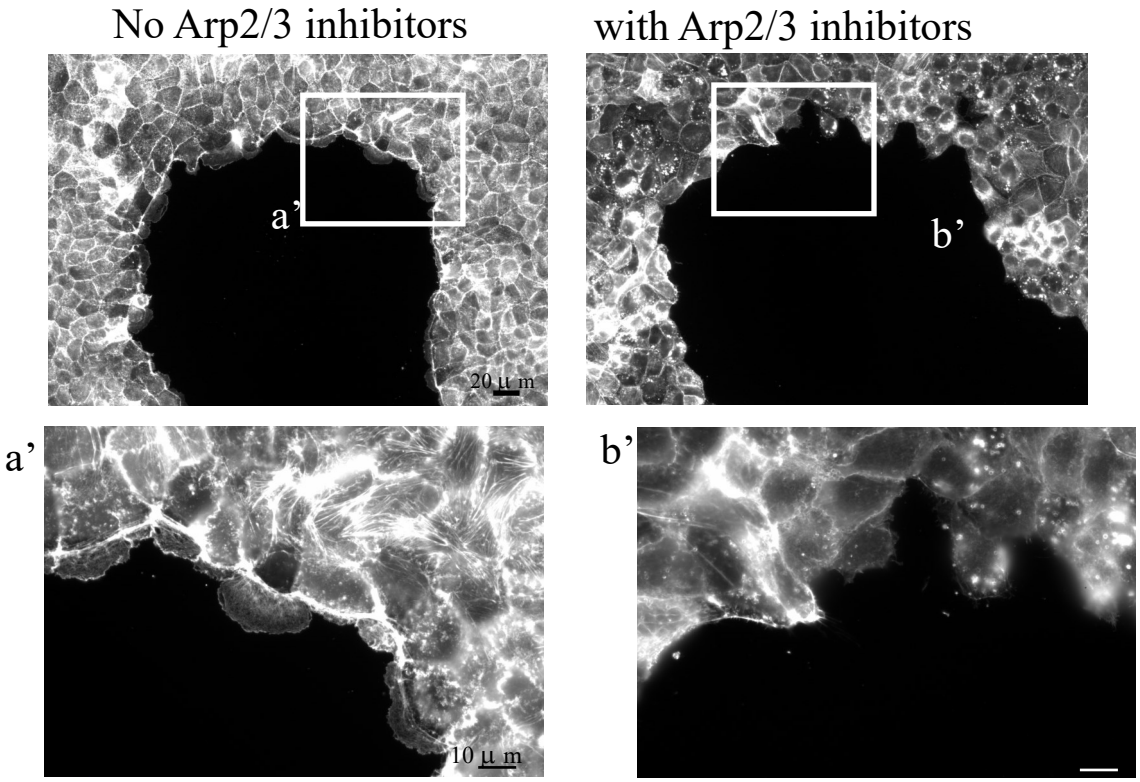

Figure 23 (cont.)

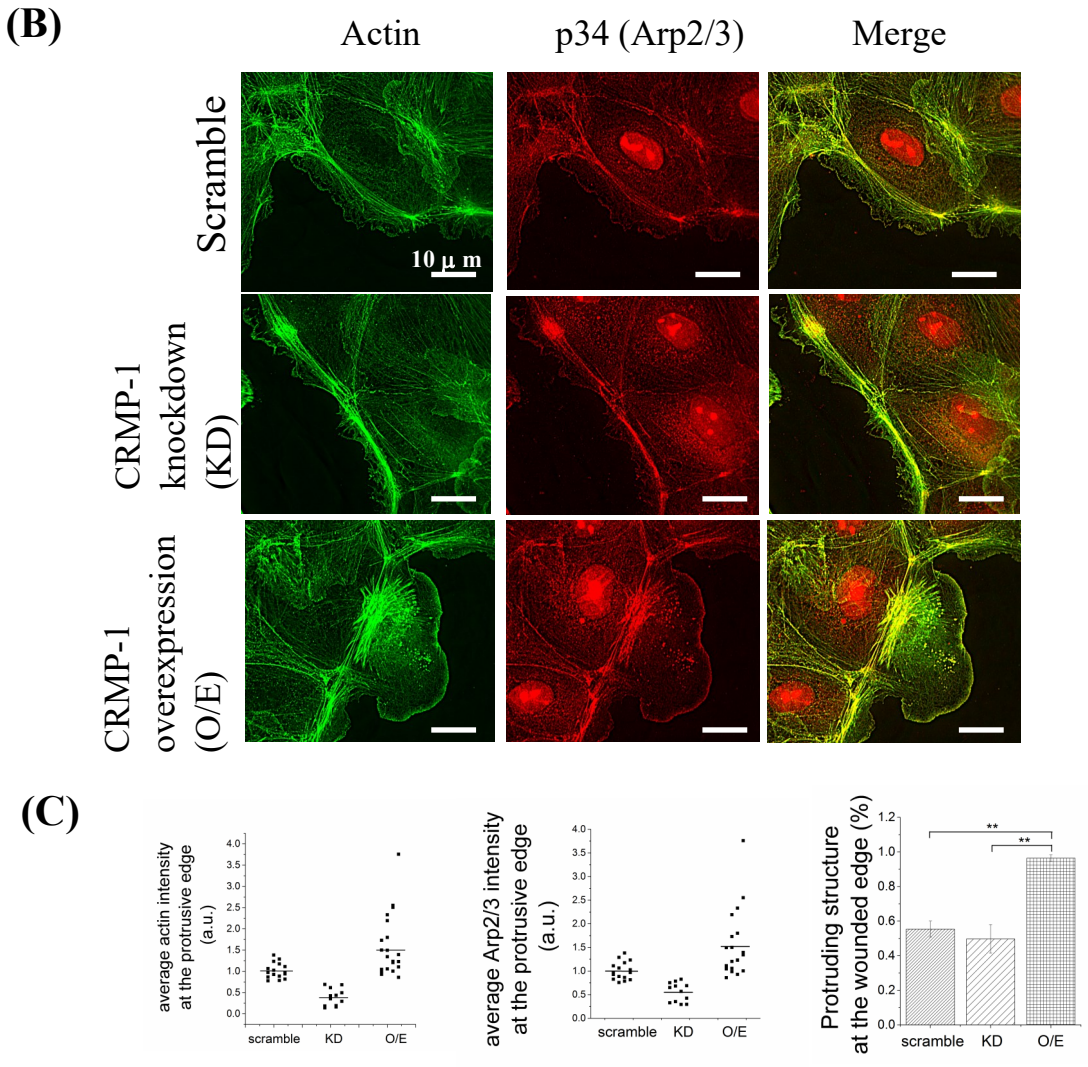

Fig. 23. CRMP-1 regulates actin polymerization at the wounded edge. (A) Wounding MDCK II monolayers induces the formation of Arp2/3-dependent lamellipodia and Arp2/3 dependent actin cables. Wounded monolayers were treated with or without Arp2/3 inhibitors (100 nM CK-636 and 100 nM CK-548). Phalloidin staining showed that actin structures were greatly diminished around the wound edge in the presence Arp2/3 inhibitors. (B) Phalloidin staining of actin and p34 subunit of Arp2/3 complex in wounded monolayers. (C) Quantifications of results from (B) indicated that overexpression of CRMP-1 resulted in higher actin signal Arp2/3 (p34) signal at the leading edge. For quantification, three repeats were done for quantifying the ratio of spreading cells or the ratio of cells with lamellipodia. KD: CRMP-1 knockdown; O/E: CRMP-1 overexpression.

Figure 24

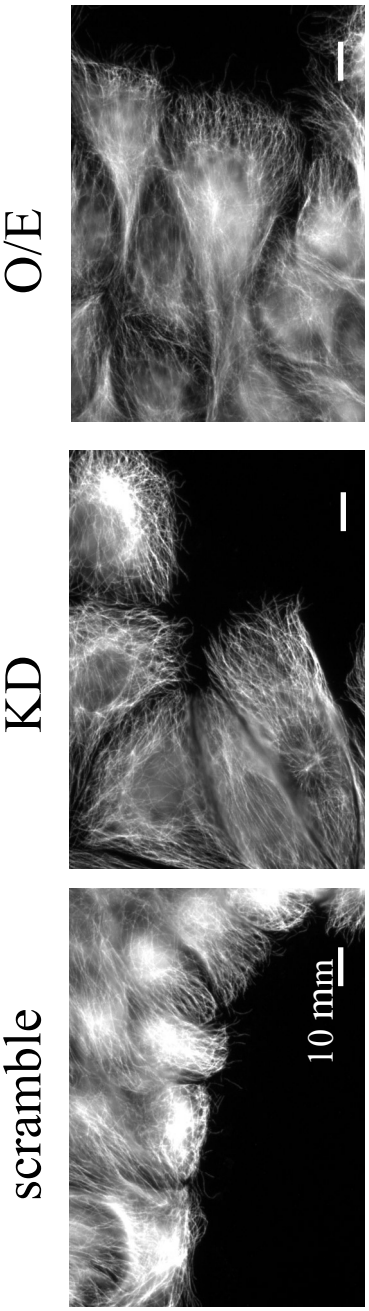

Fig. 24. No apparent change in microtubule structures while manipulating CRMP-1 function. Tubulin staining of wounded edge of scramble, CRMP-1 depleted (KD) and CRMP-1 overexpressing (O/E) cells

Figure 25

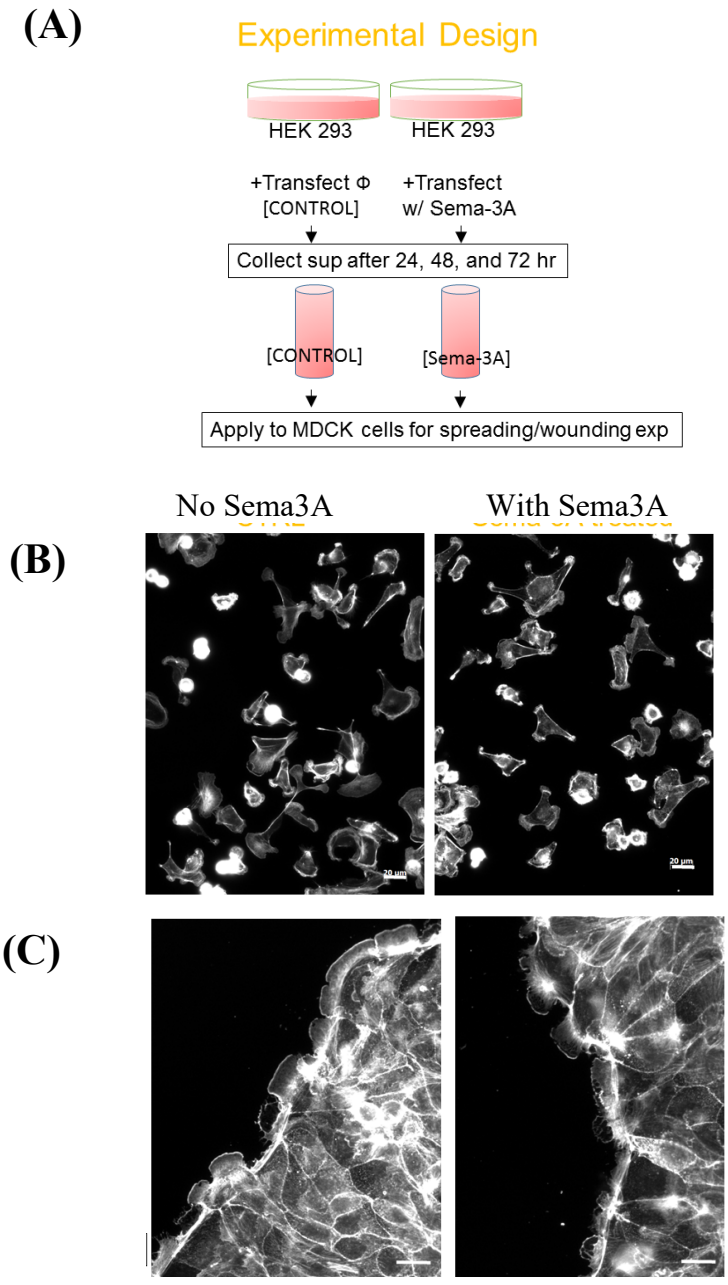

Fig. 25. Preliminary result shows that no attenuation of cell spreading or protrusive structure formation in the presence of Semaphorin 3A. (A) Experimental set-up. (B) &(C) Phalloidin staining showing the morphology of the cell in the presence or absence of Sema3A during (B) cell spreading and (C) wound healing. Scale bar: 20 μm.

Figure 26

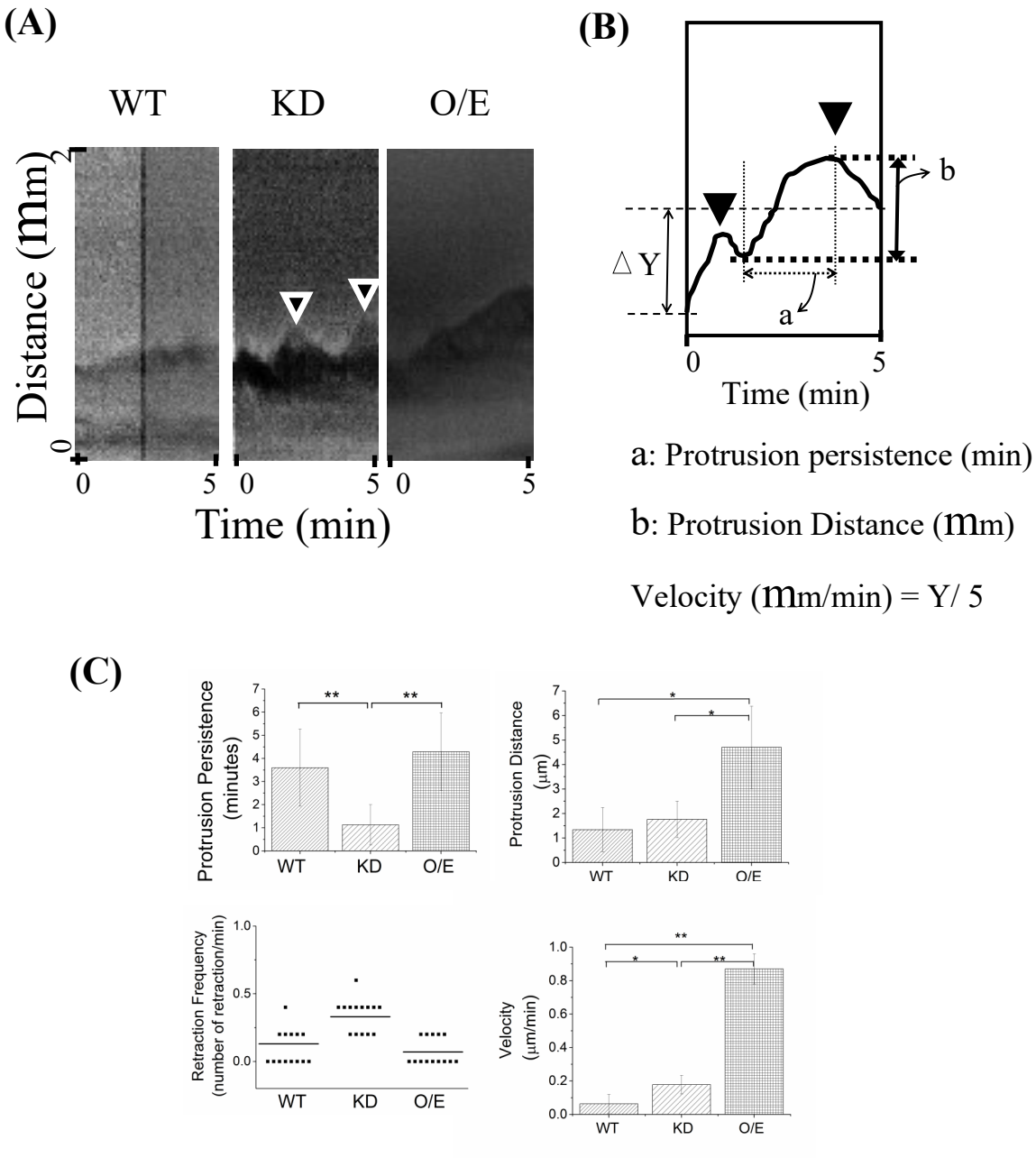

Fig. 26. CRMP-1 contributes to the persistence of the protruding edge in wounded monolayers. (A) Representative kymograph of the protrusive edge. X-axis represent the time (minutes); Y-axis represents the distance (μ m). Triangle indicates the start of the retraction. (B) Schematic representation of the parameters and the equation used for data analysis. (C) Leading edge of CRMP-1 knockdown monolayers exhibit high retraction frequency. CRMP-1 overexpressing cells protrude more persistent compared to wild-type and CRMP knockdown cells. WT: wild-type; KD: CRMP-1 knockdown: O/E: CRMP-1 overexpressing cells (O/E). * $p<0.05$. ** $p<0.01$.

Figure 27

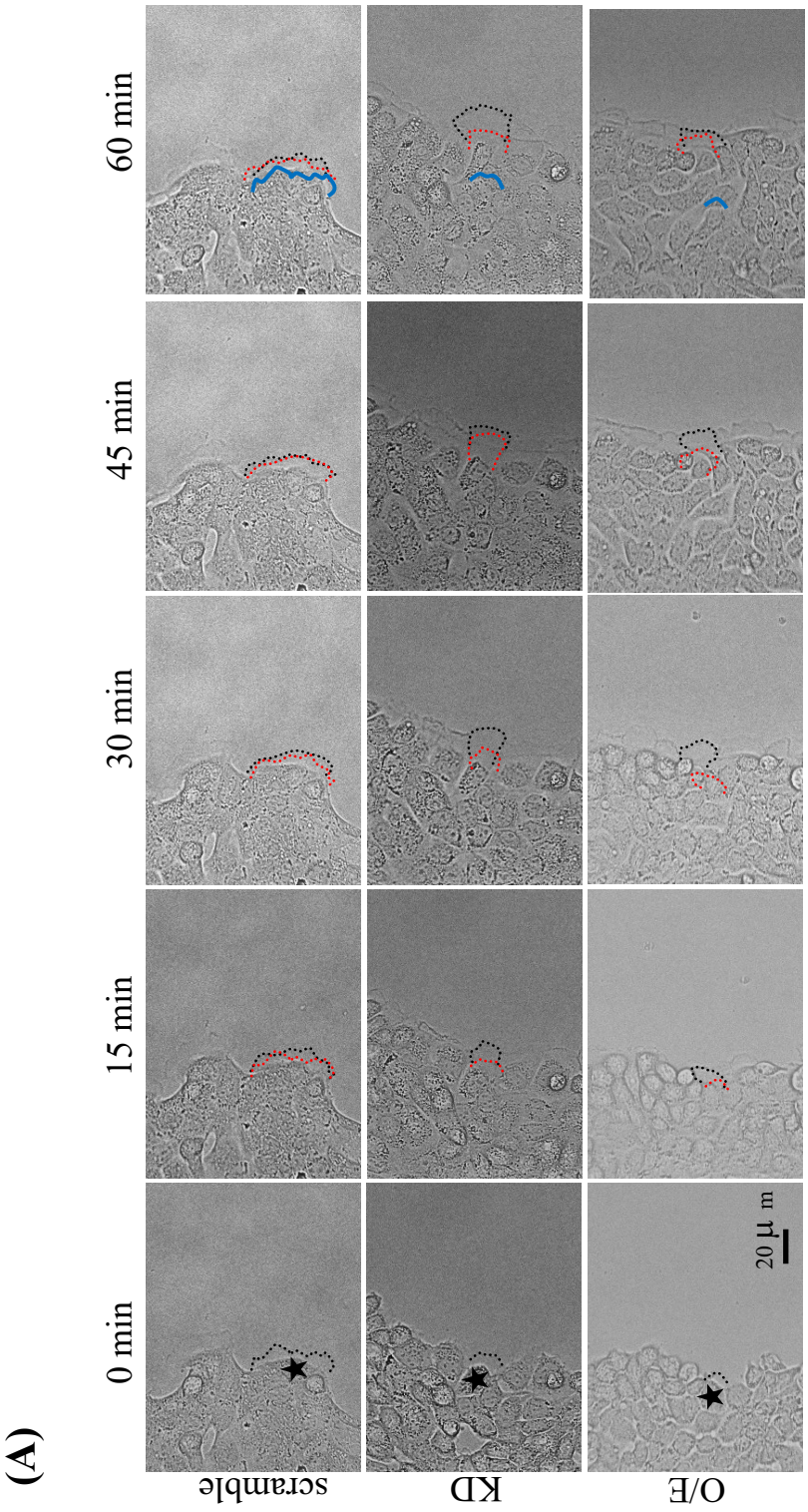

Figure 27 (cont.)

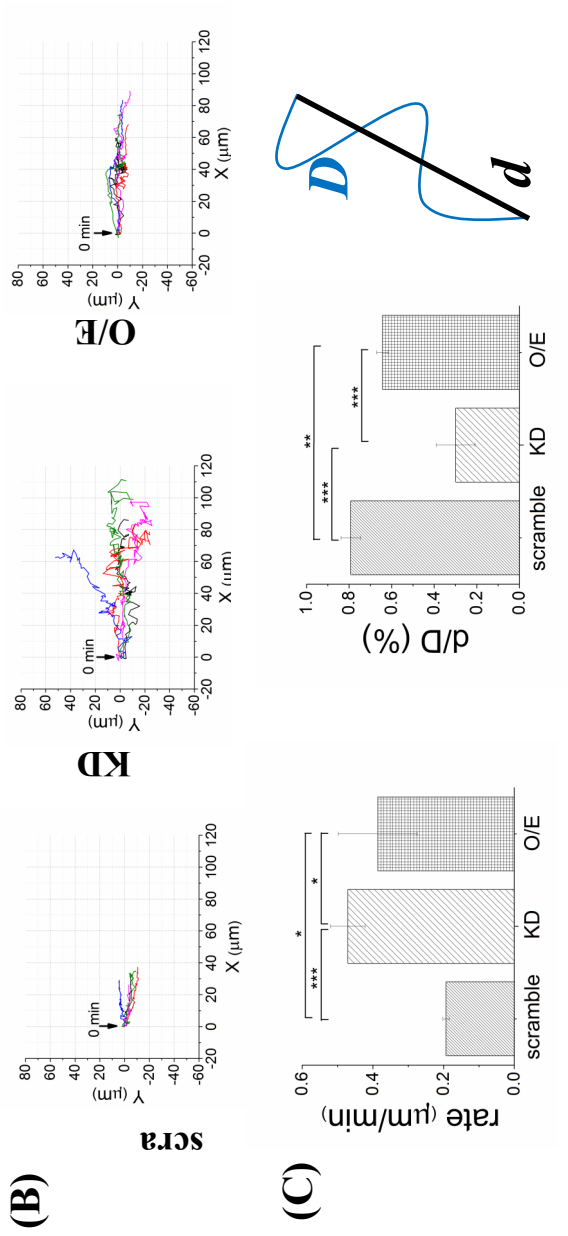

Fig. 27. CRMP-1 contributes to the directionality in wounded monolayers. (A) Time-lapse images of lamellipodia movement in wounded monolayers over 60 minutes. Representative cells that were tracked are highlighted with a star. In each image, the current position of the leading edge is marked in black, the position of the leading edge 15 minutes earlier is marked in red, the relative position of leading edge from 0 minutes is marked in blue. (B) Trajectories of the protrusive edge over 300 minutes. (C) Quantification of (B) reveals that CRMP-1 contributes to the rate and the directional migration of advanced edge.

APPENDIX A

Figures for the submission to *Journal of Cell Biology* (2016)

Figure A.1

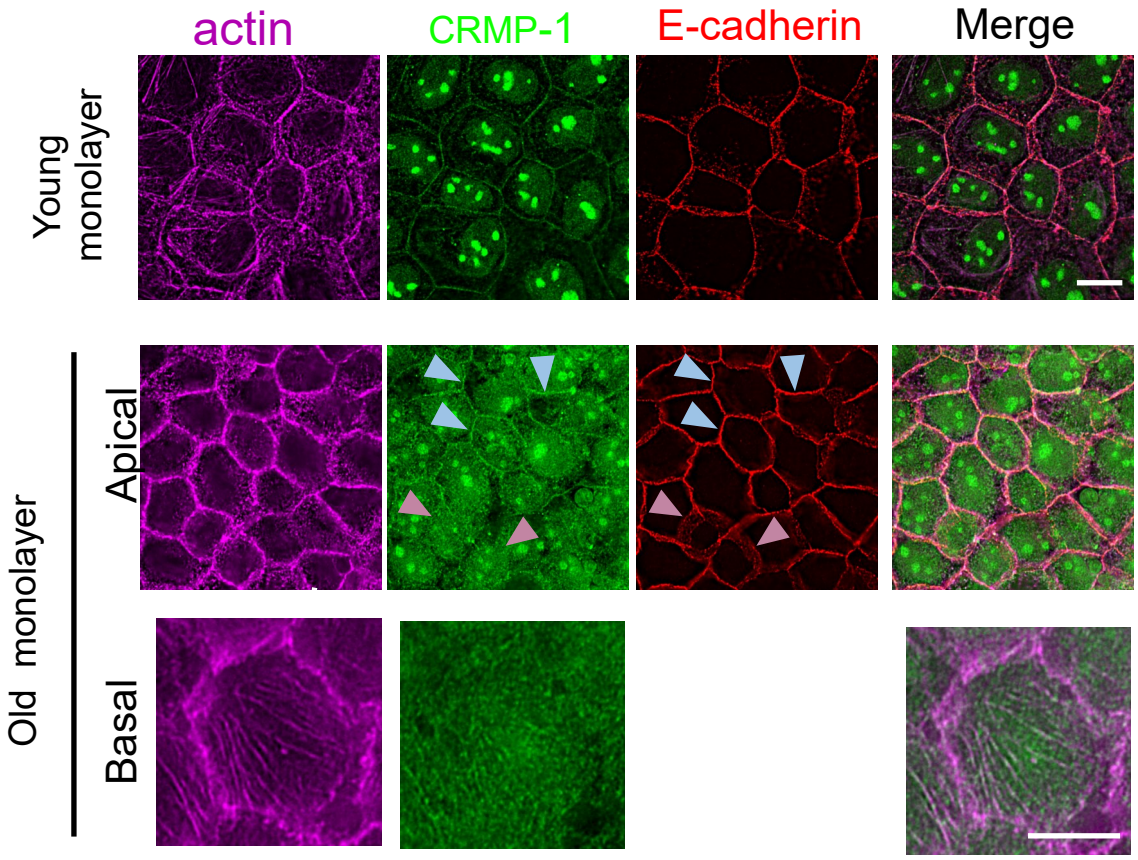

Figure A.1. CRMP-1 is expressed in epithelial MDCK cells and localizes to junctional and cortical actin. Immunostaining of a confluent monolayers of MDCK cells showing that CRMP-1 (green) localizes with actin (purple) at cell-cell contacts, which are marked with E-cadherin (red). CRMP-1 signal at this location can be detected in the apical surface of the young monolayer (1st day of confluency) (upper panel), the old monolayer (6th day of confluency) (middle panel), but not at the lateral membrane. Blue arrowheads indicate the apical membrane; pink arrowheads indicate the lateral membrane. CRMP-1 can be detected at the basal surface of the cell, yet its signal does not colocalize with any specific actin structures (lower panel). Scale bar: 10 μ m.

Figure A.2

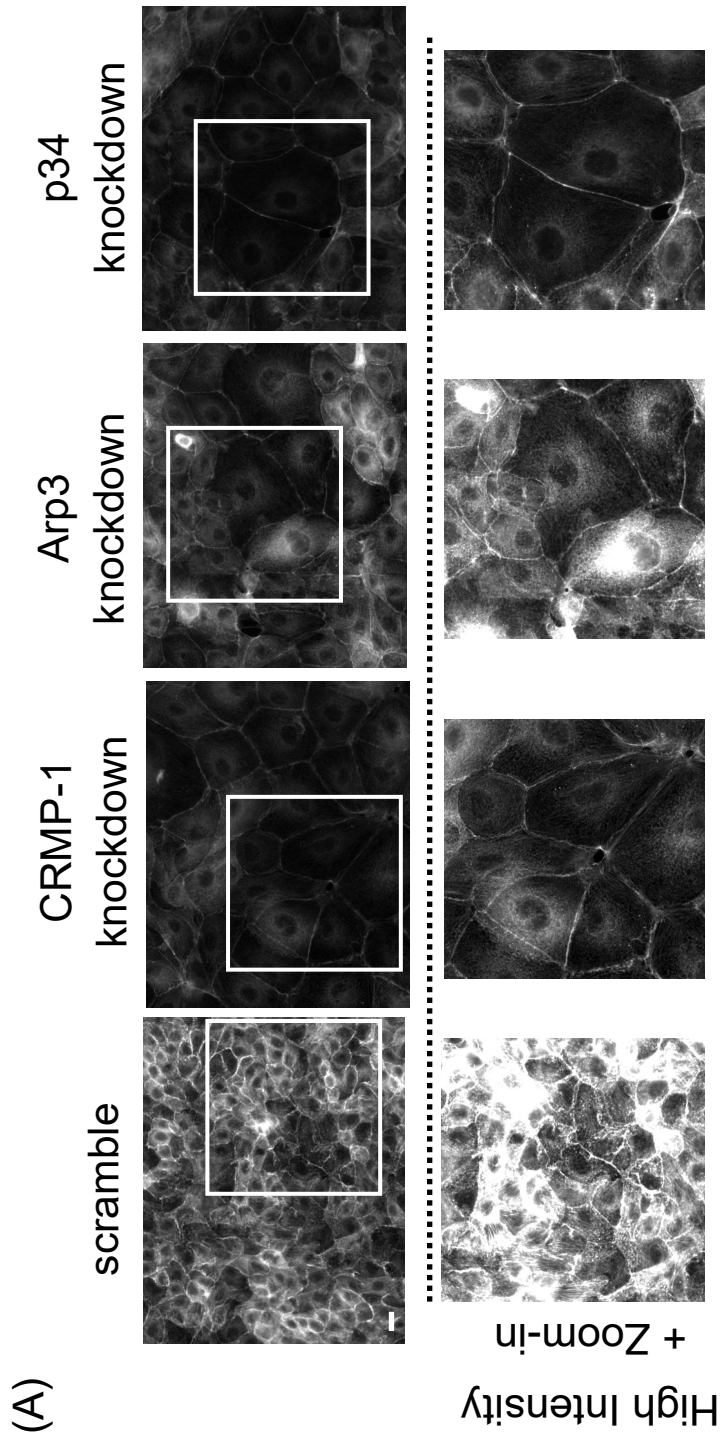
(A)
scramble
CRMP-1 knockdown
Arp3 knockdown
p34 knockdown
High Intensity
+ Zoom-in

Figure A.2 (cont.)

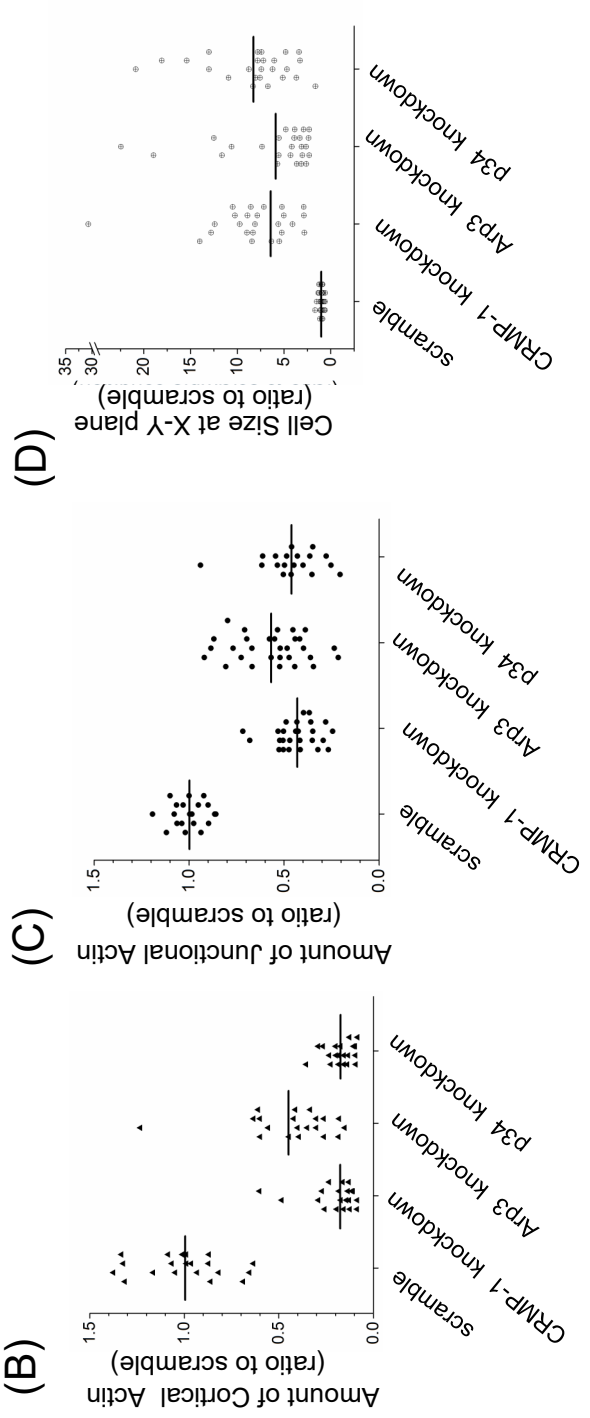

Figure A.2 (cont.)

Figure A.2. Perturbing CRMP-1 or Arp2/3 function results in the loss of cortical actin and junctional actin. (A) Actin staining in confluent MDCK monolayers of control cells (scramble) and knockdown cells (CRMP-1 knockdown, Arp3 knockdown or p34 knockdown). Scale bar: 20 μ m. (B)-(D) Quantification of (A). The amount of (B) cortical actin and (C) junctional actin decreases in the knockdown cells. For quantification, n≥20. (D) Cell size in the x-y plane. In this set of measurements, control cells transfected with the scrambled shRNA have an average area around 282 μ m^2, which was standardized to 1 in the y-axis. 25 cells were measured in each condition. (E) WAVE2 localize to cell boundaries. (F) Phalloidin staining reveals that WAVE2 knockdown cells shows similar phenotype as Arp2/3 and CRMP-1 knockdowns. Scale bar: 20 μ m.

Figure A.3

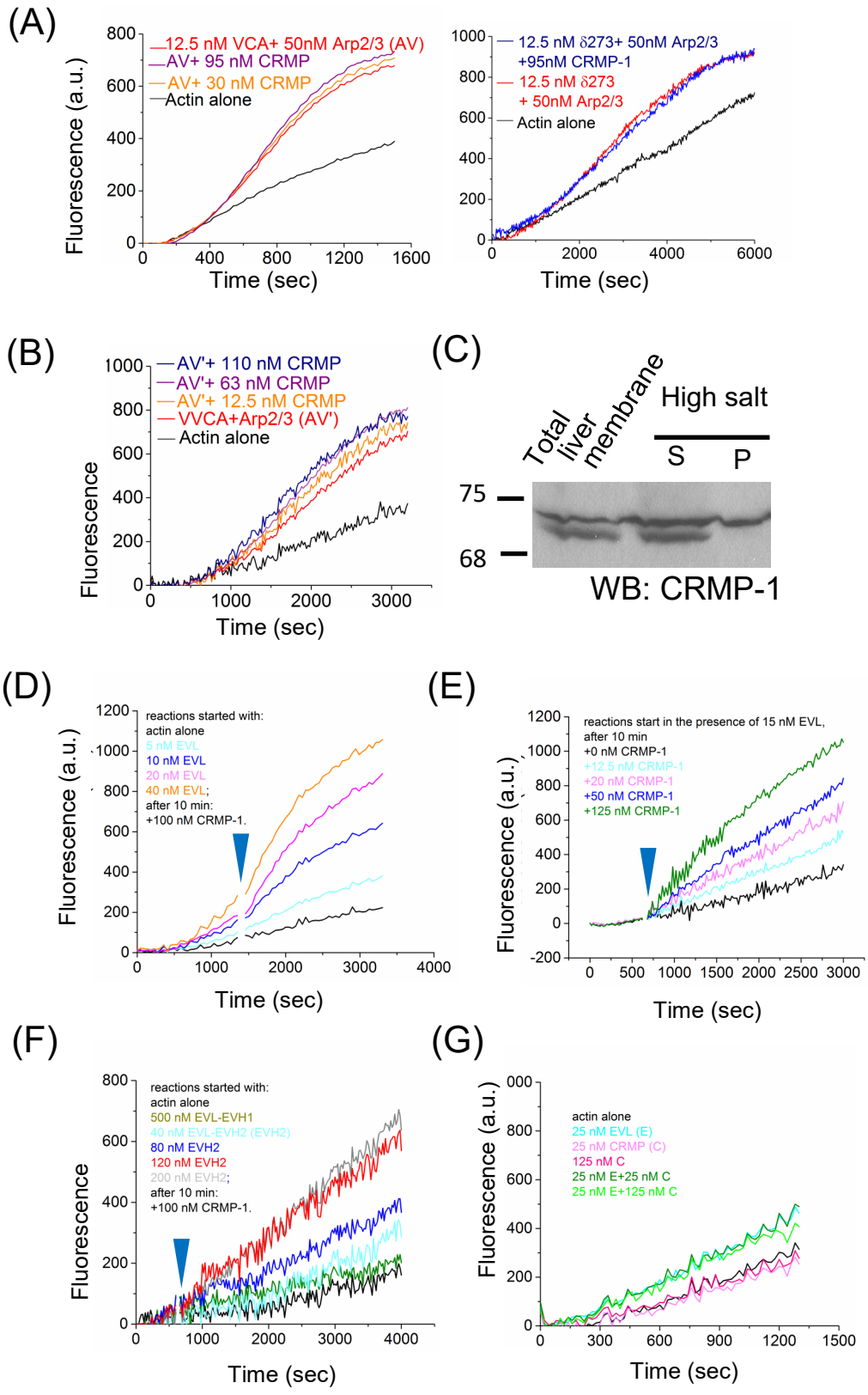
(A)
12.5 nM VCA+ 50nM Arp2/3 (AV)
AV+ 95 nM CRMP
AV+ 30 nM CRMP
Actin alone
Fluorescence (a.u.)
Time (sec)
12.5 nM δ273+ 50nM Arp2/3
+95nM CRMP-1
12.5 nM δ273
+ 50nM Arp2/3
Actin alone
Time (sec)
(B)
AV'+ 110 nM CRMP
AV'+ 63 nM CRMP
AV'+ 12.5 nM CRMP
VVCA+Arp2/3 (AV')
Actin alone
Fluorescence
Time (sec)
(C)
Total liver membrane
High salt
S
P
75
68
WB: CRMP-1
(D)
reactions started with:
actin alone
5 nM EVL
10 nM EVL
20 nM EVL
40 nM EVL;
after 10 min:
+100 nM CRMP-1.
Fluorescence (a.u.)
Time (sec)
(E)
reactions start in the presence of 15 nM EVL,
after 10 min
+0 nM CRMP-1
+12.5 nM CRMP-1
+20 nM CRMP-1
+50 nM CRMP-1
+125 nM CRMP-1
Fluorescence (a.u.)
Time (sec)
(F)
reactions started with:
actin alone
500 nM EVL-EVH1
40 nM EVL-EVH2 (EVH2)
80 nM EVH2
120 nM EVH2
200 nM EVH2;
after 10 min:
+100 nM CRMP-1.
Fluorescence
Time (sec)
(G)
actin alone
25 nM EVL (E)
25 nM CRMP (C)
125 nM C
25 nM E+25 nM C
25 nM E+125 nM C
Fluorescence (a.u.)
Time (sec)

Figure A.3 (cont.)

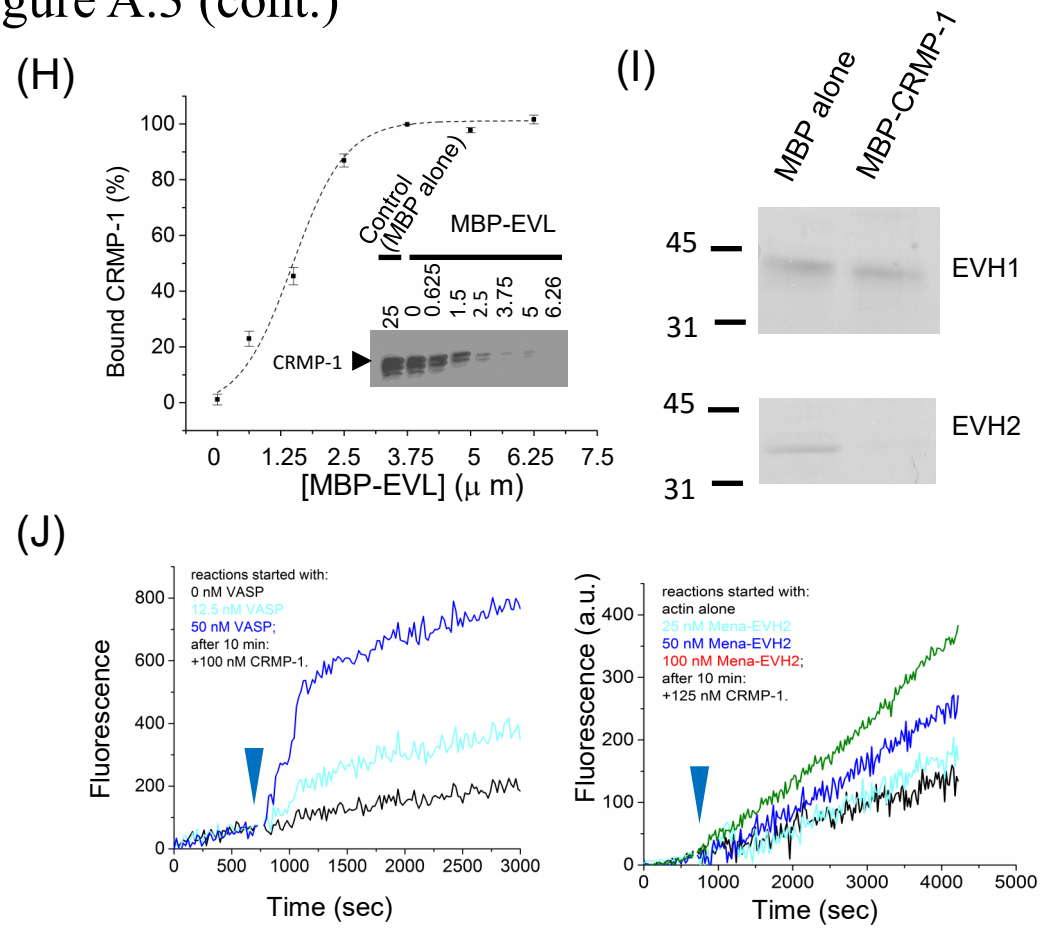

Figure A.3. CRMP-1 works with VASP family proteins to facilitate actin polymerization. (A) CRMP-1 does not contribute to Arp2/3 polymerization in the presence of constitutively active WAVE truncations. Left panel: VCA-induced Arp2/3 reaction; right panel: δ 273-induced reaction. The δ 273 construct contains VCA and proline-rich domain of WAVE-2. (B) CRMP-1 does not facilitate Arp2/3 polymerization mediated by VVCA of N-WASP. (C) Immunobloting of CRMP-1 on liver plasma membranes. (D) & (E) CRMP-1 contributes to EVL-mediated actin polymerization. Increasing concentration of EVL was provided at the beginning of the reaction, a constant amount of CRMP-1 was added later (D). CRMP-1 provides a dose-dependent effect when the reaction was started with a constant amount of EVL (E). (F) CRMP-1 promotes actin polymerization with the EVH2 domain, but not the EVH1 domain, of EVL. (G) Providing both CRMP-1 and EVL at the beginning of actin polymerization do not increase the rate of actin polymerization. (H) CRMP-1 interacts with EVL. The binding curve of CRMP-1 to MBP-tagged EVL. (insert) western blotting of CRMP-1 in the supernatants showing CRMP-1 depletion after incubating with different amount of EVL. Numbers above each lane indicate total protein concentration on the beads. (Concentration: EVL was calculated as tetramer; MBP alone was calculated as monomer). (I) EVH2 of EVL interacts with MBP-tagged CRMP-1, but EVH1 domain does not. The coomassie staining shows the amount of EVL truncates remaining in the supernatant after incubating with the immobilized MBP or MBP-tagged CRMP-1. (J) CRMP-1 has affect on VASP-mediated (left) or MENA-EVH2-mediated (right) actin polymerization. Blue arrowhead indicates the time when CRMP-1 was added into the reaction.

Figure A.4

(A)

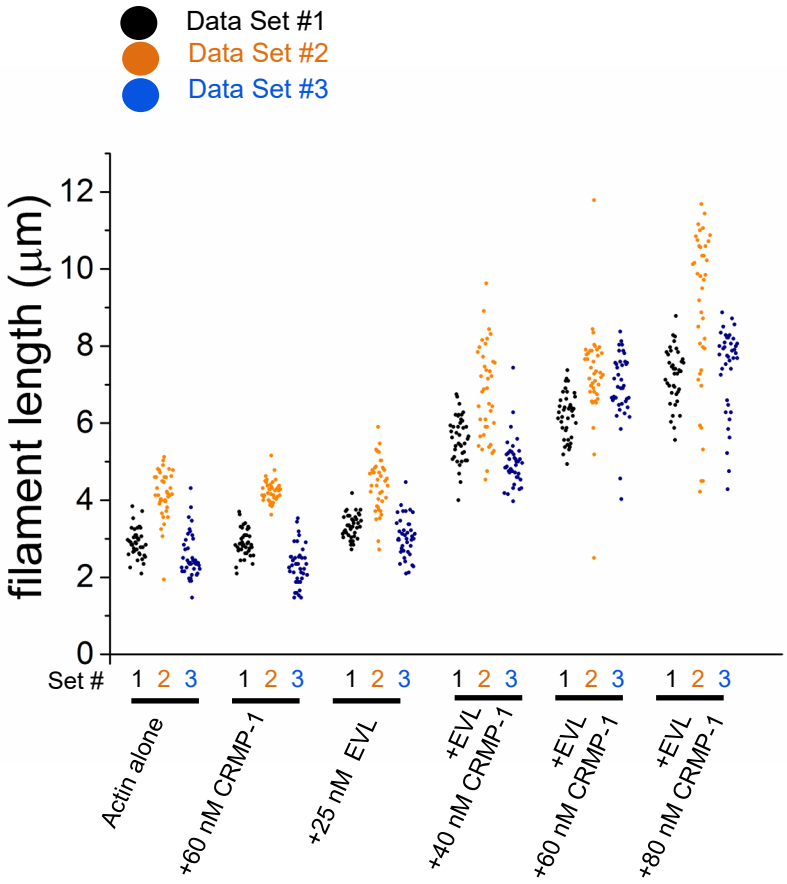

(B)

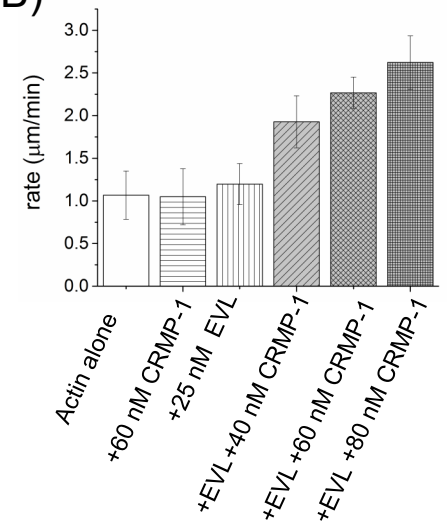

(C)

Condition	# of filaments
Actin alone	155
+CRMP-1	132
+EVL	141
+EVL + 40 nM CRMP-1	147
+EVL + 460 nM CRMP-1	128
+EVL +80 nM CRMP-1	160

Figure A.4 (cont.)

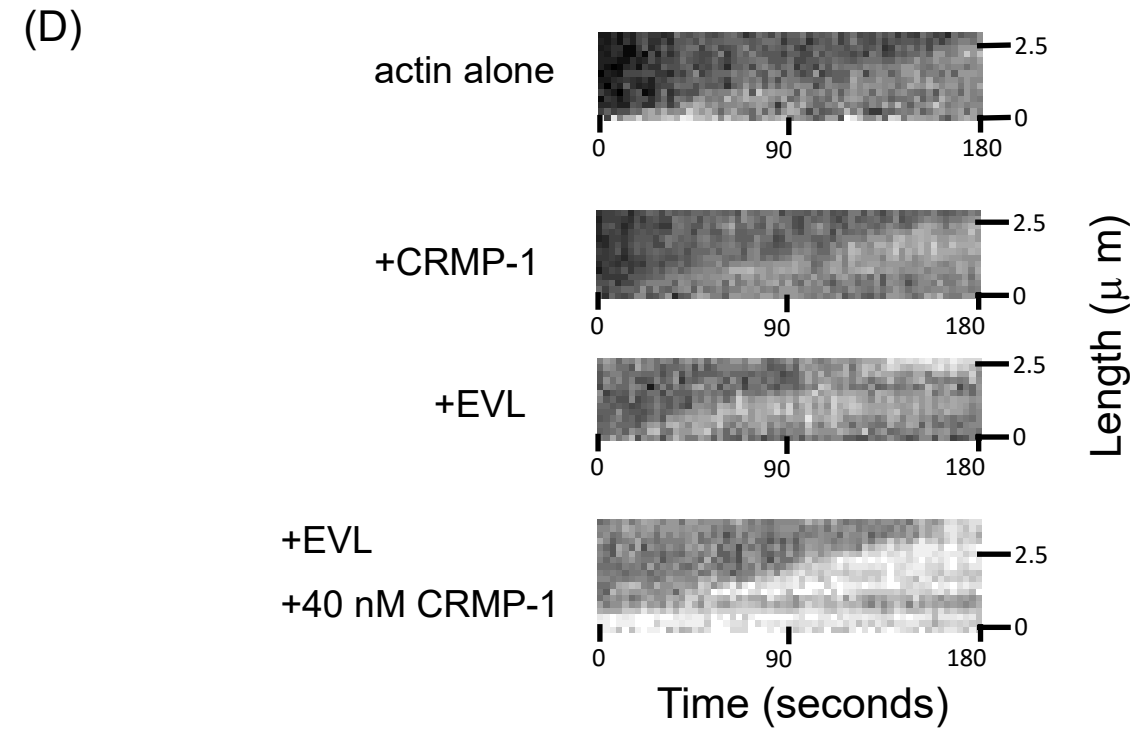

Figure A.4. Single filament experiments show that CRMP-1 facilitate EVL-mediated actin elongation. (A) Quantitative result of single filament experiments showing that CRMP-1 further increases the length of EVL– bounded filament. The filament were first polymerized with actin alone or in the presence of CRMP-1 or EVL for 1 minute in the test tube. Different concentrations of CRMP-1 were added into EVL pre-polymerized reactions. The reaction were immediately applied on a coverslip and recorded for 3 minutes, with 3 second per frame. The length of the filaments grow in different conditions were quantified. Three repeats were done, as shown in the plot as set #1, #2 and #3. (B) Quantification shows that CRMP-1 increases filament elongation rate in the presence of EVL. (C) CRMP-1 and EVL might not nucleate actin filament, since similar number of filaments was detected for different conditions. (D) Representative kymographs from single filament experiments.

Figure A.5

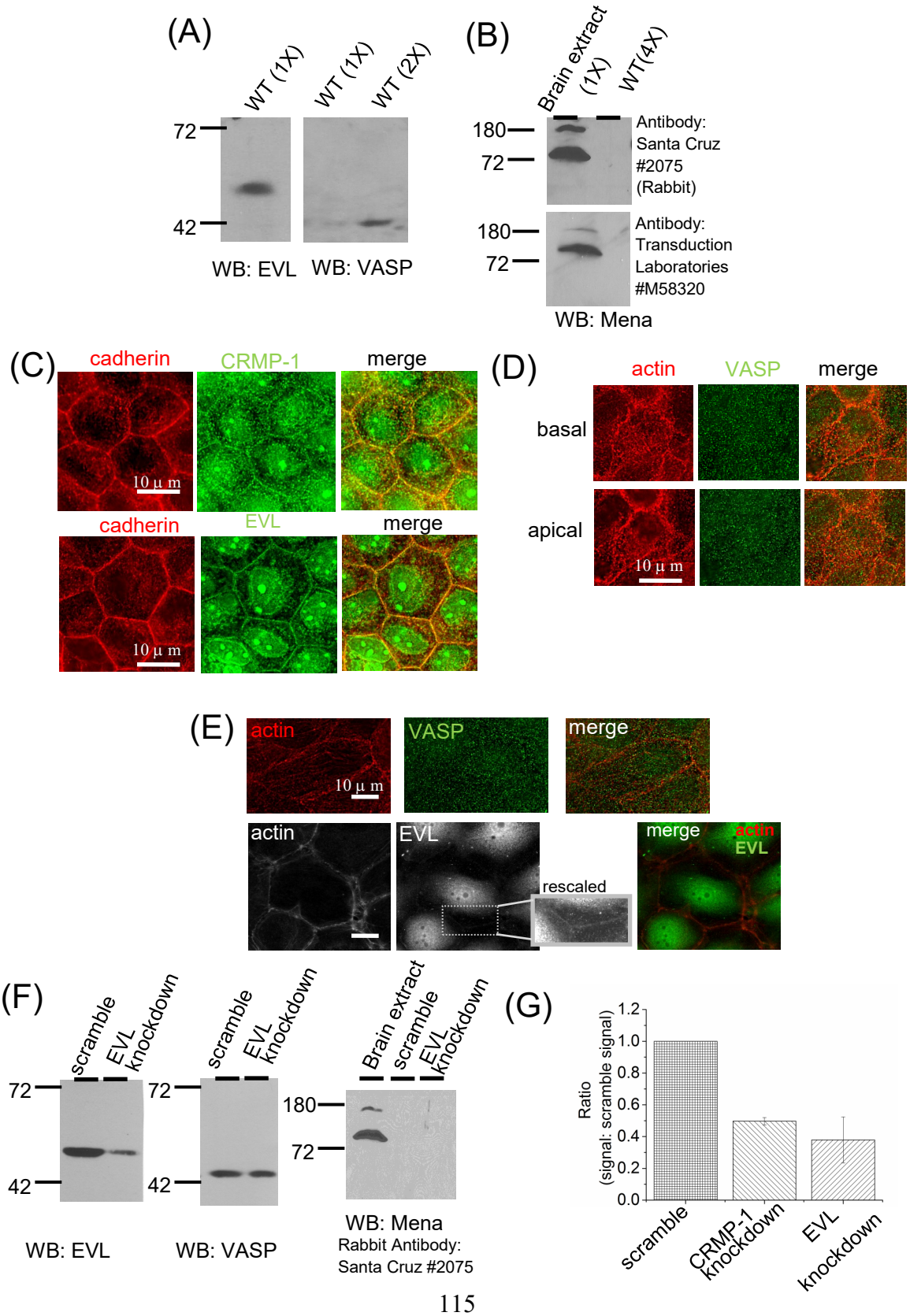
(A)
WT (1X)
WT (1X)
WT (2X)
72
42
WB: EVL
WB: VASP
(B)
Brain extract (1X)
WT(4X)
180
72
Antibody: Santa Cruz #2075 (Rabbit)
Antibody: Transduction Laboratories #M58320
WB: Mena
(C)
cadherin
CRMP-1
merge
10 µ m
cadherin
EVL
merge
10 µ m
(D)
actin
VASP
merge
basal
apical
10 µ m
(E)
actin
VASP
merge
10 µ m
actin
EVL
rescaled
merge
actin
EVL
(F)
scramble
EVL knockdown
72
42
scramble
EVL knockdown
72
42
Brain extract
scramble
EVL knockdown
180
72
WB: EVL
WB: VASP
WB: Mena
Rabbit Antibody: Santa Cruz #2075
(G)
Ratio (signal: scramble signal)
1.2
1.0
0.8
0.6
0.4
0.2
0.0
scramble
CRMP-1 knockdown
EVL knockdown

Figure A.5 (cont.)

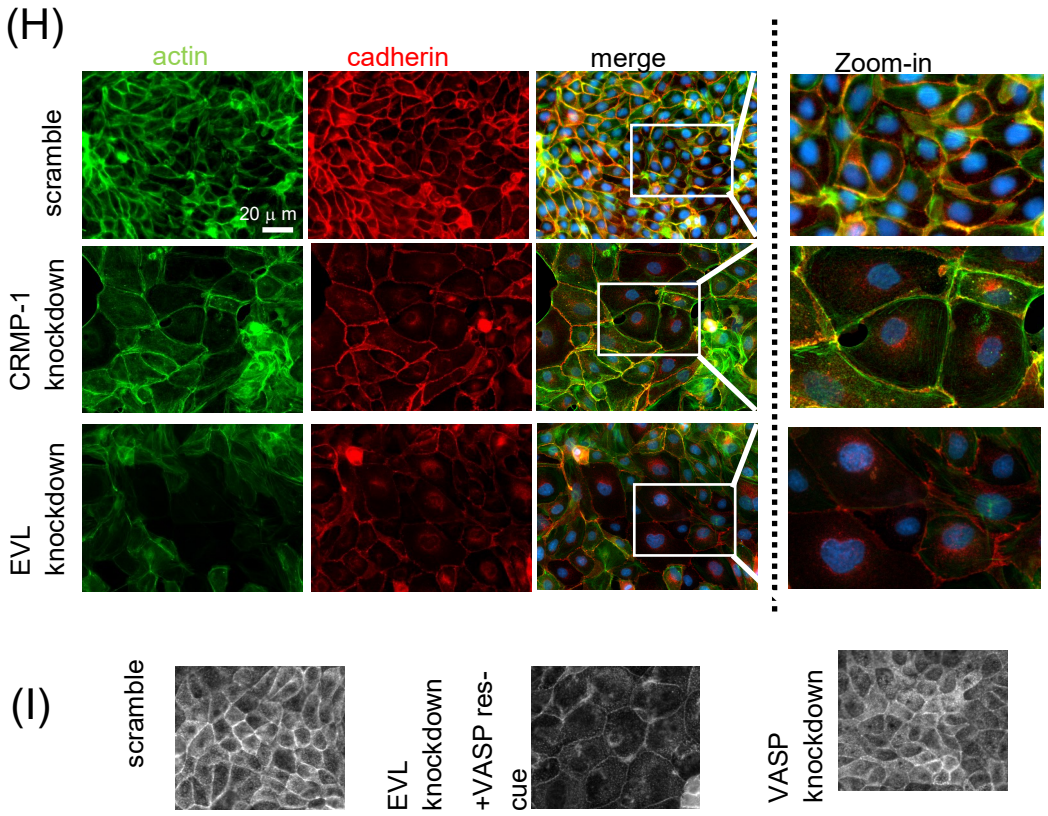

Figure A.5. CRMP-1 and EVL regulates the amount of actin in MDCK cells. (A) Western blotting results indicate that MDCK cells express EVL and VASP. (B) MENA is not expressed in MDCK cell. The two blots showed the result from using two commercial antibodies. WT: wild-type cells. X indicates the amount of whole lysate loaded into the well. For example, 2X means double volume of the sample were loaded. 1X contains approximately 150 μ g of protein. (C) CRMP-1 and EVL locates to cell-cell border. Red: cadherin; green: CRMP-1 or EVL. Scale bar: 10 μ m. (D) VASP does not show specific localization in the wildtype cell. (E) In CRMP-1 knockdown cells, VASP still has no specific localization; yet EVL is still at the junction. (F) EVL shRNAs are

Figure A.6

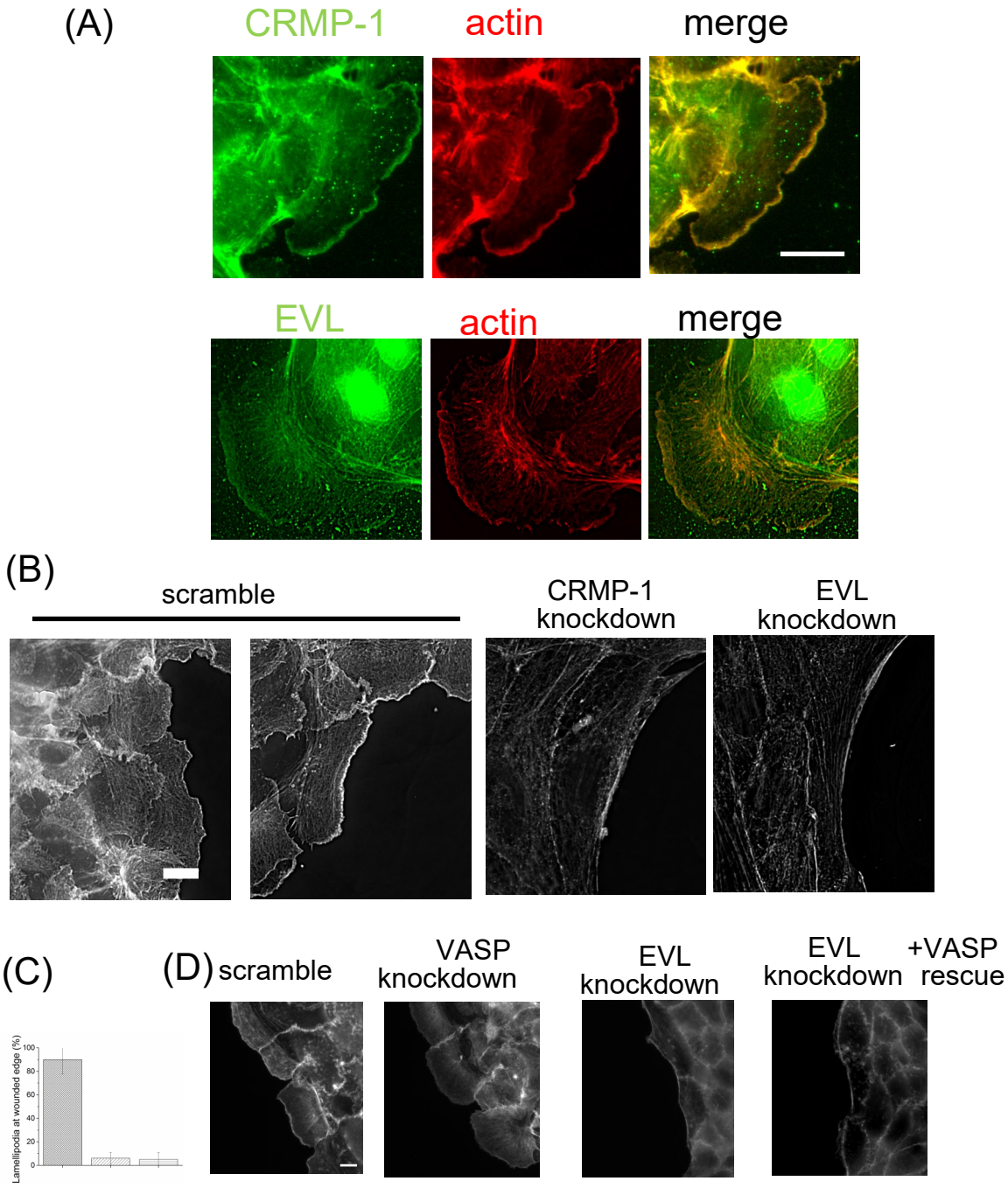

Figure A.6. CRMP-1 and EVL contribute to the lamellipodia formation in MDCK cells. (A) Immunostaining showing that CRMP-1 and EVL localize to the leading edge of the protruding structures in response to wounding. (B) Phalloidin staining shows that in CRMP-1 or EVL depleted cells, the formation of lamellipodia was perturbed. (C) Quantification of (B) shows that the amount of lamellipodia formation is greatly reduced in the knockdown cells. (D) Depletion of VASP did not affect lamellipodia formation. VASP did not rescue EVL-depleted cell regarding to its ability of forming lamellipodia. Scale bar: 20 μ m.

APPENDIX B

Figure. B.1

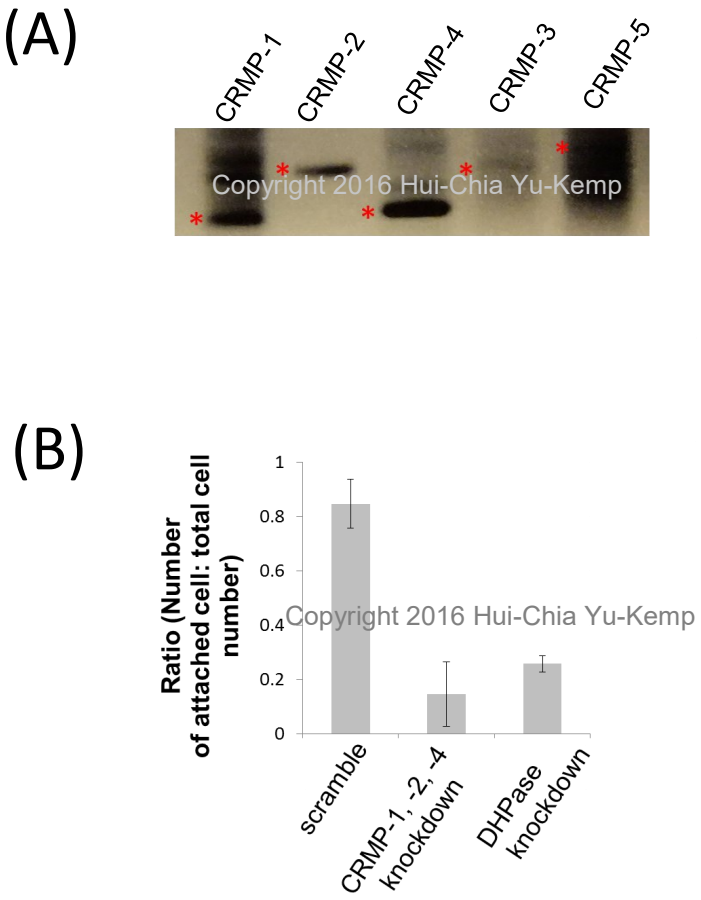

Fig. B.1 MDCK cells express different CRMPs. (A) RT-PCR analysis of CRMP family proteins in MDCK cells. (B) Depletion of CRMPs or DHPase in MDCK affects cell size.

Figure. B.2

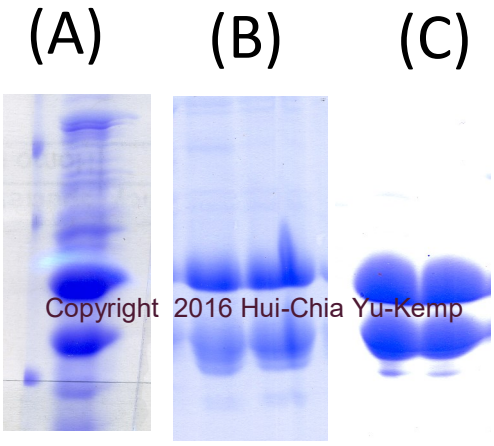

Fig. B.2. Purification of recombinant CapZ. Coomassie gel shows CapZ in (A) total lysate, (B) fractions after hydroxyapatite column, and (C) fractions after Q column.